8-2013

# NOVEL INDUCERS OF GLIOTOXIN PRODUCTION IN ASPERGILLUS FUMIGATUS

Taylor J. Schoberle

NOVEL INDUCERS OF GLIOTOXIN PRODUCTION IN *ASPERGILLUS FUMIGATUS*

By:

Taylor Jane Schoberle, M.S.

APPROVED:

_____
Supervisory Professor: Dr. Gregory May

_____
Dr. Michelle Barton

_____
Dr. Kevin Morano

_____
Dr. Michael Lorenz

_____
Dr. Dimitrios Kontoyiannis

---

APPROVED:

_____
Dean, The University of Texas Graduate
School of Biomedical Sciences at Houston

# NOVEL INDUCERS OF GLIOTOXIN PRODUCTION IN *ASPERGILLUS FUMIGATUS*

A

DISSERTATION

Presented to the Faculty of
The University of Texas
Health Science Center at Houston
and
The University of Texas
MD Anderson Cancer Center
Graduate School of Biomedical Sciences
in Partial Fulfillment

of the Requirements

of the Degree of

DOCTOR OF PHILOSOPHY

by

Taylor Jane Schoberle, M.S.
Houston, Texas

August, 2013

## Dedication

I dedicate this dissertation to my family and friends, whose love and support helped me achieve this degree. I would also like to dedicate this dissertation to my PhD advisor, Dr. Gregory May, who has served as a great mentor throughout my M.S. degree and Ph.D. degree.

## Acknowledgements

I would like to acknowledge Dr. John S. McMurray and Pijus Mandal for their invaluable help with the RP-HPLC analysis. I would also like to acknowledge Dr. Timothy Hughes, Ally Yang, and Matt Weirauch for their work on the protein binding microarray analysis.

NOVEL INDUCERS OF GLIOTOXIN PRODUCTION IN *ASPERGILLUS FUMIGATUS*

Publication No._____

Taylor Jane Schoberle, M.S.

Supervisory Professor: Dr. Gregory May, PhD

Secondary metabolites are produced by numerous organisms and can either be benign to humans or harmful. Genes involved in the synthesis and transport of these secondary metabolites are frequently found in gene clusters, which are often located in subtelomeric regions of the chromosome. These clusters are often coordinately regulated, being almost exclusively dependent on transcription factors that are located within the clusters themselves. Secondary metabolites are also regulated by a variety of factors, including nutritional factors, environmental factors and developmental processes. Gliotoxin, which is produced by a variety of *Aspergillus* species, *Trichoderma* species, and *Penicillium* species, exhibits immunosuppressive properties and has therefore been the subject of research for many laboratories. There have been a few proteins shown to regulate the gliotoxin cluster, most notably GliZ, a $Zn_2Cys_6$ binuclear finger transcription factor that lies within the cluster, and LaeA, a putative methyltransferase that globally regulates secondary metabolism clusters within numerous fungal organisms, although no study has demonstrated the direct binding of any protein to a promoter region in the gliotoxin cluster.

I report here two novel proteins, GipA, a $C_2H_2$ transcription factor and GipB, a hybrid sensor kinase, which are involved in regulating the gliotoxin biosynthetic cluster. GipA plays

an important role in gliotoxin production, as high-copy expression of *gipA* induces gliotoxin biosynthesis and loss of *gipA* reduces gliotoxin biosynthesis by 50%. GipB is also involved in regulating gliotoxin production, as high-copy expression of *gipB* induces gliotoxin biosynthesis, but only during certain stages of asexual development. Furthermore, loss of *gipB* reduces gliotoxin biosynthesis by 10%. Based on data obtained from this project, I propose a model for the regulation of *gliA*, the efflux pump of the gliotoxin cluster, which involves GipB signaling through both GliZ and GipA. I propose that GliZ and GipA are interdependent, as mutation of the GipA DNA binding site in the *gliA* promoter negatively affects both GliZ-mediated and GipA-mediated induction of *gliA*. This is further supported by the fact that GliZ cannot fully induce *gliA* in the absence of GipA and vice versa. This is the first time that anyone has shown evidence of a protein directly binding to the gliotoxin cluster. Even though biosynthetic clusters are often coordinately regulated, my model raises the possibility that *gliA* is independently regulated, as the layout of the binding site in the *gliA* promoter is not present upstream of any other genes in the gliotoxin cluster, except for *gliZ*.

## Table of Contents

## List of Figures:

## List of Tables

# Chapter 1:

# General Introduction

## 1.1 Secondary Metabolism

Secondary metabolites are small, low-molecular weight molecules made by numerous organisms that are not essential for normal growth, but can play important roles in defense or signaling [1-4]. Oftentimes, there is a link between production of secondary metabolites and specific stages of morphological differentiation [1, 5]. Although these compounds are manufactured by a plethora of organisms, especially soil-dwelling bacteria and fungi, each individual metabolite is subject to restricted taxonomic distribution, as metabolites are not produced in a highly conserved fashion [1-3]. For example, gliotoxin is produced by *Aspergillus fumigatus* and *A. oryzae*, but not *A. nidulans* [6, 7].

Secondary metabolites can be benign in nature, such as pigments or molecules used in interspecies communication, but they can also be malignant, exhibiting antimicrobial or toxic activities to eliminate competing organisms [5, 8]. Some of these compounds have been exploited by scientists because of their potential benefit to humans. For example, penicillin, produced by *Penicillium chrysogenum*, is used as an antibiotic and lovastatin, produced by *A. terreus*, reduces cholesterol [9]. Indeed, a literature survey examining 1,500 fungal metabolites between 1993 and 2001 discovered that more than half of these molecules had antibacterial, antifungal, and antitumor activity [2]. While some of these secondary metabolites benefit humans, others cause harm. Aflatoxin, produced by *A. flavus*, is carcinogenic, and gliotoxin, produced by *A. fumigatus*, exhibits immunosuppressive properties [3, 6, 10, 11]. There are also compounds produced by fungal species that are both harmful and beneficial to humans, such as ergot alkaloids. These compounds, when consumed by humans, can cause convulsions, vasoconstriction, and hallucinations, yet have been used medically to hasten labor and treat migraines [2].

Several classes of fungal secondary metabolites exist: polyketides, non-ribosomal peptides, terpenes, and indole alkaloids [1-3] (Fig. 1.1). Polyketides are produced by type I polyketide synthases (PKS) and are the most abundant of all fungal secondary metabolites. These type I polyketide synthases are multidomain proteins that bear homology to eukaryotic fatty-acid synthases. Aflatoxin, lovastatin, and the yellow spore pigment intermediate naphthopyrone (WA) from *A. nidulans* are among the best genetically characterized polyketides [2]. Multidomain, multimodular enzymes, known as non-ribosomal peptide synthetases (NRPS) are responsible for creating non-ribosomal peptides [2, 3]. Module-specific amino acids are recognized and activated by NRPSs, which results in the formation of a covalent bond between each amino acid and the 4'-phosphopantetheine cofactor, through a conserved serine. Tethered amino acids form peptide bonds and the resulting peptide is subsequently released. Penicillin, cephalosporin, and gliotoxin all fall within this class of fungal secondary metabolites [2].

Terpenes, best known as odoriferous plant metabolites, such as camphor and turpentine, are composed of several isoprene units. Terpene cyclases, which are essential for the production of terpenes, share structural homology, but exhibit low primary sequence similarity, suggesting these cyclases have been subject to rapid divergent evolution. Fungal terpenes include carotenoids, gibberellins, and trichothecenes [2]. Tryptophan and dimethylallylpyrophosphate commonly serve as precursors for indole alkaloids, although this is not absolute. One of the best characterized pathways synthesizes ergotamine, although other tryptophan-derived alkaloids include fumigaclavines and fumitremorgens from *A. fumigatus* [2].

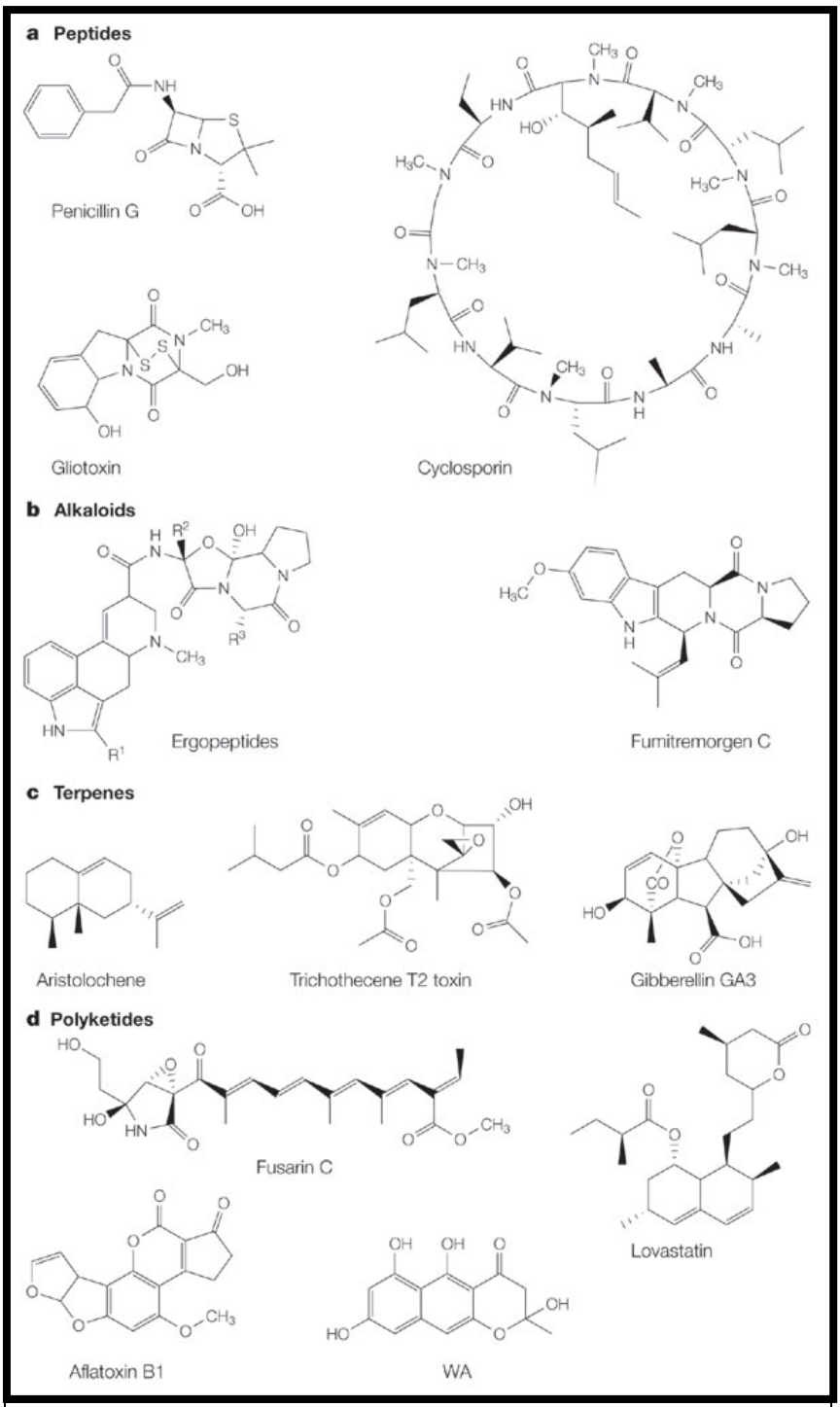


Figure 1.1. The main classes of fungal secondary metabolites. Reprinted by permission from Macmillan Publishers Ltd: Nature Reviews Microbiology [2], copyright 2005.

## 1.2 Cluster-specific Regulation of Secondary Metabolism

Originally, eukaryotic genes involved in functionally related pathways were believed to be unlinked in the genome. Owing to the discovery of gene clusters in fungi involved in a variety of mechanisms, such as nutrient use, mating type, pathogenicity, and secondary metabolism, this dogma of unlinked pathways was abandoned [2]. It is now widely accepted that genes involved in these various primary and secondary metabolic processes are indeed frequently found as clusters [1-3, 8]. Furthermore, secondary metabolism clusters have more recently been shown to be oftentimes located in subtelomeric positions [12]. These clusters are typically coordinately regulated, being almost completely dependent on induction from transcription factors located within the clusters themselves [2, 3, 8, 13, 14]. Aside from these pathway-specific transcription factors, there are numerous other regulatory elements that affect the expression of secondary metabolite clusters. Nutritional and environmental factors, as well as developmental processes, have been shown to affect secondary metabolite production in multiple fungal species [2, 3].

### *1.2.1 Transcription Factors Located within Clusters*

Secondary metabolism gene clusters often contain regulatory elements that are essential for the coordinate expression of the biosynthetic enzymes and transport proteins encoded within the cluster [2, 3]. Zinc binuclear ($Zn(II)_2Cys_6$) transcription factors are uniquely found in fungi and represent the most common type of regulators located within these clusters [2, 3, 15, 16]. AflR, a $Zn_2Cys_6$ transcription factor, is located within the aflatoxin/sterigmatocystin gene cluster and is required for production of both metabolites [2, 3, 11]. The aflatoxin and sterigmatocystin gene clusters contain most of the same enzymes, except the sterigmatocystin gene cluster lacks the genes necessary for the final

biochemical steps, therefore, sterigmatocystin is a precursor to aflatoxin [11]. *A. nidulans* produces sterigmatocystin, while *A. flavus* and *A. parasiticus* produce aflatoxin. Aflatoxin/sterigmatocystin production is abolished when *aflR* is disrupted or mutated and amplified when *aflR* is over-expressed [2, 3, 11, 17].

$Zn_2Cys_6$ transcription factors, like *aflR*, generally recognize and bind as homodimers to palindromic sequence motifs, such as CGG($N_x$)CCG [15-18]. Interestingly, although the palindromic sequences of these binding motifs can be similar or identical for multiple $Zn_2Cys_6$ transcription factors, the length and base composition of the linker sequence is highly variable. Therefore, this linker sequence greatly contributes to the specificity of binding for each individual transcription factor [16, 18, 19]. For instance, Gal4 and Ppr1 are two $Zn_2Cys_6$ transcription factors in *Saccharomyces cerevisiae* that regulate different pathways. Gal4 is responsible for transcription of various galactose-inducible genes and Ppr1 activates transcription of genes in the pyrimidine metabolic pathway [16, 18, 19]. Both transcription factors recognize binding sites that are flanked by CGG palindromic repeats, but have differently sized linker sequences, Gal4 recognizes an 11 bp linker and Ppr1 recognizes a 6 bp linker. Even though the CGG repeats, which are crucial for Gal4 or Ppr1 binding, are identical, these two proteins do not recognize the other's binding site and therefore remain specific to their respective pathways [16, 18, 19].

Although $Zn_2Cys_6$ transcription factors represent the most common type of in-cluster regulatory elements, other types of cluster-specific transcription factors have been identified. TRI6 and MrTRI6 are $C_2H_2$ transcription factors that control production of trichothecene in *Fusarium sporotrichiodes* and *Myrothecium roridum*, respectively [2, 8, 20]. *Cochliobolus carbonum* contains an ankyrin repeat protein, ToxE, which regulates HC-toxin production. Furthermore, CPCR1 and AcFKH1, which are members of subfamilies of

winged helix transcription factors, are required for the production of cephalosporin C in *Acremonium chrysogenum* [2, 8, 20].

### *1.2.2 Alternative Pathway-specific Regulation*

Aside from cluster-specific transcription factors, there are members of secondary metabolite clusters that have been shown to affect expression of other genes within the cluster. For example, *gliP* encodes an NRPS in the gliotoxin cluster and catalyzes the first step in the biosynthesis of gliotoxin. Not only does loss of *gliP* abolish gliotoxin production, but it also causes a significant decrease in the other gliotoxin-specific genes [21-24]. In addition, disruption of *sirA*, the ABC transporter for the sirodesmin biosynthetic cluster in *Leptosphaeria maculans*, positively affects the expression of *sirP*, the NRPS of the sirodesmin cluster [25, 26]. Although gene clusters are often coordinately regulated by the cluster-specific transcription factor, some members can be independently regulated. For example, *gliT* encodes an oxidoreductase of the gliotoxin biosynthetic cluster, which is required for self-protection against gliotoxin. Even though *gliT* expression is decreased when the $Zn_2Cys_6$ transcription factor, *gliZ*, is deleted, exogenous gliotoxin induces the expression of *gliT*, even in a *ΔgliZ* background [3, 27].

## 1.3 Fungal Development and Secondary Metabolism

Within the genus *Aspergillus* are between 260 and 837 species, which are classified into ten different teleomorph genera based on their sexual stages [28]. For example, *A. nidulans* belongs to the teleomorph genus *Emericella*, while *A. flavus* and *A. fumigatus* are categorized into the *Petromyces* and *Neosartorya* genera, respectively [28]. Many

*Aspergillus* species can reproduce both asexually, by developing conidia, and sexually, via ascospore development [28]. Vegetative growth of filamentous fungi entails germination of conidia or ascospores into hyphae, which can lead to the formation of mycelial colonies, development of biofilms, initiation of asexual development (conidiation), or initiation of sexual development, among other things, depending on external stimuli [28, 29]. Environmental cues, such as light, oxygen, salt, and nutrients, can affect the expression of genes involved in regulating the different developmental programs [28, 30]. Oftentimes, the environmental signals that promote a certain developmental program will also affect secondary metabolite production [31]. For instance, asexual development can be induced in submerged liquid cultures by nutrient starvation or stress, which can also positively influence production of secondary metabolites [28]. Conversely, exposure to constitutive darkness will promote sexual development, which also enhances secondary metabolism [30, 32].

### *1.3.1 Fungal Development*

The process of germination can be divided into three stages. In the first stage, a spore will abandon the dormant state in response to environmental cues, such as exposure to water and air, sometimes in addition to inorganic salts, amino acids, or fermentable sugars [28, 33]. In the second stage, spores begin to swell isotropically due to water uptake, which decreases the microviscosity of the cytoplasm. Moreover, cellular functions are directed to the synthesis of new plasma membrane and cell wall components [28]. The third stage is reached when the spore initiates polarized growth to form a germ tube, which requires redirection of morphogenetic machinery to the site of polarization [28] (Fig. 1.2).

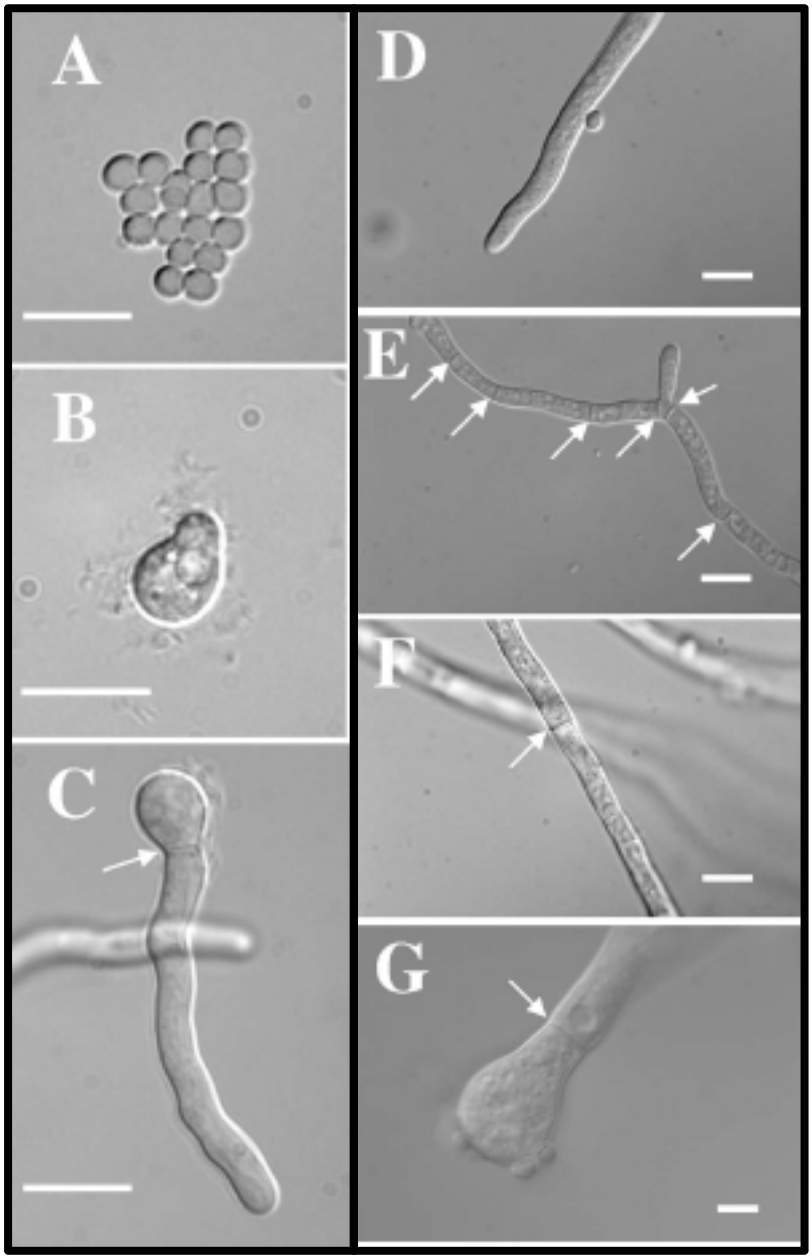


Figure 1.2. Growth and germination of *A. fumigatus*. (A) Dormant conidia (0 hrs growth). (B) Swollen conidia at the beginning of germ-tube formation (3 hrs growth). (C) Germling with newly formed septum (white arrow) (6 hrs growth). (D) Hyphal tip. (E-G) Examples of hyphae with mature septa (white arrows). Modified and reprinted by permission from American Society for Microbiology: Eukaryotic Cell [34], copyright 2008.

When grown at 37°C, *A. fumigatus* can achieve germ tube formation within 4.5 hours of inoculation. Protein synthesis is important in these early stages of germination, as there is an up-regulation of genes involved in protein synthesis in germinating spores of *A. fumigatus*. Furthermore, isotropic growth of conidia can be prevented by the protein synthesis inhibitor cyclohexamide, but not by inhibitors of the cytoskeleton or nucleotide synthesis [28, 33].

Once germination is initiated, germlings undergo hyphal proliferation. Hyphae are tube-like structures that consist of repeated elongated cellular units. Hyphae proliferate by polarized growth at the apex of the tip cell, similar to germ tube formation, which involves expansion of the plasma membrane and biosynthesis of cell wall components [1, 35] (Fig. 1.2c). Elongated cells within hyphae are separated by porous walls, called septae, through which cytoplasm and also entire nuclei can migrate towards the growing tip [1] (Fig. 1.2). One conidial cell or ascospore will generally give rise to multiple hyphal extensions as a result of apical branching [35]. Vegetative growth is a required precursor to other developmental programs in filamentous fungi, with the exception of dimorphic fungi [1] (Fig. 1.3). Differentiation capability is defined by the ability of vegetative hyphae to reach a competence state [35]. In *A. nidulans*, competence can be reached between 12 and 20 hours after germination of the spore, depending on the growth rate [1]. In *A. fumigatus*, developmental competence is reached 9 to 10 hours after inoculation in rich medium [36].

When vegetative hyphae have reached a competence state, asexual development (conidiation) is initiated, which involves the formation of the conidiophore [1, 35]. The process of conidiation can be divided into several distinct phases, beginning with the outgrowth of a stalk from a specialized, thick-walled foot cell within the mycelium [1, 28, 30]. Once the stalk has fully extended (in *A. nidulans*, stalks reach a height of about 100 μM

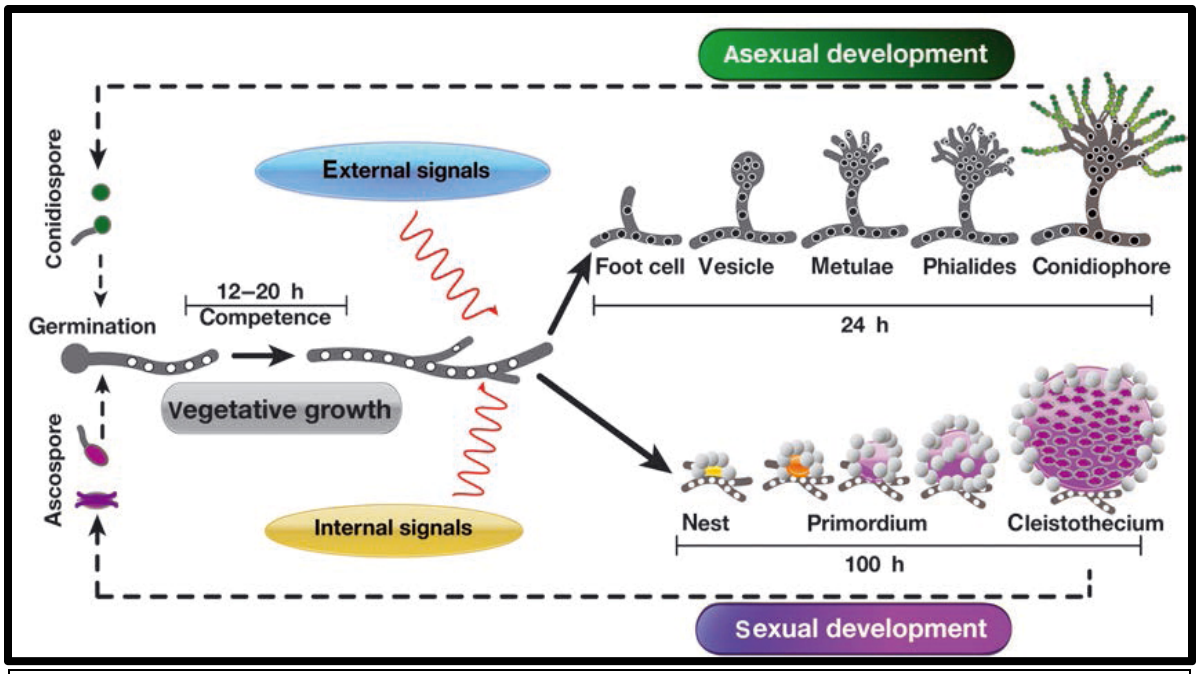


Figure 1.3. The different developmental stages of *A. nidulans*. Vegetative growth is a necessary precursor for either asexual development or sexual development. External and internal signals both contribute to the switch from vegetative growth to unique developmental programs. Reprinted by permission from John Wiley and Sons: FEMS Microgiology Reviews [1], copyright 2011.

[28]), the tip of the stalk swells to form a multinucleate vesicle, from which sterigmata bud [1, 28, 30, 35, 37]. In uniserate organisms, such as *A. fumigatus*, there is only one layer of sterigmata, termed phialides, however, in biserate fungi, such as *A. nidulans* and *A. niger*, two layers of sterigmata form from budding: (1) metulae and (2) phialides [28]. Finally, phialides generate multiple chains of single-celled conidia from asymmetric mitotic division, with the possibility of more than 10,000 conidia arising from a single conidiophore [28, 30, 35] (Fig. 1.4a-e). Exposure to light serves as a major activation signal for asexual development [30]. In addition, conidiophore formation generally occurs upon exposure to an air interface, which is thought to activate internal signals that regulate the genes involved in conidiation [28, 30, 35]. In some instances, though, conidiophore development can occur in submerged cultures, in response to external stress or nutrient limitations [28]. Once fully mature, conidia can be widely dispersed through the air or by water, contributing to fungal survival by widespread distribution [1, 28].

Although researchers have only observed a sexual cycle in about one-third of known *Aspergillus* species, genomic analysis has revealed the presence of genes specifically involved in sexual development in most of these fungi, indicating that they too may be capable of sexual development [28]. For instance*, A. fumigatus* has just recently been shown to form sexual fruiting bodies under experimental conditions, although this process took an extended period of time [28, 38]. With respect to sexual reproduction, a fungal organism is either homothallic, containing both mating types and therefore able to undergo sexual reproduction without a compatible partner, or heterothallic, containing only one mating type and thus requiring a compatible partner to undergo sexual reproduction [1, 28]. *A. fumigatus* is heterothallic, while *A. nidulans* is homothallic [1, 28]. The beginning of sexual development is represented by the formation of Hülle cells, which is followed by

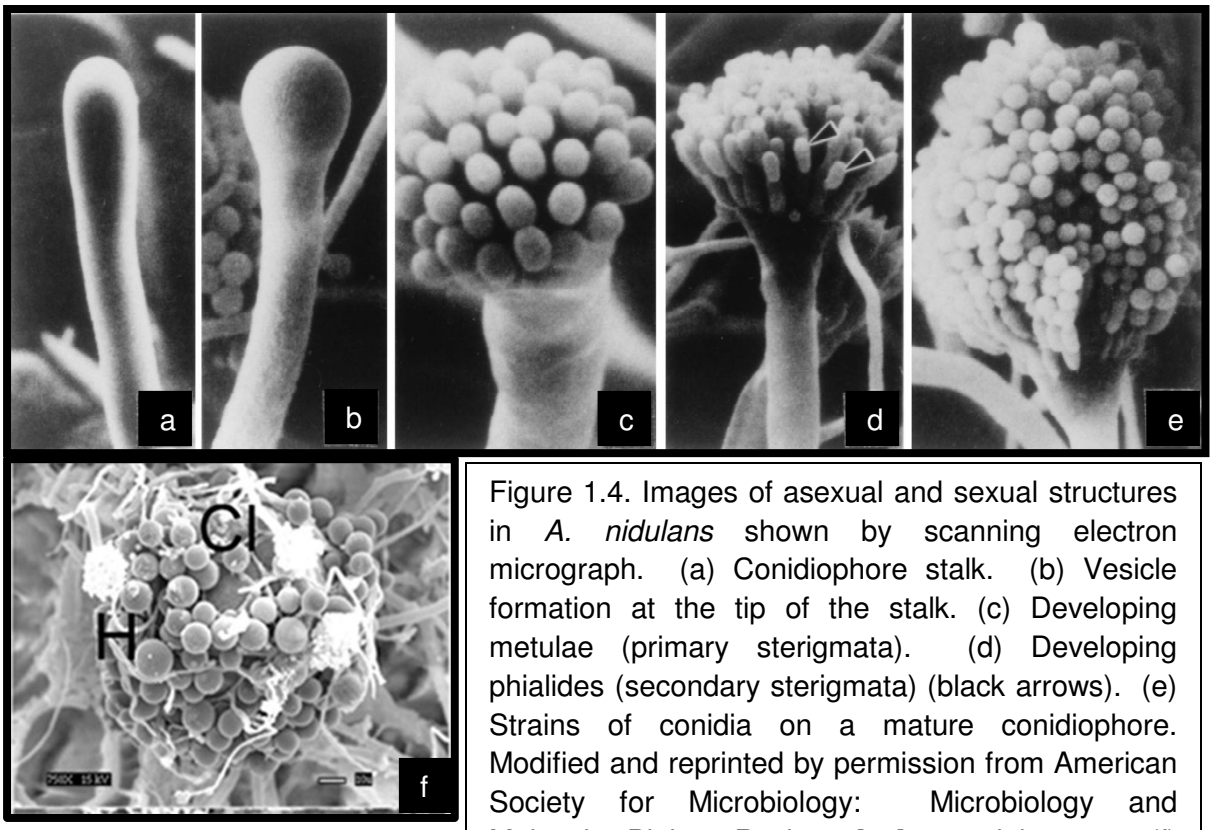


Figure 1.4. Images of asexual and sexual structures in *A. nidulans* shown by scanning electron micrograph. (a) Conidiophore stalk. (b) Vesicle formation at the tip of the stalk. (c) Developing metulae (primary sterigmata). (d) Developing phialides (secondary sterigmata) (black arrows). (e) Strains of conidia on a mature conidiophore. Modified and reprinted by permission from American Society for Microbiology: Microbiology and Molecular Biology Reviews [35], copyright 1998. (f) Mature cleistothecium (CI) (sexual fruiting body) surrounded by Hülle cells (H). Modified and reprinted by permission from American Society for Microbiology: Eukaryotic Cell [39], copyright 2012.

hyphal fusion and the emergence of a dikaryon. These Hülle cells surround the dikaryon and pack into a “nest”, eventually differentiating into thick-walled globose cells believed to provide both protection and nutrition to the maturing cleistothecium, or sexual fruiting body [1, 28] (Fig. 1.4f). Nuclear fusion followed by meiosis and post-meiotic mitosis gives rise to eight nuclei, which are separated by membranes to become spores. Ascospores become binucleate through a second post-meiotic mitosis. A single cleistothecium can contain a high number of asci, which each contain eight ascospores [28].

### *1.3.2 Secondary Metabolism and Asexual Development*

There are three categories of secondary metabolites that are often associated with conidiation: (1) metabolites required to activate conidiation (the extracellular sporulation-inducing factor [ESID], (2) pigments important for conidiophore development (melanin), and (3) mycotoxins [5]. Although production of certain mycotoxins does not appear to be essential for conidiation (for instance *A. nidulans* mutants deficient in sterigmatocystin production still undergo asexual development) a relationship between asexual development and mycotoxin production has been established. A number of studies have reported that *Aspergillus* mutants deficient in conidiation also display a deficiency in aflatoxin production [5, 40].

FluG, which produces an ESID in response to external signals, activates downstream targets to induce asexual development, one of these targets being FlbA [5, 28, 30, 35, 40-43] (Fig. 1.5). Loss of either *fluG* or *flbA* abolishes conidiophore formation and promotes hyperproliferative vegetative growth or the “fluffy” phenotype. FlbA is an RGS (regulator of G-protein signaling) protein that negatively regulates FadA, a G$\alpha$ subunit of a

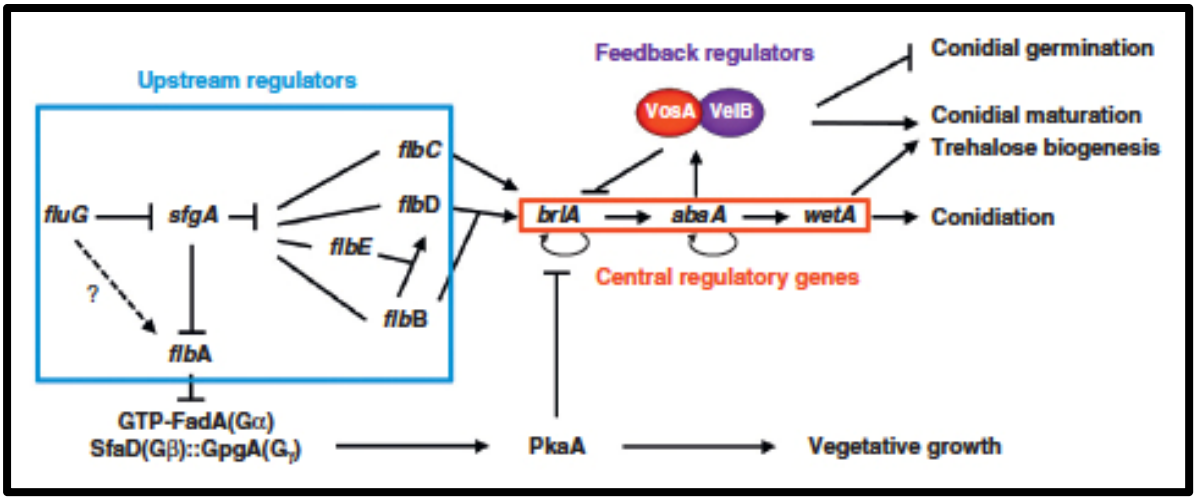


Figure 1.5. Model of upstream and central genetic regulators of asexual development. Reprinted from Current Opinion in Microbiology, Vol. 15/No. 6, Hee-Soo Park and Jae-Hyuk Yu, Genetic Control of asexual sporulation in filamentous fungi, pg. 669-677, 2012, with permission from Elsevier [30].

heterotrimeric G-protein complex that promotes vegetative growth and represses asexual development [5, 28, 30, 35, 40, 42, 44] (Fig. 1.5), therefore a constitutively active form of FadA resembles a *ΔflbA* mutant [43]. In *A. nidulans*, loss of *fluG* or *flbA* also abolishes sterigmatocystin production [2, 5, 40, 45, 46]. Interestingly, although over-expression of *flbA* in *A. nidulans* results in premature sterigmatocystin production, over-expression of *fluG* in submerged culture does not [5, 40]. Furthermore, in a *ΔflbA* mutant, over-expression of *aflR* does not reinstate sterigmatocystin production, indicating that these regulatory networks can be complex [5]. A mutant expressing a dominant active form of FadA also loses the ability to produce sterigmatocystin, suggesting that FluG activates FlbA, which supports the inactivation of FadA and subsequent sterigmatocystin production through induction of AflR [5, 40, 43, 45].

While FadA negatively regulates sterigmatocystin production, it positively regulates penicillin production in *A. nidulans* [2, 5, 47]. Furthermore, a FadA homologue in *Fusarium sporotrichioides* positively regulates trichothecene production, as expression of a dominant active form of FadA increases trichothecene biosynthesis [2, 5, 47]. Contrary to what is observed with a FadA dominant active mutant in *A. nidulans*, loss of either SfaD, the Gβ subunit, or GpgA, the Gγ subunit, causes reduced sterigmatocystin production [5, 43]. To positively regulate vegetative growth, FadA G-protein signaling induces the production of cAMP, which promotes PKA activation [5, 28, 45, 48]. Not surprisingly, over-expression of *pkaA* in *A. nidulans* represses conidiophore development and blocks sterigmatocystin production [2, 5, 45]. StuA, a transcriptional modifier of asexual development, has now been associated with regulation of secondary metabolism in several fungi, such as *P. chrysogenum* and *F. graminear* [9].

*1.3.3 Secondary Metabolism and Sexual Development: Light vs. Dark*

Secondary metabolite production is also associated with sexual development [1, 49]. When *A. nidulans* is grown in light, sterigmatocystin production is minimal, but when grown in the dark, which induces sexual development, levels of sterigmatocystin increase [30]. This differential expression has been linked to the formation of a heterotrimeric complex, called the Velvet complex, composed of VeA, VelB, and LaeA, which regulates the balance between sexual and asexual development [1, 28, 30, 50, 51]. Regulatory proteins that are in the velvet family, VeA, VelB, VosA, and VelC, are highly conserved among ascomycetes and basidiomycetes [1]. Velvet family proteins all contain a conserved velvet domain, which comprises 150 amino acids [1, 30].

An N-terminal-truncated mutant of VeA (*veA1*) produces more conidia and less sexual fruiting bodies than a wild-type strain. Furthermore, *A. nidulans* requires red light to induce conidiation, but the *veA1* mutant allows conidial development in the absence of light, suggesting that a domain in the N-terminus of VeA is responsible for light-mediated VeA activity [1, 28, 35]. A strain in which *veA* or *velB* has been deleted does not produce any sexual fruiting bodies in any conditions. In addition, over-expression of *veA* results in constitutive formation of sexual fruiting bodies, regardless of light exposure [1, 28]. LaeA is a putative methyltransferase that was identified in a screen for *A. nidulans* mutants that lost the ability to produce sterigmatocystin [50, 51]. LaeA contributes to light-dependent support of asexual development, as loss of *laeA* in *A. nidulans* renders the fungus unable to suppress sexual fruiting body formation in light. This phenotype is opposite of *ΔveA*, which cannot produce any sexual fruiting bodies regardless of light or dark exposure [1, 28]. LaeA forms a trimeric complex with VeA and VelB, which coordinates sexual development in darkness. This complex is low in concentration in light, as VeA and VelB remain in the cytoplasm and LaeA is confined to the nucleus [28]. Upon exposure to darkness, VeA

levels are increased and VeA forms a complex with VelB, which translocates to the nucleus (Fig. 1.6). It is here that VeA interacts with LaeA to form the trimeric complex with VelB [1, 28].

VeA, VelB, and LaeA are not only important for sexual and asexual development, but they also control secondary metabolism. Indeed, loss of *veA* in *A. nidulans*, results in a loss of penicillin and sterigmatocystin production [1]. This link of VeA to secondary metabolism has also been shown in other fungal species, such as *A. flavus* and *A. parasiticus*, which lose the ability to produce aflatoxin when *veA* is deleted, and *F. verticilloides*, which is unable to produce fumonisin and fusarins in a *Δve1* (*veA* homologue) background [1]. Additionally, deletion of *vel1* in *F. fujikuroi* represses fumonisins and fusarins, deletion of *velA* in *P. chrysogenum* negatively affects penicillin biosynthesis, and deletion of *veA* in *A. chrysogenum* drastically reduces expression of cephalosporin biosynthesis genes [1, 9]. VelB also plays a role in secondary metabolite production, as loss of *velB* from *A. nidulans* results in a decrease in sterigmatocystin [52]. A shift to dark increases sterigmatocystin production in this deletion strain, but only to light-exposed wild-type levels of sterigmatocystin production [52]. LaeA is a global regulator of secondary metabolism, as loss of *laeA* abolishes overall production of secondary metabolites in numerous *Aspergillus* species [1, 51, 53]. Not surprisingly, over-expression of *laeA* leads to an abundance of penicillin and lovastatin in *A. nidulans* and *A. terreus*, respectively [50, 51]. With the presence of the SAM methyltransferase domain, LaeA has been proposed to affect secondary metabolism by counteracting H3K9 methylation in the sterigmatocystin cluster [1, 53].

FphA is a phytochrome-like receptor that senses and responds to red light, while LreA and LreB constitute the blue-light sensing apparatus [30, 54, 55]. FphA interacts with

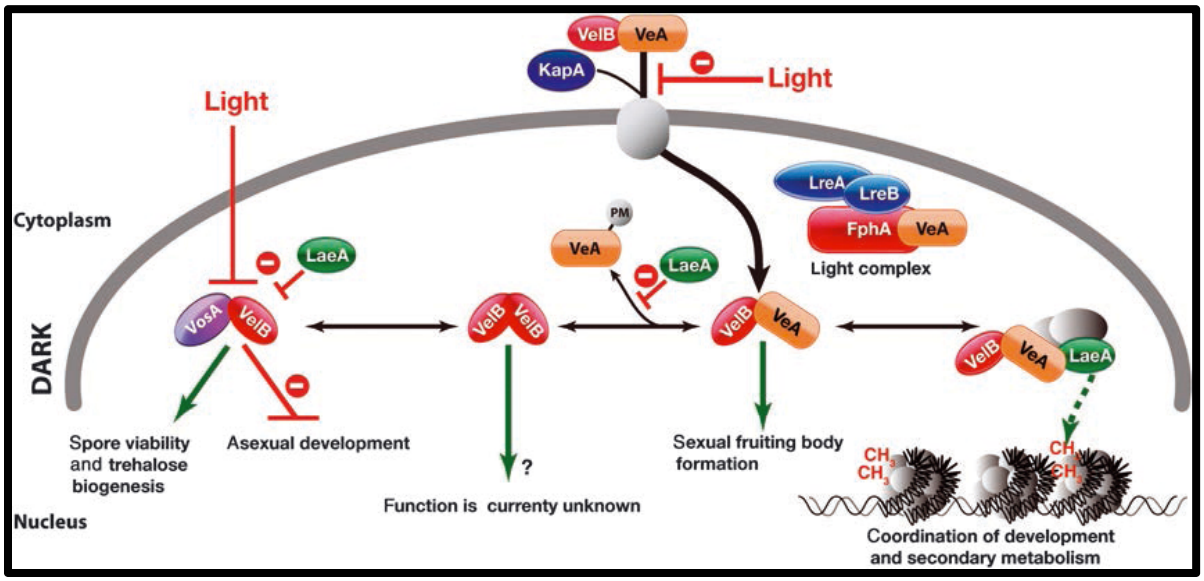


Figure 1.6. Model of light vs. dark regulation of sexual development and secondary metabolism. Reprinted by permission from John Wiley and Sons: FEMS Microgiology Reviews [1], copyright, 2011.

VeA, as well as LreA and LreB [1, 30] (Fig. 1.6). FphA acts to promote asexual development, but represses sterigmatocystin production. Alternatively, LreA and LreB promote sexual development, as well as the production of sterigmatocystin [1, 56]. Interestingly, the opposite effect is seen for penicillin production in *A. nidulans*, as loss of *fphA* reduces penicillin production and mutations in *lreA* and *lreB* cause a slight increase in penicillin production [1, 56].

### 1.4 Regulation of Secondary Metabolism in Response to Environmental Factors

Fungal organisms are extremely versatile with respect to abiotic growth conditions. Fungi can grow in a wide range of conditions and utilize a variety of substrates for nutritional requirements [28]. Global regulatory proteins have been identified that react to specific environmental cues. These proteins generally regulate large sets of genes that are involved in degradation of alternative nutrient sources or protection of intracellular processes against environmental extremes [20, 57]. For instance, to degrade pectin within plant material, fungi synthesize and secrete pectinases; to degrade starch, fungi synthesize and secrete amylases; and to degrade elastin in the human lung, infectious fungi can synthesize and secrete elastase [28]. Interestingly, optimal growth conditions favor lower levels of secondary metabolite production, perhaps to save energy when defense is not necessary. Conversely, nutrient starvation or harsh environmental factors induce production of secondary metabolites. This could be a result of the need to eliminate competition so as to have access to whatever alternative nutrient sources are available. A link has been established between the activity of many of these global regulatory elements and the expression of gene clusters responsible for producing secondary metabolites [3] (Fig. 1.7).

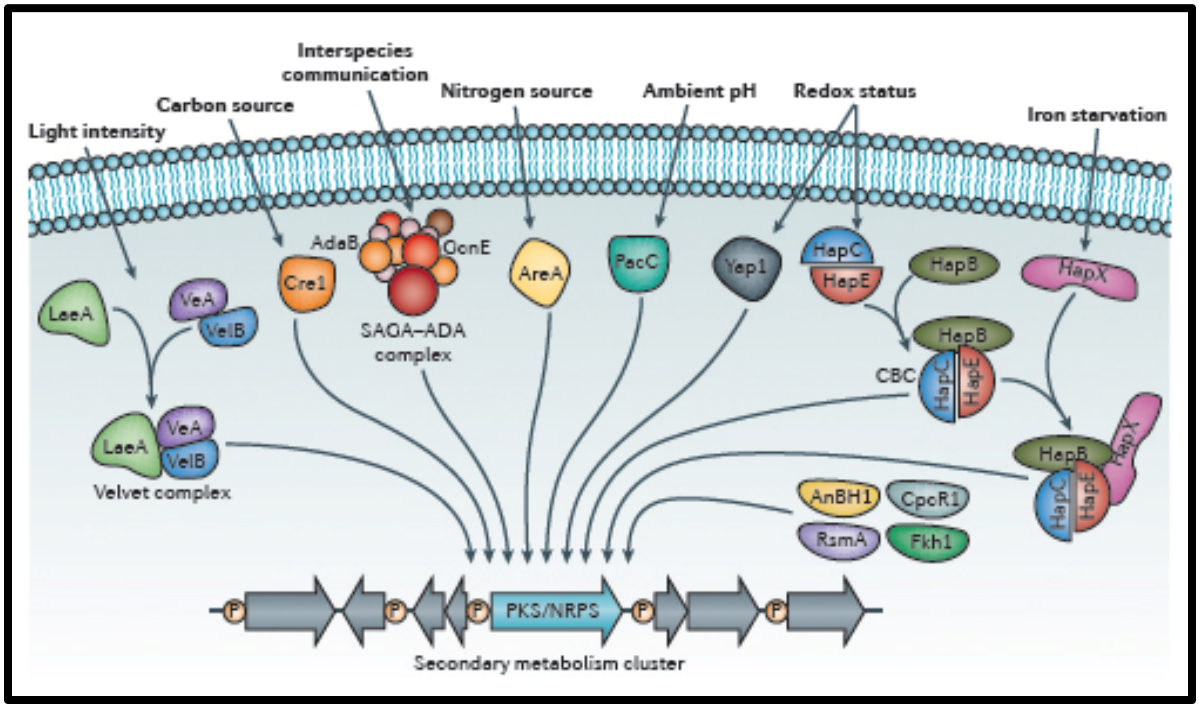


Figure. 1.7. Environmental and developmental global regulatory elements involved in secondary metabolite production. Reprinted by permission from Macmillan Publishers Ltd: Nature Reviews Microbiology [3], copyright 2013.

*1.4.1 Nitrogen Metabolite Repression*

Metabolite repression occurs in response to nitrogen source, which has been studied in great detail. AreA, the global positive regulator of nitrogen metabolite repression in *A. nidulans* and *A. fumigatus*, induces genes involved in alternative nitrogen source utilization [58-60]. In the presence of a preferred nitrogen source, such as ammonium or glutamine, AreA is repressed by various mechanisms, physical interaction with the repressive element NmrA being one of them [58, 60-62]. When preferred nitrogen sources are not available, AreA is released from NmrA to activate its targets, some of which include secondary metabolism clusters, generally in conjunction with pathway-specific transcriptional activators [59-61].

AreA is a member of the GATA family of transcription factors and posesses a DNA binding domain that contains a single $Cys_2/Cys_2$-type zinc finger motif [1, 58-60]. These types of DNA binding proteins are so named because they recognize binding sites that contain a core GATA sequence (e.g. AreA binds to 5'-HGATAR-3') [1, 58-60, 62]. In *A. nidulans*, *areA* is highly expressed in the presence of non-preferred nitrogen sources, yielding three different mRNA transcripts of 3.9, 3.6, and 3.2 kb [60]. There are numerous micro open reading frames (μORFs) and 13 GATA binding elements upstream of the *areA* start site, suggesting that AreA is under transcriptional control (by autoregulation) and post-transcriptional control [60]. Furthermore, the 3' untranslated region (UTR) of *areA* affects mRNA stability and the turnover rate of the *areA* transcript varies based on nitrogen status [63]. In wild-type cells, *areA* mRNA has a half-life of 40 minutes when only non-preferred nitrogen sources are available, but in the presence of preferred nitrogen sources, the half-life decreases to 7 minutes [60]. In contrast, when part of the 3' UTR region is deleted from *areA*, the half-life of the mRNA transcript is 25 minutes, regardless of the nitrogen sources available [60]. Further regulation of AreA is achieved through the binding of NmrA to a

conserved region adjacent to the zinc finger and the 12 carboxyl-terminal residues [60]. Indeed, deletion of *nmrA* from *A. nidulans* results in partial derepression of *amdS*, which encodes acetamidase and is subject to nitrogen metabolite repression [61]. MeaB, a bZIP transcription factor, binds to the promoter of *nmrA* and activates its transcription in both nitrogen-preferred and non-preferred conditions [58].

The nitrate assimilation system has been extensively studied in *A. nidulans* and encodes the structural genes nitrate reductase (*niaD*) and nitrite reductase (*niiA*), *crnA*, a nitrate transporter, and *nirA*, the pathway-specific transcription factor that controls induction of the cluster genes [58, 62, 64-66]. The two structural genes, *niaD* and *niiA*, share an intergenic region and are divergently transcribed, requiring activation from both NirA and AreA [58, 59, 64]. Interestingly, AreA not only binds to GATA elements within the *niaD-niiA* intergenic region to induce nitrate assimilation, but also plays a role in chromatin remodeling [58, 59]. There are six nucleosomes present in the *niaD-niiA* bidirectional promoter when nitrate is absent from surrounding medium. When nitrate becomes available, these nucleosomes are remodeled, which creates an “open” chromatin structure. The chromatin remodeling requires active AreA [58, 59].

As mentioned above, AreA also positively regulates secondary metabolite clusters. For example, in *A. nidulans*, sterigmatocystin production is repressed in the presence of ammonium and induced when nitrate is the sole nitrogen source [1, 5, 67]. Interestingly, nitrogen sources have the opposite effect in *A. parasiticus*, where growth in the presence of ammonium results in higher levels of aflatoxin production [1, 5, 67]. Furthermore, AreA positively regulates gibberellin production in *Gibberella fujikuroi*. In *Fusarium verticillioides*, however, AreA is required for production of fumonisin B1, as an *ΔareA* mutant is devoid of fumonisin $B_1$, even with the addition of ammonium phosphate [3]. This suggests that while

AreA serves as an activator for most gene clusters, there might be alternate roles for AreA with secondary metabolite gene expression.

### *1.4.2 Carbon Catabolite Repression*

Carbon catabolite repression via the global transcriptional repressor, CreA, is present in a wide range of fungal species. When an organism is exposed to a preferred carbon source, such as glucose, CreA acts to repress genes involved in the degradation and utilization of alternative carbon sources, such as ethanol [68, 69]. CreA also exerts repressive effects on secondary metabolism clusters in preferred carbon conditions, as it has been shown that penicillin production in *A. nidulans* is carbon catabolite repressed [10, 68].

CreA, a $C_2H_2$ transcription factor, was first discovered in *A. nidulans* in experiments searching for suppressor mutations for *areA* loss-of-function mutations [68, 69]. There are several nutrients, such as acetamide and proline, which can serve as both nitrogen and carbon sources and are therefore regulated by both CreA and AreA [57, 68]. For example, growth of *A. nidulans* on both preferred nitrogen and carbon sources completely represses proline catabolism. Mutants deficient in *areA* activity are unable to use proline as a nitrogen source when exposed to preferred carbon sources, but a shift to a non-preferred carbon will alleviate this repression and allow proline to be catabolized [57, 68]. CreA generally recognizes the consensus sequence 5'-SYGGRG-3' and appears to be self-regulated, as *creA* mRNA in *A. nidulans* is higher when cultures are grown on glycerol or L-arabinose, compared to growth on glucose [68, 69]. Furthermore, a number of putative CreA binding sites are present within its own promoter [68]. Interestingly, although several loss-of-function mutations have been characterized, *creA* is an essential gene, as deletion of *creA*

in *A. nidulans* is lethal. This suggests that either derepression of certain systems under CreA control is lethal or CreA has an unknown positive function that is essential to the fitness of the organism [68].

The repressive activity of CreA is thought to occur to ensure that the energetically most favorable carbon sources are utilized and to prevent energy waste on the synthesis of alternate catabolic systems. There are three groups of systems that are regulated by carbon catabolite repression: (1) genes encoding enzymes involved in catabolism of less preferred carbon sources, (2) gluconeogenic and glyoxylate cycle enzymes, (3) genes involved in secondary metabolism [69]. Regulation of ethanol metabolism in *A. nidulans* is one of the most extensively studied examples of carbon catabolite repression. CreA affects ethanol catabolism by repressing *alcR*, the transcriptional activator of all genes associated with ethanol catabolism, as well as *alcA*, encoding alcohol dehydrogenase I, and *aldA*, encoding aldehyde dehydrogenase [68]. The binding site of AlcR and CreA overlap in the *alcR* promoter and studies have shown that the two proteins compete for binding. AlcR does not activate ethanol catabolism in the absence of ethanol, but when cultures are grown in both ethanol and glucose, a smooth transition between repression and induction is observed [68]. Upon consumption of the glucose, CreA loses affinity for its binding site in the *alcR* promoter, allowing binding of AlcR and subsequent activation of ethanol catabolism genes [68].

As mentioned above, secondary metabolism is also regulated by CreA and carbon catabolite repression. When *A. chrysogenum* is grown in high glucose concentrations, cephalosporin production is reduced, in part by the repression of *ipnA* and *cefEF* by Cre1 (CreA homologue) [70]. In addition, glucose represses penicillin production in *P. chrysogenum* [10, 70]. Furthermore, penicillin production in *A. nidulans* is subjected to carbon catabolite repression, although this may not be entirely based on CreA activity.

Transcript levels of *ipnA* mRNA, involved in the production of penicillin, are decreased in glucose medium and a loss-of-function mutation in *creA* only slightly depresses *ipnA*. A single CreA binding site is present in the promoter region if *ipnA*, however this binding site was revealed to be nonfunctional in an *ipnA-lacZ* expression analysis [10, 68].

### *1.4.3 pH-mediated Regulation*

The ability to respond to a wide range of pH is advantageous to microbial organisms, as large variations in ambient pH are commonly encountered. Being extremely versatile, *Aspergillus* species have been shown to survive in a pH range of 3.0 to 10.5 [28, 71]. This versatility is in part due to the activity of PacC, a global regulatory protein that responds to ambient pH. In alkaline pH, PacC induces genes primarily expressed in alkaline conditions and represses genes primarily expressed in acidic conditions [1, 72]. Secondary metabolism appears to be regulated by PacC, as pH causes differential expression of a variety of biosynthetic clusters [3, 73].

PacC is a $C_2H_2$ zinc finger transcription factor that is activated in alkaline pH conditions. PacC is translated as an inactive precursor and is only activated after proteolytic cleavage, which requires PalH and PalI, two potential plasma membrane pH sensors, PalB, a signaling protease, PalA, PalC, and PalF [74-76] (Fig. 1.8). Upon translation, the C-terminal domain of PacC interacts with two domains upstream, which creates a “closed” conformation and prevents accessibility of PacC to PalB. When alkaline pH is sensed, possibly by PalH and PalI, PacC shifts to an “open” confirmation, which allows PalB to catalyze the proteolytic cleavage of PacC after residues ~493-500, within a conserved signaling protease box [74-76]. The activity of PalB is assisted by PalA,

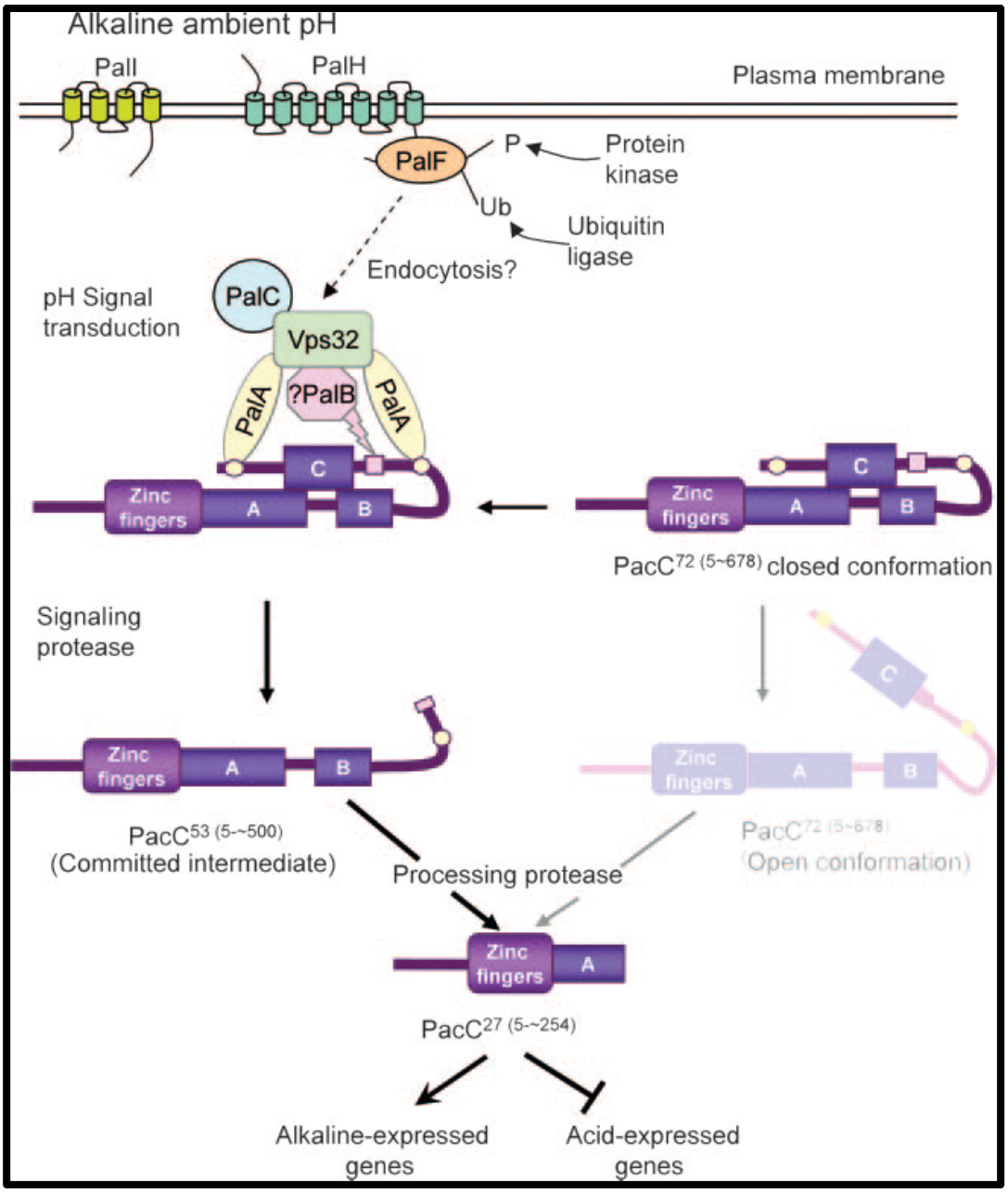


Figure 1.8. Model of the two proteolysis steps required for PacC activation. This process involves PalI, PalH, PalF, PalC, PalA, and PalB. Reprinted by permission from American Society for Microbiology: Eukaryotic Cell [75], copyright 2007.

binding to two YPXL/I motifs on either side of the signaling protease box, PalC and PalF. Loss of this C-terminal region, which is crucial for the "closed" conformation, leaves PacC in an "open" conformation and commits the protein to the second processing step, involving cleavage at residues ~252-254 [74-76]. The first proteolytic cleavage step is regulated by ambient pH, while the second cleavage step is not. In its active form, PacC targets genes through the sequence 5'-GCCARG-3' [74-76].

Early studies of murine intraperitoneal injection with *A. nidulans* revealed an association between alkaline phosphatase production, which is activated by PacC in alkaline pH, and virulence, which could be partially explained by the fact that changes in pH affect secondary metabolism [76]. PacC induces penicillin production in *A. nidulans* in alkaline conditions [1, 3, 5, 70, 73]. In contrast, PacC represses sterigmatocystin production in alkaline conditions, as a mutant expressing a constitutively active PacC protein produces higher levels of penicillin and lower levels of sterigmatocystin [1, 3, 5, 73]. Genes involved in the biosynthesis of ochratoxin A in *A. ochraceus* are down-regulated in alkaline pH, which suggests that PacC is regulating this cluster [20]. Furthermore, fumonisin biosynthesis is negatively regulated by Pac1 (PacC homologue) in *F. verticillioides*, as a disrupted Pac1 mutant produced higher levels of fumonisin when grown on maize kernels [77]. This mutant also produced fumonisin in medium buffered to pH 4.5 or pH 8.4, suggesting that this mutant does not respond to ambient pH [77].

### *1.4.4 Cross-pathway Control Regulation*

Amino acid biosynthesis is vital for metabolic processes in fungi, which is controlled by a global regulatory system referred to as the general control of amino acid biosynthesis (Gcn) in *S. cerevisiae* and as cross-pathway control (Cpc) in filamentous fungi [1, 78, 79].

This global regulation enables a fungal organism to synthesize amino acids in conditions of amino acid starvation.

This regulatory system has been extensively studied in *S. cerevisiae*, with Gcn4 serving as the transcriptional regulator and Gcn2 serving as the protein kinase, which recognizes a build-up of uncharged tRNAs [80]. Gcn4 is a member the bZIP-type family of transcriptional activators, with a leucine-zipper structure important for dimerization and a basic DNA binding domain at the C terminus [79]. Upon induction, Gcn4 binds to the recognition element 5'-ATGASTCAT-3' and activates a variety of gene clusters involved in amino acid biosynthesis, such as the proline biosynthesis cluster and the arginine biosynthesis cluster [79]. Gcn4 has been shown to be under translational control due to the presence of four μORFs in its promoter region. Mutational analysis has revealed that the first and fourth μORFs are sufficient for the translational regulation. In normal conditions, these two μORFs are translated, which prevents reinitiation of the translational machinery at the actual *gcn4* ORF. When cells are starved for amino acids, the translational machinery scans past the fourth μORF and reinitiates at the actual *gcn4* ORF [78-80] (Fig. 1.9). In addition, a negative regulator, Cpc2, reduces Gcn4 activity in nonstarvation conditions, independent of the translational regulation [79].

CpcA, the homologue to Gcn4 in *A. nidulans*, exhibits some of the same attributes as Gcn4. CpcA has a basic leucine-zipper structure in the C-terminal region, but only one leucine, as opposed to Gcn4, which has four repeated leucines [79]. Furthermore, *cpcA* has only two μORFs in its 5' UTR, as opposed to *gcn4*, which has four μORFs, although only two appear to be sufficient for the translational regulation [79]. The 5' UTR of *cpcA* also contains two CpcA/Gcn4 recognition elements, suggesting that *cpcA* is autoregulated

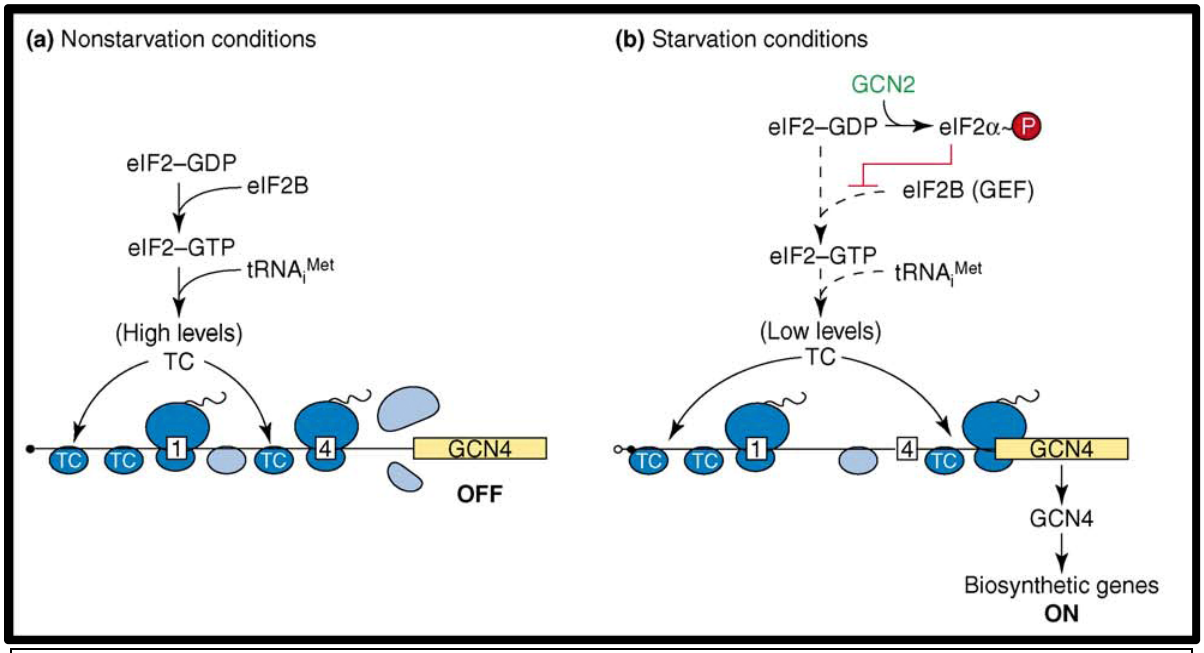


Figure 1.9. Model of post-transcriptional control of *gcn4* involving µORFs 1 and 4. (a) In normal conditions, ribosomal machinery translates µORF 1 and reinitiates at µORF 4, preventing reinitiation and translation at the *gcn4* start site. (b) Under amino acid starvation, ribosomal machinery translates µORF 1, scans past µORF 4 and reinitiates at the *gcn4* start site. Modified and reprinted from Trends in Biochemical Sciences, Vol. 31/No. 10, Alan G. Hinnebusch, eIF3: a versatile scaffold for translation initiation complexes, pg. 553-562, 2006, with permission from Elsevier [81].

at the transcriptional level, in addition to the translational regulation. Indeed, when point mutations were introduced to both μORFs, there was an increase in *cpcA* mRNA and protein levels, but when point mutations were additionally added to the recognition elements, mRNA and protein levels of *cpcA* were drastically reduced [79].

Not much research has been done to explore the effect of CpcA on secondary metabolism, although CpcA does appear to negatively regulate the production of sirodesmin PL in *L. maculans*. Exposure of wild-type *L. maculans* to artificially-induced amino acid starvation did not induce the sirodesmin cluster, as mRNA transcript levels of *sirZ*, the cluster-specific transcription factor, and *sirP*, remained unchanged to those in normal conditions [82]. However, when *cpcA* was silenced, mRNA transcript levels of *sirZ* and *sirP* increased in artificially-induced amino acid starvation. Furthermore, *sirP* mRNA transcript levels in the *cpcA*-silenced mutant were higher than those of the wild-type strain even in normal conditions. Although CpcA does seem to regulate sirodesmin PL biosynthesis, it is unknown whether this regulation is a consequence of CpcA directly binding to promoter regions within the cluster or of an indirect effect of CpcA activity [26, 82]. Furthermore, studies have shown that CpcA negatively regulates penicillin biosynthesis in *A. nidulans*, as over-expression of *cpcA* results in reduced expression of *ipnA* and *acvA*, two genes essential to penicillin biosynthesis [26, 70, 83].

### 1.5 Additional Regulatory Elements of Secondary Metabolism

An additional complex of proteins that regulates secondary metabolism is the HAP-like CCAAT-binding complex (Fig. 1.7). This complex is evolutionarily conserved in eukaryotic organisms and has been designated with various names in different organisms [2, 3, 5, 20]. For instance, this complex is HAP in *S. cerevisiae* and *Arabidopsis thaliana*,

AnCF (formally PENR1) in *Aspergilli*, and CBF in *Xenopus laevis*. Within the AnCF complex are three subunits: HapB, HapC, and HapE [2, 3, 5, 20]. Complete formation of the complex is required for DNA binding and transcriptional regulation. Numerous genes are positively regulated by this complex, including *ipnA* and *aatA*, which are part of the penicillin biosynthetic cluster in *A. nidulans* [2, 3, 5, 20]. Furthermore, penicillin production in a number of fungal species is dependent on the activity of this HAP-like complex [70].

RsmA, a putative YAP-like bZIP protein, was identified in *A. nidulans* in a multicopy suppressor screen for restoration of sterigmatocystin production in mutants lacking members of the velvet complex [84]. Over-expression of AnRsmA partially restores sterigmatocystin production in *ΔlaeA* and *ΔveA* backgrounds and significantly enhances sterigmatocystin production in the presence of an intact velvet complex. Furthermore, mutation of one or both RsmA binding sites, which are present in the AflR-AflJ intergenic region, reduces sterigmatocystin production [84].

### 1.6 *Aspergillus fumigatus*

*A. fumigatus* is a saprophytic ascomycete that is ubiquitous in nature, thanks to the dispersion of conidia in air and by water. Conidia are hydrophobic and are generally between 2 to 3 μm in diameter, giving them buoyancy that aids in dispersion [6]. Any given environment is estimated to contain between 1 and 100 conidia/$m^3$, which results in humans experiencing daily exposure to *A. fumigatus*. Due to the size of conidia, upon inhalation, they can avoid mucociliary clearance and reach the alveoli of the lungs [6]. *A. fumigatus* has the ability to grow in a wide range of temperatures and pH, making it easy for this organism to adapt to various ecological environments. For instance, being a thermophilic organism, *A. fumigatus* can survive in temperatures as high as 70°C [6, 85].

The ability to adapt to harsh environments gives *A. fumigatus* an advantage over other organisms and contributes to the infectious nature of the fungus [85].

*A. fumigatus,* an opportunistic pathogen, is the leading cause of mold infections worldwide that causes severe problems in immune-compromised populations [6, 86]. These populations include: AIDS patients, cancer patients receiving chemotherapy, solid organ transplant/skin graft patients and victims of chronic granulomatous disease [13, 21, 87, 88]. Exposure to conidia can cause invasive aspergillosis or severe allergic reactions [6, 85]. Even with current antifungal medications, the mortality rates of infected individuals can still exceed 50% [21, 22, 32]. Over the past 20 years, hospitals have witnessed an increase in *A. fumigatus* infections, possibly due to an increase in patient transplants, widespread use of immunosuppressive therapies, as well as a higher incidence in HIV or AIDS [89, 90]. Inhalation of conidia through the airways is the primary route of infection for *A. fumigatus*. Once inside the alveoli, spores are exposed to alveolar neutrophils and macrophages, which serve as the first line of defense [6, 89, 90]. In immune-competent individuals, clearance of spores is quick and further invasive disease is not allowed to occur. However, immune dysfunction can result in improper elimination and subsequent germination of the spores [86]. Hyphae of *A. fumigatus* can penetrate tissue, allowing for a more severe or disseminated infection [86]. There are numerous virulence factors produced by this fungus that contribute to its pathogenesis. True virulence factors contribute to the damage the fungus can inflict upon the host, but do not greatly affect growth of the fungus. Among these are secondary metabolites or mycotoxins that can possess carcinogenic or immune-modulating properties [8].

## 1.7 *Aspergillus fumigatus* and Secondary Metabolism

*A. fumigatus* is predicted to contain 30 secondary metabolism clusters, the majority of which have not been characterized [53, 91]. There has been debate on the number of secondary metabolism clusters, which are usually predicted based on the presence of a PKS, NRPS, or the like. In 2007, one group published data defining 22 secondary metabolism clusters in *A. fumigatus*, at least 50% of which were regulated by LaeA [91]. In 2012, another paper was published, which listed 34 PKS and NRPS genes, possibly defining 9 additional secondary metabolism clusters in *A. fumigatus*, based on web-based programs specifically designed to define these clusters through algorithms [53]. Among the secondary metabolites that have been identified are melanin, gliotoxin, fumagillin, fumitremorgen B, pseurotin A, gibberellin, helvolic acid, and aflatoxin [4, 6]. As seen in other organisms, secondary metabolism cluster dispersal in *A. fumigatus* displays a bias towards sub-telomeric regions of the chromosome [12, 91] (Fig. 1.10). Evidence suggests that secondary metabolites produced by *A. fumigatus* contribute to its virulence, which is supported by the fact that loss of *laeA*, a global regulator of secondary metabolite production, severely attenuates the virulence of this fungus in a murine model of infection [24, 53]. One of the most well-studied secondary metabolites produced by *A. fumigatus* is gliotoxin, which is also produced by *Eurotium chevalieri, Gliocladium fimbriatum*, and several other *Aspergillus* species, *Trichoderma* species, and *Penicillium* species [14, 24, 25, 92].

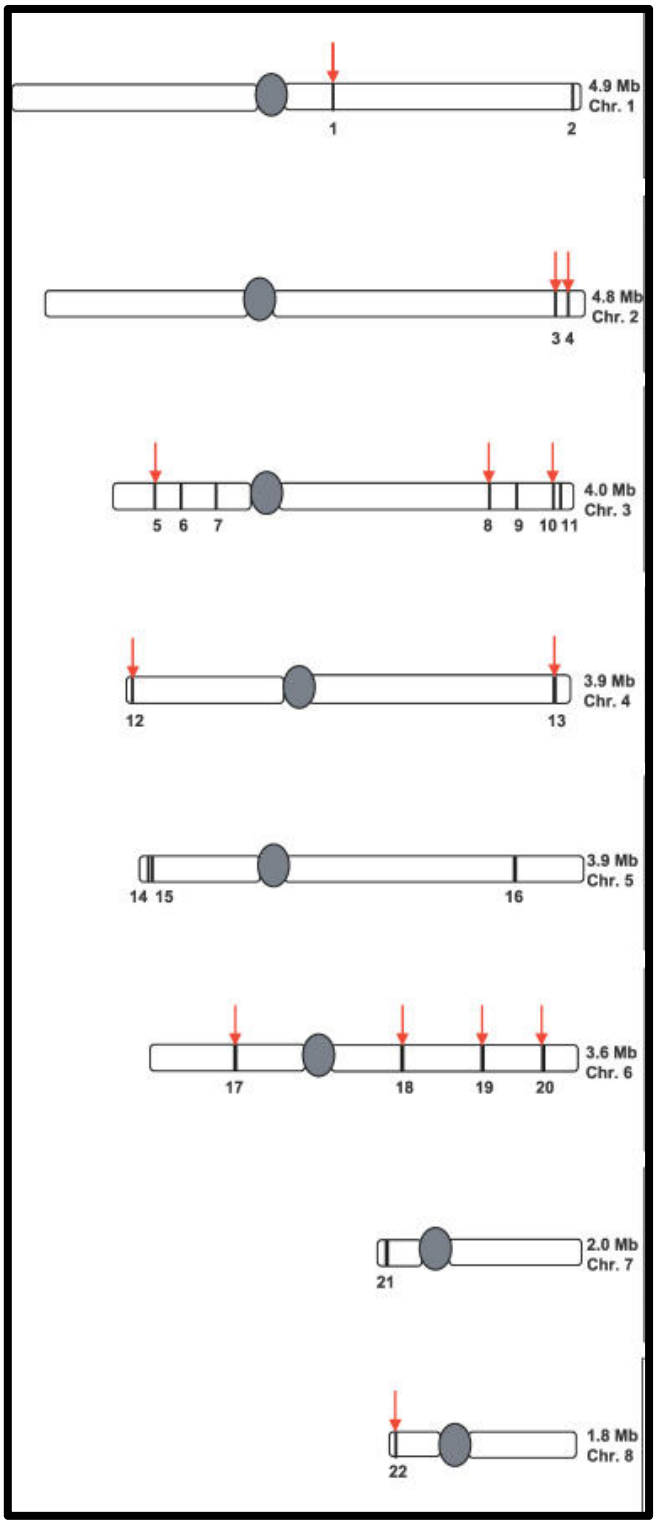


Figure 1.10. Schematic of *A. fumigatus* chromosomes with locations of secondary metabolite gene clusters (indicted as black bars). Red arrows identify clusters that are partially or completely regulated by LaeA [91]. Open-access article.

*1.7.1 Gliotoxin*

Gliotoxin ($C_{13}H_{14}N_2O_4S_2$) is a member of the epipolythiodioxopiperazine (ETP) class of toxins, which are characterized by a disulfide bridge across a dioxopiperazine ring [14, 21-25, 53, 87, 88, 93-95]. The oxidized form of gliotoxin is taken up into host immune cells in a glutathione- dependent fashion, where it is rapidly reduced to the dithiol form [26, 94] (Fig. 1.11). Constant redox cycling causes accumulation of this dithiol form within the target cell, with only a small percentage of gliotoxin existing in the oxidized form at any given time [26, 53]. The oxidized form is thought to be the biologically active form, but some scientists believe the reduced form has activities of its own [92]. Once inside target cells, gliotoxin is able to affect cellular functions essential to the immune response. For instance, gliotoxin has been shown to prevent neutrophils from engulfing surrounding fungal cells by targeting the actin cytoskeleton and can prevent the generation of superoxide anions by targeting the activation of NADPH oxidase [24, 25, 87, 95, 96]. Gliotoxin has recently been shown to inhibit angiogenesis [92, 97]. In addition, gliotoxin is able to inhibit NFkB via prevention of IkB degradation in several cell types [24, 88, 92, 98]. This leads not only to apoptosis, but also a loss of cytokine production, therefore the cell cannot signal to other cells of the immune system about the fungal invasion [24, 88, 94]. Several other actions of gliotoxin result in apoptosis of the host cell, such as the activation of BAK via conformational changes and the production of reactive oxygen species via redox cycling [24, 26, 99]. Being a redox active toxin, gliotoxin can also induce internal disulfide bond formation of cysteine residues in the host cell, which results in inhibition of protease activities. [24, 87, 88, 93-96]. Once the target cell begins the process of apoptosis and glutathione levels are depleted, gliotoxin is converted back to its oxidized form and exits the target cell, after which uptake into surrounding target cells occurs [93]. Gliotoxin has been detected in lungs

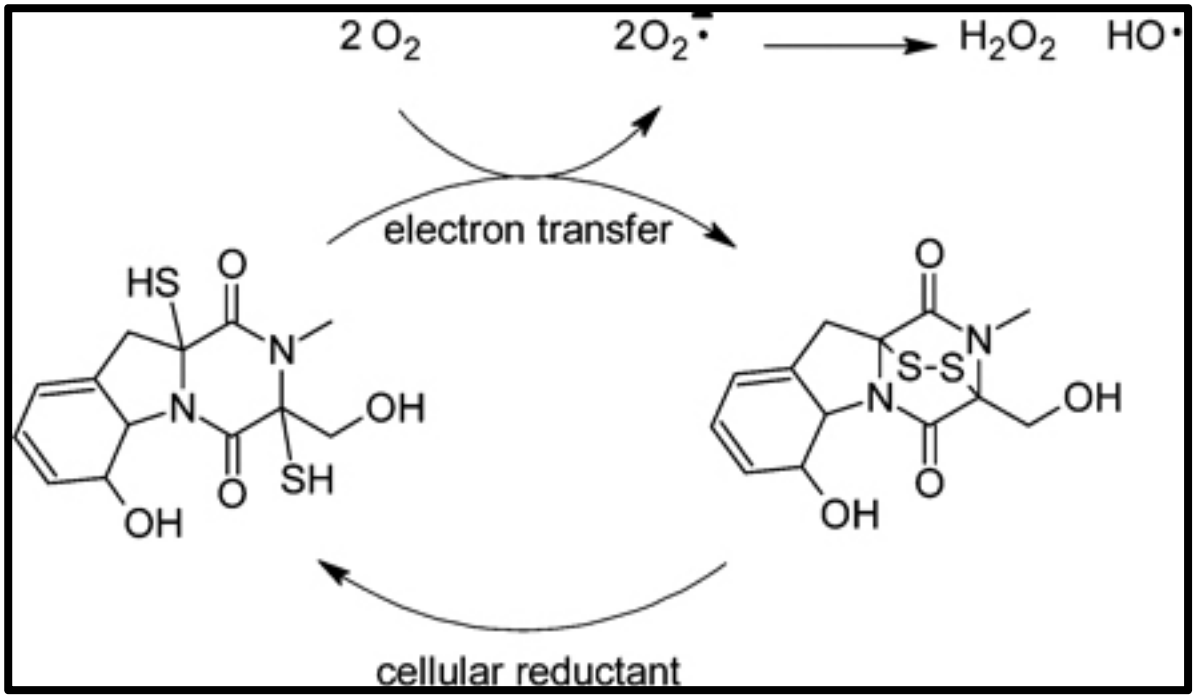


Figure 1.11. Redox cycling of gliotoxin between the oxidized (disulphide) form and the reduced (dithiol) form. This continuous process generates reactive oxygen species. Reprinted with permission of Society for General Microbiology: Microbiology [100], copyright 2005.

and sera of mice and humans suffering from aspergillosis [24, 101]. Furthermore, out of 100 clinical and environmental strains of *A. fumigatus*, more than 96% produced gliotoxin [102].

### *1.7.2 Regulation of Gliotoxin*

As with other secondary metabolites, most of the genes responsible for the production and transport of gliotoxin exist within a gene cluster. The gliotoxin biosynthesis cluster was first identified based on its homology to the sirodesmin PL biosynthesis gene cluster in the ascomycete *L. maculans* [7, 14, 25, 26] (Fig. 1.12). Within this cluster lies a $Zn_2Cys_6$ binuclear finger transcription factor, GliZ, thought to be responsible for general gliotoxin induction and regulation. Indeed, over-expression of *gliZ* leads to an increase in gliotoxin production and deletion of *gliZ* results in loss of gliotoxin production [13, 24, 92]. A DNA binding site has been proposed for GliZ ($TCGGN_3CCGA$), but has not been tested. This site is present within the promoter region of every gene within the gliotoxin cluster, except *gliZ* and *gliA* [15]. Gliotoxin itself positively regulates expression of the genes within the gliotoxin cluster, as deletion of *gliP*, the non-ribosomal peptide synthetase (NRPS) responsible for the first step in the biosynthetic pathway for gliotoxin, virtually eliminates expression of the other genes in the cluster [22, 24, 27]. This loss in gene expression can be reversed by the addition of exogenous gliotoxin to culture medium [22, 24, 27]. Interestingly, *gliT*, encoding an oxidoreductase required for resistance of the fungus to gliotoxin, is induced by exogenous gliotoxin even in the absence of *gliZ* [27]. In addition, FlbA, mentioned above, negatively regulates *gliT* expression, as a *ΔflbA* mutant in *A.*

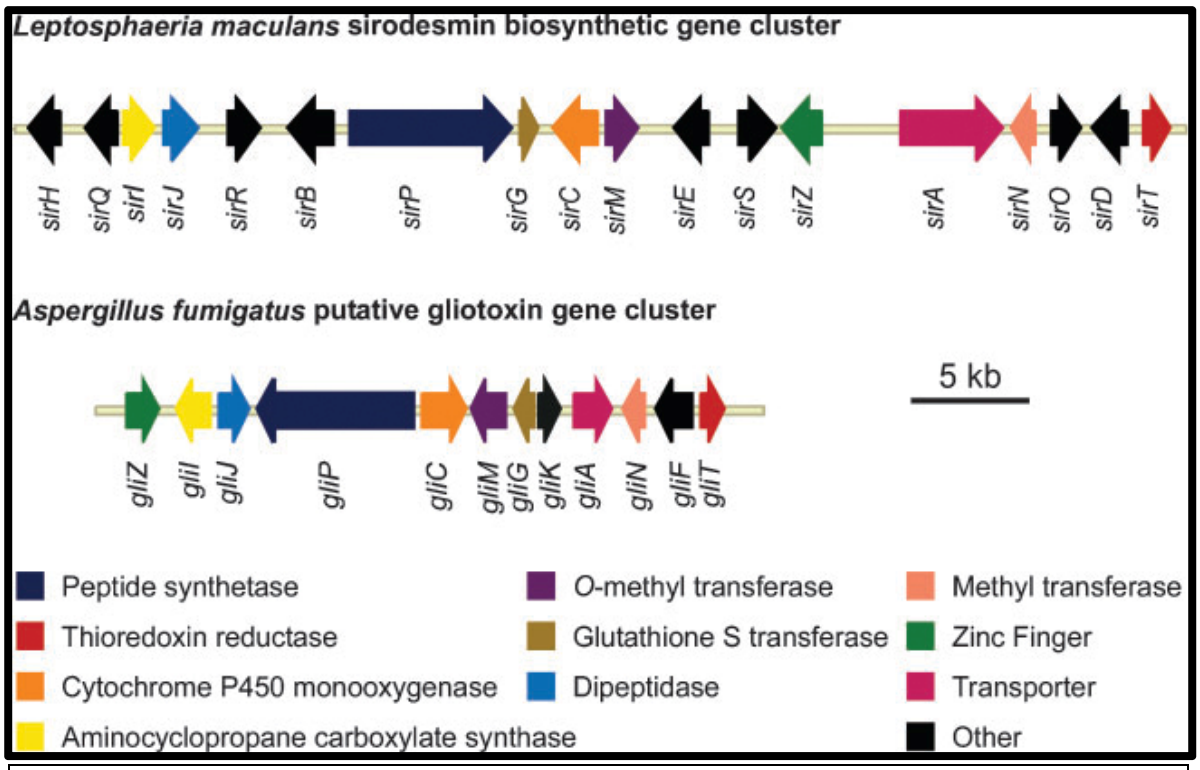


Figure 1.12. Layout of the sirodesmin biosynthetic gene cluster from *L. maculans* and the gliotoxin biosynthetic gene cluster from *A. fumigatus*. Homologues between the two clusters are colored. Reprinted with permission of Society for General Microbiology: Microbiology [100], copyright 2005.

*fumigatus* displays an accumulation of *gliT* mRNA and protein, without affecting *gliZ* expression or overall gliotoxin production [103]. This demonstrates regulation of genes within the cluster that are independent of the coordinate regulation by GliZ.

LaeA, mentioned above, has also been shown to regulate the gliotoxin cluster, as gliotoxin is among the secondary metabolites that are lost with deletion of *laeA* [32, 50, 51]. Furthermore, loss of *vel1* in *T. virens* (homologous to VeA in *Aspergilli*) results in a loss in gliotoxin production [104]. This is not surprising, since VeA, VelB, and LaeA form a heterotrimeric complex that regulates secondary metabolism and sexual development in several fungal species [1, 28, 30, 50, 51]. SfaD and GpgA, encoding the only Gβ subunit and Gγ subunit, respectively, in *A. fumigatus*, are involved in spore germination and vegetative growth. In addition, SfaD and GpgA contribute to gliotoxin production, as loss of either protein reduces gliotoxin synthesis [105]. FlbB, a bZIP transcription factor involved in asexual development, is required for gliotoxin production in liquid submerged cultures, but not in air-exposed solid cultures [106]. Additionally, StuA, involved in asexual development, appears to partially regulate the gliotoxin cluster, as loss in *stuA* results in a down-regulation of several genes within the gliotoxin cluster [107].

RsmA positively regulates the gliotoxin cluster through LaeA and GliZ, as loss of either protein abolishes the inducing effects of RsmA over-expression [108]. Interestingly, over-expression of RsmA is able to partially restore sterigmatocystin production in a *ΔlaeA* background in *A. nidulans*, but this is not the case in *A. fumigatus*. In addition, loss of *rsmA* negatively affects sterigmatocystin production in *A. nidulans*, but has no effect on gliotoxin production in *A. fumigatus* [84, 108]. Map kinase signaling is another element that is important for gliotoxin production, as a strain lacking *mpkA*, the map kinase in the cell wall integrity pathway, is significantly reduced in gliotoxin production [109]. Nutrient starvation,

murine infection, and exposure of germlings to neutrophils have also been shown to up-regulate the gliotoxin biosynthesis cluster through microarray analysis [12, 24].

# Chapter 2:

# Materials and Methods

All primers used in this study are listed in Table 2.1.

## 2.1 Strains and Growth Conditions

All strains used in this study and genotypes are listed in Table 2.2. I maintained Af293.1, Af293.1-GL, 1160, Af293.1-SD1, and Af293.1-SD2 on YAG medium supplemented with uridine and uracil (0.5% yeast extract, 1% glucose, trace elements and vitamin mix as modified [110], 10 mM $MgCl_2$, 1.5% agar, 5 mM uridine, and 10 mM uracil,). I grew Ama.G, Ama.Z, Ama.A, Ama-gliZ.G, Ama-gliZ.Z, Ama-gliZ.A, Ama-gipA.G, Ama-gipA.Z, Ama-gipA.A, Ama-gipB.G, Ama-gipB.Z, and Ama-gipB.A on YAG medium with 400 µg/ml hygromycin. I maintained all other strains on YAG medium. Unless otherwise noted, I grew all strains at 37℃ for 48 hrs. For phenotypic growth assays of high-copy and deletion strains, I inoculated approximately 1000 spores of each strain onto MMVAT (1× MM salts [20 mM ammonium tartrate, 7 mM KCl, 2 mM $MgSO_4 \cdot 7H_2O$], 1% glucose, 12 mM $KPO_4$ pH 6.8, trace elements, vitamin mix as modified [110], and 1.25% agar), MMVAT with 10 µg/ml gliotoxin, and YAG. MMVAT plates were incubated for 72 hours. I repeated plate growth assays twice for a total of three independent tests. I measured radial growth of each colony and scanned plates on the final day of growth. For spore counts, I evenly spread $1x10^{10}$ spores onto YAG medium and incubated plates for 48 hours at 37℃. I collected all spores from the plate with 1x Tween-20 solution and counted total spores with a hemocytometer. I calculated spores/$cm^2$ based on the surface area of the medium.

## 2.2 Genetic Screen

I used fusion PCR (f-PCR) to create a *gliA*$^P$-*lacZ*-*gliA*$^T$ construct. For the first reaction, I created three cassettes: *gliA*$^P$, *lacZ*, and *gliA*$^T$, using primer pairs GliA F1 and GliA 5' R, lacZ F and lacZ R, and GliA 3' F and GliA R, respectively. I obtained these three

| Name | Sequence |
|---|---|
| GliA F1 | 5’-**ggggacaagtttgtacaaaaaagcaggctaa**gatagcaacagtagccaatgt-3’ |
| GliA 5’ R | 5’-cgtaatcatggtcataatggtcgatgtcagtagagagctg-3’ |
| lacZ F | 5’-ctgacatcgaccattatgaccatgattacggattcactgg-3’ |
| lacZ R | 5’-gtttcgaccagatacttatttttgacaccagaccaactgg-3’ |
| GliA 3’ F | 5’-tggtgtcaaaaataagtatctggtcgaaacatgtctgctt-3’ |
| GliA R | 5’-**ggggaccactttgtacaagaaagctgggtc**taagctcgggatggagtgatt-3’ |
| GliZ attB 1 | 5’-**ggggacaagtttgtacaaaaaagcaggctgc**gaccgcagctgattggag-3’ |
| GliZ attB 2 | 5’-**ggggaccactttgtacaagaaagctgggtc**gattccctttgtgccgcc-3’ |
| AMA-NotI F | 5’-aaataagcttgcatgcgc-3’ |
| AMA-NotI R | 5’-gccagtgaattcgagctc-3’ |
| 6g01910 F | 5’-**ggggacaagtttgtacaaaaaagcaggctg**cgggtttggtttggttgttgtgctt-3’ |
| 6g01910 R | 5’-**ggggaccactttgtacaagaaagctgggtc**gagggcgtggtgaacgttc-3’ |
| 4g00320 F | 5’-**ggggacaagtttgtacaaaaaagcaggctg**ccagcagaccattctcgtttgcattc-3’ |
| 4g00320 R | 5’-**ggggaccactttgtacaagaaagctgggtc**ttcgaggaacctgggttgcg-3’ |
| M13F | 5’-cgccagggttttcccagtcacgacg-3’ |
| M13R | 5’-ggaaacagctatgaccatga-3’ |
| 01910 5’ F | 5’-**ggggacaactttgtatagaaaagttgaa**GCGGCCGCgcttacttacagtacggagtacgg-3’ |
| 01910 5’ R | 5’-**ggggactgcttttttgtacaaacttgc**gcccggcggaggaat-3’ |
| 01910 3’ F | 5’-**ggggacagctttcttgtacaaagtggaa**tccgttttctacgagcattgttctc-3’ |
| 01910 3’ R | 5’-**ggggacaactttgtataataaagttgc**ttcatggtgccgtgctcg-3’ |
| gipA 3kb F | 5’-**ggggacaagtttgtacaaaaaagcaggctgc**accccgtttttgtggttgcgc-3’ |
| gliZ 5’ F | 5’-**ggggacaactttgtatagaaaagttgaa**GCGGCCGCgggagtcgagagatgcatgaa-3’ |
| gliZ 5’ R | 5’-**ggggactgcttttttgtacaaacttgc**tgtggatgtcggggacga-3’ |
| gliZ 3’ F | 5’-**ggggacagctttcttgtacaaagtggaa**gctgttctcacctctttttttttttt-3’ |
| gliZ 3’ R | 5’-**ggggacaactttgtataataaagttgc**cgagctcgtcgaccagta-3’ |
| gipA C2H2 F | 5’-**ggggacaagtttgtacaaaaaagcaggctgc**cagcaaatgtacggcgggca-3’ |
| gipA C2H2 R | 5’-**ggggaccactttgtacaagaaagctgggtc**tcagctgtgcccattggtatcaacg-3’ |
| SDMut1 F | 5’-gacttaacggagactctgccgccacgccgaatcacagcgg-3’ |
| SDMut1 R | 5’-ccgctgtgattcggcgtggcggcagagtctccgttaagtc-3’ |
| SDMut2 F | 5’-gacttaacggagactttgggtgagcgccgaatcacagcgg-3’ |
| SDMut2 R | 5’-ccgctgtgattcggcgctcacccaaagtctccgttaagtc-3’ |

Table 2.1. Oligonucleotides used throughout this study. Bolded regions are *att* sites. Underlined regions are extensions for fusion PCR. Uppercase regions are NotI sites.

| Strain | Genotype | Origin |
|---|---|---|
| Af293 | Wild type | FGSC |
| Af293.1 | pyrG1 | This Lab[111] |
| Af293.1-GL | pyrG1; pDHGL | This Study |
| AMA.GL | pyrG1; pDHGL; pDONR AMA | This Study |
| AMA-gliZ.GL | pyrG1; pDHGL; pDONR AMA-gliZ | This Study |
| AMA-gipA.GL | pyrG1; pDHGL; pDONR AMA-gipA | This Study |
| AMA-gipB.GL | pyrG1; pDHGL; pDONR AMA-gipB | This Study |
| 1160 | pyrG1; nkuB::AfpyrG; pyrG::5FOA | FGSC[112] |
| 1160G | pyrG1; nkuB::AfpyrG; pyrG::5FOA; pDONR G | This Lab |
| *ΔgliZ* | pyrG1; nkuB::AfpyrG; pyrG::5FOA; pDHGL; gliZ::pyrG | This Study |
| *ΔgipA* | pyrG1; nkuB::AfpyrG; pyrG::5FOA; gipA::pyrG | This Study |
| *gipA*(R) | pyrG1; nkuB::AfpyrG; pyrG::5FOA; gipA::pyrG; pDONR HPH-gipA | This Study |
| *ΔgipB* | pyrG1; nkuB::AfpyrG; pyrG::5FOA; gipB::pyrG | This Study |
| *gipB*(R) | pyrG1; nkuB::AfpyrG; pyrG::5FOA; gipB::pyrG; pDONR HPH-gipB | This Study |
| *ΔgipA.0* | pyrG1; nkuB::AfpyrG; pyrG::5FOA; gipA::pyrG; pyrG::5FOA | This Study |
| *ΔgliZ/ΔgipA* | pyrG1; nkuB::AfpyrG; pyrG::5FOA; gipA::pyrG; pyrG::5FOA; gliZ::pyrG | This Study |
| *ΔgipB.0* | pyrG1; nkuB::AfpyrG; pyrG::5FOA; gipB::pyrG; pyrG::5FOA | This Study |
| *ΔgipA/ΔgipB* | pyrG1; nkuB::AfpyrG; pyrG::5FOA; gipB::pyrG; pyrG::5FOA; gipA::pyrG | This Study |
| Af293.1-SD1 | pyrG1; pDHSD1 | This Study |
| Af293.1-SD2 | pyrG1; pDHSD2 | This Study |
| Af293.1-SD3 | pyrG1; pDHSD3 | This Study |
| AMA.SD1 | pyrG1; pDHSD1; pDONR AMA | This Study |
| AMA-gliZ.SD1 | pyrG1; pDHSD1; pDONR AMA-gliZ | This Study |
| AMA-gipA.SD1 | pyrG1; pDHSD1; pDONR AMA-gipA | This Study |
| AMA.SD2 | pyrG1; pDHSD2; pDONR AMA | This Study |
| AMA-gliZ.SD2 | pyrG1; pDHSD2; pDONR AMA-gliZ | This Study |
| AMA-gipA.SD2 | pyrG1; pDHSD2; pDONR AMA-gipA | This Study |
| pyrG+ | pyrG1; AnpyrG | This Study |
| ΔgliZ.1 | pyrG1; gliZ::pyrG | This Study |
| ΔgipA.1 | pyrG1; gipA::pyrG | This Study |
| AMA.G | pyrG1; pyrG; pDONR AMA/HPH | This Study |
| AMA-gliZ.G | pyrG1; pyrG; pDONR AMA/HPH-gliZ | This Study |
| AMA-gipA.G | pyrG1; pyrG; pDONR AMA/HPH-gipA | This Study |
| AMA-gipB.G | pyrG1; pyrG; pDONR AMA/HPH-gipB | This Study |
| AMA.Z | pyrG1; gliZ::pyrG; pDONR AMA/HPH | This Study |
| AMA-gliZ.Z | pyrG1; gliZ::pyrG; pDONR AMA/HPH-gliZ | This Study |
| AMA-gipA.Z | pyrG1; gliZ::pyrG; pDONR AMA/HPH-gipA | This Study |
| AMA-gipB.Z | pyrG1; gliZ::pyrG; pDONR AMA/HPH-gipB | This Study |
| AMA.A | pyrG1; gipA::pyrG; pDONR AMA/HPH | This Study |
| AMA-gliZ.A | pyrG1; gipA::pyrG; pDONR AMA/HPH-gliZ | This Study |
| AMA-gipA.A | pyrG1; gipA::pyrG; pDONR AMA/HPH-gipA | This Study |
| AMA-gipB.A | pyrG1; gipA::pyrG; pDONR AMA/HPH-gipB | This Study |

Table 2.2. Genotype of all strains used in this study.

fragments by PCR using e2TAK DNA polymerase (Takara Bio Inc., Otsu, Shiga, Japan), following manufacturer recommendations. The *gliA*$^{P}$ fragment had a 3' extension identical to the first 15 base pairs of *lacZ*. The *lacZ* fragment had a 5' extension identical to the last 15 base pairs of *gliA*$^{P}$ and a 3' extension identical to the first 15 base pairs of *gliA*$^{T}$. The *gliA*$^{T}$ fragment had a 5' extension identical to the last 15 base pairs of *lacZ*. I used Af293 genomic DNA as template for the *gliA*$^{P}$ and *gliA*$^{T}$ regions and λGT11 as template for *lacZ*. For the second reaction, I fused the three fragments together using GliA F1 and GliA R as primers. I amplified a 50 µl reaction containing 50 fmol of each fragment, 0.3 µM of each primer, 500 µM of deoxynucleoside triphosphates, buffer 3 at a 1X concentration, and 1 µl of Expand Long DNA Template Mix (Roche Applied Science, Indianapolis, IN) per manufacturer's instructions (briefly, 94°C for 2 min, 10 cycles of 94°C for 10 sec, 62°C for 30 sec, 68°C for 4.5 min and 15 cycles of 94°C for 15 sec, 62°C for 30 sec, 68°C for 4.5 min, increasing the final extension time by 20 sec with each cycle).

I cloned the fusion product into pDONR HPH A using a BP recombination reaction (Invitrogen, Grand Island, NY). I transformed the reaction mix into TOP10 cells (Invitrogen, Grand Island, NY) by electroporation, as recommended by the manufacturer. I grew the transformation mix on LB (1% Tryptone, 0.5% yeast extract, 1X SOB salts [10mM NaCl, 2.5mM KCl], 1.5% agar) + 50 µg/ml kanamycin at 37ºC overnight. I picked colonies and transferred to 2 ml of LB liquid + 50 µg/ml kanamycin to grow overnight in a 37ºC shaking incubator. I isolated plasmid DNA from each culture using a miniprep kit (Qiagen, Hilden, Germany). I digested plasmid DNA with specific enzymes to verify the correct insertion. I designated this vector as pDHGL.

I grew Af293.1 in MAG medium (2% malt extract, 0.2% peptone, 1% glucose, trace elements and vitamin mix as modified [110]) supplemented with 5 mM uridine and 10 mM uracil. I performed the transformation as previously described [113], keeping pDHGL as a

circular vector. I grew transformants on MMVAT supplemented with 5 mM uridine, 10 mM uracil, 0.2 M sucrose, and 400 µg/ml hygromycin at 37ºC for 3-5 days. I identified the presence of pDHGL by Southern hybridization [114] of the *lacZ* coding region (Fig. 2.1a). I also streaked transformants onto MMVSN supplemented with uridine and uracil (as described above for MMVAT, except 1xMM salts contain 20mM sodium nitrate instead of ammonium tartrate) and 40 µg/ml X-gal to grow at 37ºC for 2 days. I screened for transformants that grew in the presence of hygromycin and developed a blue pigment on 5-bromo-4-chloro-3-indolyl-β-D-galactopyranoside (X-gal), signaling that *lacZ* expression was working properly (Fig. 2.1b). I designated this strain as Af293.1-GL.

For the first round of the high-copy inducer screen, I grew Af293.1-GL in MAG supplemented with uridine and uracil. I transformed the AMA1-Not1 *A. fumigatus* genomic library [115] into Af293.1-GL as described previously [113], but with changes. I combined each transformation mix with 50 ml CM top agar (MMVAT, as described above, 0.1% yeast extract, 0.2% peptone, 0.1% tryptone, 1% CM supplement [27 mM adenine HCl, 33.5 mM methionine, 173 mM arginine, and 1.3 mM riboflavin], and 1% agar) supplemented with 1 M sucrose and spread the mixture over 10 plates (5 ml/plate). I grew transformants on CM supplemented with 0.2 M sucrose and 40 µg/ml X-gal at 37ºC for 3-5 days. I screened for transformants that were both prototrophic for uridine and uracil and producing blue pigment. I prepared genomic DNA from transformants [51] and transformed 1 µl of genomic DNA into TOP10 cells (Invitrogen, Grand Island, NY) by electroporation, as recommended by the manufacturer. I grew the transformation mix on LB + 100 µg/ml ampicillin at 37ºC overnight. I picked colonies and transferred to 2 ml of LB liquid + 100 µg/ml ampicillin to grow overnight in a 37ºC shaking incubator. I isolated plasmid DNA from each culture using a miniprep kit (Qiagen, Hilden, Germany) and digested it with KpnI to identify individual plasmids.

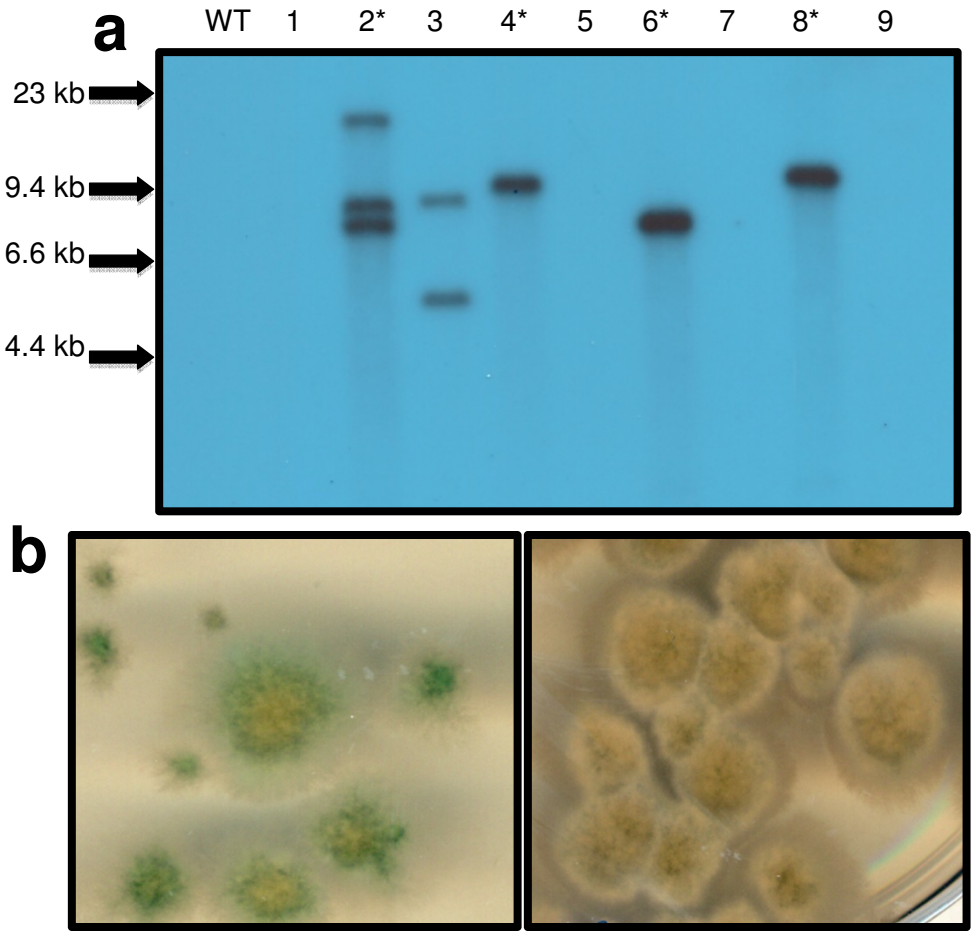


Figure 2.1. Presence and activity of *lacZ* expression cassette in Af293.1-GL transformants. (a) Southern hybridization of Af293.1-GL transformants. Genomic DNA was digested with EcoRI overnight at 37°C then run on a 0.8% agarose gel. The *lacZ* coding region was used as the probe. WT is wild-type (Af293.1) and is expected to have no band. Proper transformants should only have one band of unknown size. Lanes with asterisks are transformants that produced blue pigment when grown on MMVSN U/U (non-repressing) medium with X-gal. (b) Example of blue pigment production in Af293.1-GL transformants. The left panel shows activation of the *lacZ* expression cassette, while the right panel displays colonies that are not induced for *lacZ* expression.

For the second round of the high-copy inducer screen, I grew Af293.1-GL in MAG supplemented with uridine and uracil. I transformed each individual plasmid isolated from the first round of the genetic screen as described above, but with the following changes. I plated two amounts of protoplasts (20 µl and 100 µl) each in 4 ml MMVAT top agar (as described above but with 1% agar) supplemented with 1 M sucrose. I grew transformants on MMVAT supplemented with 0.2 M sucrose and 40 µg/ml X-gal at 37℃ for 3-4 days and put plates in the 4℃ refrigerator to facilitate blue pigment production. Plasmids causing at least 80% of colonies to turn blue were sequenced using primers AMA-NotI F and AMA-NotI R. I also grew transformants in 10 ml CM at 37℃ stationary overnight. I collected mycelia, froze in liquid nitrogen, and lyophilized overnight. I collected total protein and performed β-galactosidase assays to measure LacZ levels quantitatively (detailed below).

For the third round of the high-copy inducer screen, I PCR amplified individual genes from genomic library plasmids, flanked by native 5' and 3' non-coding regions (NCRs). For *gipA* (Afu6g01910) and *gipB* (Afu4g00320) I used the primer pair 6g01910 F and 6g01910 R and the primer pair 4g00320 F and 4g00320 R, respectively. I amplified the fragments from Af293 genomic DNA using e2TAK DNA polymerase (Takara Bio Inc., Otsu, Shiga, Japan) and following manufacturer recommendations. I cloned the PCR fragments into pDONR AMA with a BP recombination reaction (Invitrogen, Grand Island, NY). I transformed the reaction mix into TOP10 cells (Invitrogen, Grand Island, NY) by electroporation, as recommended by the manufacturer. I grew the transformation mix on LB + 100 µg/ml ampicillin at 37ºC overnight. I picked colonies and transferred to 2 ml of LB liquid + 100 µg/ml ampicillin to grow overnight in a 37ºC shaking incubator. I isolated plasmid DNA from each culture using a miniprep kit (Qiagen, Hilden, Germany). I digested plasmid DNA with specific enzymes to verify the correct insertion. I designated these vectors as pDONR AMA-*gipA* and pDONR AMA-*gipB*. I created a control vector, pDONR

AMA-*gliZ*, which contained the *gliZ* coding region flanked by promoter and terminator regions. I generated this vector as described above for pDONR AMA-*gipA* and pDONR AMA-*gipB* using primers GliZ attB 1 and GliZ attB 2.

I grew Af293.1GL in MAG medium, supplemented with uridine and uracil. I performed the transformation as previously described [113], with changes, using pDONR AMA, pDONR AMA-gliZ as controls. After the 3 hour incubation of protoplasts, I carried out all reactions at half the specified volume. I used 500 ng – 750 ng of circular vector DNA for each reaction. I plated two amounts of protoplasts (20 µl and 50 µl) each in 4 ml of MMVAT top agar supplemented with 1 M sucrose. I grew transformants on MMVAT medium supplemented with 0.2 M sucrose at 37ºC for 2-3 days. To measure LacZ levels quantitatively, I grew transformants in 10 ml CM at 37°C stationary overnight. I collected mycelia, froze in liquid nitrogen, and lyophilized overnight. I collected total protein and performed β-galactosidase assays (detailed below). I chose three strains to use for future analysis: AMA.GL, AMA-gliZ.GL, and AMA-gipA.GL.

**2.3 λ Phage Library Screen**

I isolated *gipA* and *gipB* cDNA clones from a λ phage library constructed with the UniZAP vector and poly(A)+ mRNA, as described by the manufacturer (Stratagene, La Jolla, California). I performed a primary screen of the λ phage library as recommended by manufacturer (Stratagene, La Jolla, California), with changes. I plated 6 plates (150 mm) for primary screening with host strain LE392 (Stratagene, La Jolla, California) and the λ phage library at 40,000 plaque-forming-units (pfu)/plate (3 plates) and 60,000 pfu/plate (3 plates). I lifted plaques with nylon membranes and crosslinked the DNA to the membranes by baking for 2 hours in an oven. I prehybridized and hybridized membranes at 42°C for 6

hours and overnight, respectively. I used *gipA* and *gipB* genomic DNA PCR products for probes [114]. I excised plugs containing positive plaques and placed them in SM (.1 M NaCl, 10 mM $MgSO_4 \cdot 7H_2O$, 50 mM Tris·HCl [pH 7.5], and .01% gelatin) at 4℃ overnight. After determining pfu concentration of plaques, I performed a secondary screen, as performed for the primary screen, with changes. I combined 500-1000 pfu with LE392 and spread over 8 plates (100 mm). I hybridized membranes using *gipA* and *gipB* genomic DNA as probes [114]. I plated excised phagemids as recommended by manufacturer (Stratagene, La Jolla, California) and plated on LB + 100 µg/ml ampicillin to grow at 37℃ overnight. I PCR amplified cDNA from excised phagemids using e2TAK DNA polymerase (Takara Bio Inc., Otsu, Shiga, Japan) and following manufacturer recommendations. I used M13 F and M13 R as primers for the reaction. Based on the PCR band sizes, I picked colonies from selected plates and transferred to 2 ml of LB liquid + 100 µg/ml ampicillin to grow overnight in a 37ºC shaking incubator. I isolated plasmid DNA from each culture using a miniprep kit (Qiagen, Hilden, Germany) and sequenced the cDNA insert using M13 F and M13 R primers. I used DNASTAR software (DNASTAR Inc., Madison, WI) to assemble and analyze the sequences obtained from the library screen.

**2.4 RNA Dot Blot Analysis**

For all dot blot assays, I grew stationary cultures in 25 ml CM (repressing) (described above) or CD (non-repressing) (87.6 mM sucrose, 35.3 mM $Na_2NO_3$, 5.8 mM $K_2HPO_4$, 2 mM $MgSO_4 \cdot 7H_2O$, 6.7 mM KCl, and 0.025 mM $(NH_4)_2Fe(SO_4)_2 \cdot 6H_2O$) at a concentration of $5x10^6$ spores/ml at 37ºC for 48 hours. I included 400 µg/ml hygromycin in dot blot assays involving Ama.G, Ama.Z, Ama.A, Ama-gliZ.G, Ama-gliZ.Z, Ama-gliZ.A, Ama-gipA.G, Ama-gipA.Z, Ama-gipA.A, Ama-gipB.G, Ama-gipB.Z, and Ama-gipB.A. I

prepared total RNA from freeze-dried mycelia using the TRIzol method [110]. I incubated total RNA with denaturing solution (50% formamide, 16% formaldehyde, 1X borate buffer [20X borate buffer: 0.4 M Boric Acid, 4 mM EDTA, pH 8.3 with NaOH], 0.025% bromophenol blue) for 10 minutes at 65°C. I quenched samples on ice for 10 minutes, then added equal volume 20x SSC (3 M NaCl, 0.3 M $C_6H_5O_7Na_3$ •$2H_2O$, pH 7.0). I placed a nylon membrane that had been equilibrated in 10x SSC for 10 minutes into a 96-well dot blot apparatus attached to a vacuum manifold. I collected samples, each containing 3 µg of RNA unless otherwise noted, in 100 µl volumes by aspiration. I aspirated 50 µl of 10x SSC through the membrane in duplicate immediately before and after samples were collected. Once all samples were aspirated, I air dried nylon membranes overnight and then baked them in an oven for 2 hours. For prehybridization and hybridization, I sealed nylon membranes in a bag using a heated sealer. I prehybridized membranes for 4-6 hours at 42°C and hybridized membranes overnight at 42°C. For DNA probes, I only used the coding region of each gene of interest (*gliA, gliP, gliZ, gliT, gipA, gipB*, actin). I used different combinations of these probes in different experiments, which is noted in the figure legends. After hybridization, I washed membranes as I would for Southern hybridization [114] and exposed them to a Typhoon 8600 PhosphorImager (GE Healthcare Life Sciences, Pittsburgh, PA) overnight. I quantified the intensity of hybridization using ImageQuant5.1 software (GE Healthcare Life Sciences, Pittsburgh, PA).

**2.5 Gliotoxin Extraction and HPLC Analysis**

I extracted spent culture medium from RNA dot blot assays in 15 ml chloroform for 30 minutes at room temperature on an orbital shaker set to 250 rpm. I transferred the chloroform phase to a 50 ml conical tube (BD Biosciences, San Jose, California) and

repeated the extraction twice for a total of 45 ml chloroform. I dried open tubes under a hood until the chloroform was completely evaporated. I added 15 ml chloroform to each tube and mixed, to concentrate the extracted material at the bottom. I dried open tubes under a hood until chloroform was completely evaporated. I added 1 ml methanol to each tube and mixed to dissolve all methanol-soluble substances and transferred extracts to microcentrifuge tubes (Fisher Scientific, Pittsburgh, PA). I dried open tubes under a hood until all methanol was completely evaporated.

I dissolved extracts in 50 µl of dimethyl sulfoxide (DMSO), spun tubes to pellet insoluble debris, and transferred DMSO to fresh microcentrifuge tubes. I quantified gliotoxin levels by running samples through a reverse-phase high performance liquid chromatography (RP-HPLC) system with a Waters 996 photodiode array detector (Waters, Milford, MA). I ran samples through a Sonoma 2.1 x 250 mm C18 column (100 Å pore size) packed with 5 µM particles (VWR, Radnor, PA). The mobile phase consisted of $H_2O$, 0.1% TFA (solution A) and 100% Acetonitrile, 0.1% TFA (solution B): 10% B up to 80% B over 30 minutes. The injection volume was 10 µl and flow rate was set at 0.4 ml/min. Gliotoxin eluted from the column at 14.7 minutes and absorbance was read at 268 nm wavelength. I determined gliotoxin concentrations by interpolation from a 9 point standard curve (39 ng to 10 µg) prepared using purified gliotoxin (Sigma-Aldrich Corp., St. Louis, MO).

**2.6 Microarray**

The DNA amplicon microarray for Af293 was created previously [116]. I grew AMA.GL and AMA-gipA.GL in 25 ml CM (described above) at 37℃ for 24 hours in stationary cultures. The spore concentration was $5x10^6$ spores/ml. I used two independent biological replicates for AMA.GL and AMA-gipA.GL growth assays. I prepared total RNA

from freeze-dried mycelia using the TRIzol method [110]. I carried out RNA labeling reactions and hybridizations as described in the J. Craig Venter Institute Microarray Protocols (http://pfgrc.jcvi.org/index.php/microarray/protocols.html). I repeated all the hybridizations in dye-swap sets. I scanned and analyzed hybridized slides as described previously [116]. I averaged all replicates for the official data used in our analysis.

### 2.7 Virulence Assays with Toll-deficient *Drosophila melanogaster*

I injected the dorsal side of the thorax of $CO_2$-anesthetized, adult, Toll-deficient *D. melanogaster* flies with a sterile 0.25 mm needle that had been dipped in a solution containing $10^7$ spores/ml of *A. fumigatus* conidia. I infected 20-25 flies per strain for each virulence assay, which was repeated at least twice. Flies were kept in a 29℃ incubator to maximize susceptibility to microbial challenge and monitored for 7 days. Flies that died within 3 hours of the injection were not included in the survival graph, as these flies most likely died as a result of the puncture wound.

### 2.8 Deletion and Complementation of *gipA* and *gipB* in Af1160

I amplified the 5' flanking region (FR) and the 3' FR from *gipA* using primers 01910 5' F, 01910 5' R, 01910 3' F, and 01910 3' R and *gipB* using primers 00320 5' F, 00320 5' R, 00320 3' F, and 00320 3' R. I engineered a unique NotI site into 01910 5' F and 00320 5' F to linearize the final deletion constructs. I amplified the fragments from Af293 genomic DNA using e2TAK DNA polymerase (Takara Bio Inc., Otsu, Shiga, Japan) and following manufacturer recommendations. I cloned the *gipA* 5' FR and *gipB* 5' FR into pDONR P4-P1R and I cloned the *gipA* 3' FR and *gipB* 3' FR into pDONR P2R-P3, using BP

recombination reactions (Invitrogen, Grand Island, NY). I transformed BP reaction mixes into TOP10 cells (Invitrogen, Grand Island, NY) by electroporation, as recommended by the manufacturer. I grew transformed cells on LB (described above) + 50 µg/ml kanamycin at 37ºC overnight. I picked colonies and transferred to 2 ml LB liquid + 50 µg/ml kanamycin to grow overnight in a 37ºC shaking incubator. I isolated plasmid DNA from each culture using a miniprep kit (Qiagen, Hilden, Germany). I digested plasmid DNA with specific enzymes to verify the correct fragment orientation.

To create the deletion constructs, I combined pDONR P4-P1R-*gipA* 5' FR, pDONR P2R-P3-*gipA* 3' FR, and pDONR 221-*AnpyrG* for the *gipA* construct and pDONR P4-P1R-*gipB* 5' FR, pDONR P2R-P3-*gipB* 3' FR, and pDONR 221-*AnpyrG* for the *gipB* construct in two LR recombination reactions with pDEST R4-R3 as the destination vector (Invitrogen, Grand Island, NY) [117]. I transformed the LR reaction mixes into TOP10 cells (Invitrogen, Grand Island, NY) by electroporation, as recommended by the manufacturer. I grew transformed cells on LB + 100 µg/ml ampicillin at 37ºC overnight. I picked colonies and transferred to 2 ml LB liquid + 100 µg/ml ampicillin to grow overnight in a 37ºC shaking incubator. I isolated plasmid DNA from each culture using a miniprep kit (Qiagen, Hilden, Germany). I digested plasmid DNA with specific enzymes to verify the correct fragment orientation. I grew bacterial cultures containing the correct plasmids in 250 ml LB liquid + 100 µg/ml ampicillin overnight in a 37ºC shaking incubator. I purified plasmid DNA by banding on cesium chloride ethidium bromide gradients [114]. I designated the plasmids pDEST R4-R3-*gipA* 5' FR-*AnpyrG*-*gipA* 3' FR and pDEST R4-R3-*gipB* 5' FR-*AnpyrG*-*gipB* 3' FR.

I grew *A. fumigatus* 1160 (obtained from FGSC) in MAG supplemented with uridine and uracil (described above). I performed the transformation as previously described [113], linearizing both deletion constructs with NotI to facilitate homologous recombination. I grew

transformants on MMV (described above) supplemented with 0.2 M sucrose at 37ºC for 3-5 days. I screened for mutants that were prototrophic for uridine and uracil. I prepared genomic DNA from transformant strains [51], and I identified deletion mutants by Southern blot analysis (Fig. 2.2a & b) [114]. I made two DNA probes using the *gipA* 5' and 3' FRs and the *gipB* 5' and 3' FRs to verify *ΔgipA* and *ΔgipB*, respectively.

To create a vector for complementation, I PCR amplified the *gipA* coding region, flanked by a 3 kilobase promoter region and 500 base pair terminator region, using primers gipA 3kb F and 6g01910 R. I used primers 4g00320 F and 4g00320 R to isolate the *gipB* coding region. I amplified the fragments from Af293 genomic DNA using e2TAK DNA polymerase (Takara Bio Inc., Otsu, Shiga, Japan) and following manufacturer recommendations. I cloned the PCR products into pDONR HPH B, as described previously for pDHGL. I designated these vectors pDONR HPH-*gipA* and pDONR HPH-*gipB*. I grew *ΔgipA* and *ΔgipB* in MAG medium (as described above). I performed the transformations as previously described for pDHGL. For Southern hybridization, I made DNA probes using the coding region of *gipA* and *gipB* (Fig. 2.3a&b). I designated these strains as *gipA*(R) and *gipB*(R). I obtained controls (1160G and *ΔgliZ*) for growth assays deletion mutants. I created 1160G by transforming pDONR G into Af1160 and I created *ΔgliZ* by transforming pDEST R4-R3-*gliZ* 5' FR-*AnpyrG-gliZ* 3' FR into Af1160, performed as described above for *ΔgipA*. I created the *gliZ* deletion construct as described previously for *ΔgipA* using primers gliZ 5' F, gliZ 5' R, gliZ 3' F, and gliZ 3' R. I used *gliZ* 5' and 3' flanking regions as a DNA probe for Southern hybridization (Fig. 2.2c).

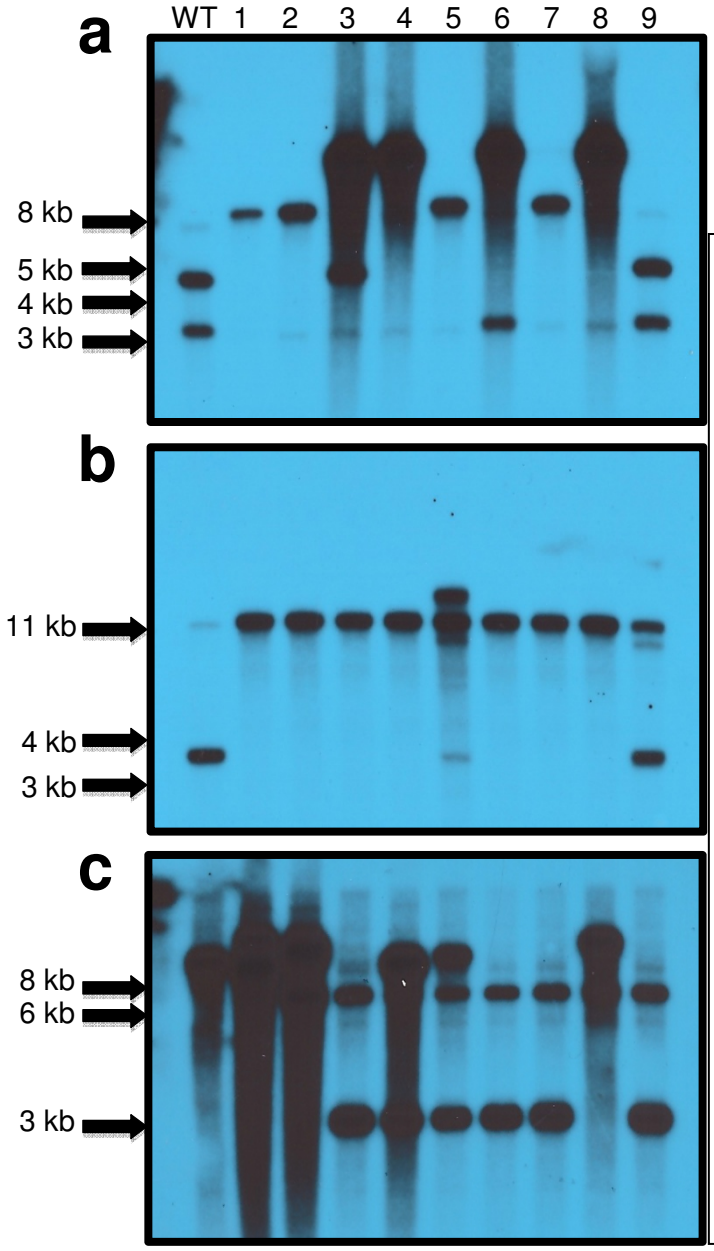


Figure 2.2. Southern hybridizations of *gipA, gipB*, and *gliZ* deletion mutants. Samples were run on a 0.8% agarose gel. WT is wild-type (Af1160). (a) *ΔgipA* transformants digested with PstI. WT should have a 4769 bp band and a 3275 bp band, while correct transformants are expected to have one 8627 bp band. The *gipA* 5' FR and 3' FR was used as a probe. (b) *ΔgipB* transformants digested with ClaI. WT should have a 11488 bp band and a 3852 bp band, while correct transformants should have one 13619 bp band. The *gipB* 5' FR and 3' FR was used as a probe. (c) *ΔgliZ* transformant digested with KpnI. WT should have one 8775 bp band, while correct transformant should have a 6314 bp band and a 2945 bp band. The *gliZ* 5' FR and 3' FR was used as a probe.

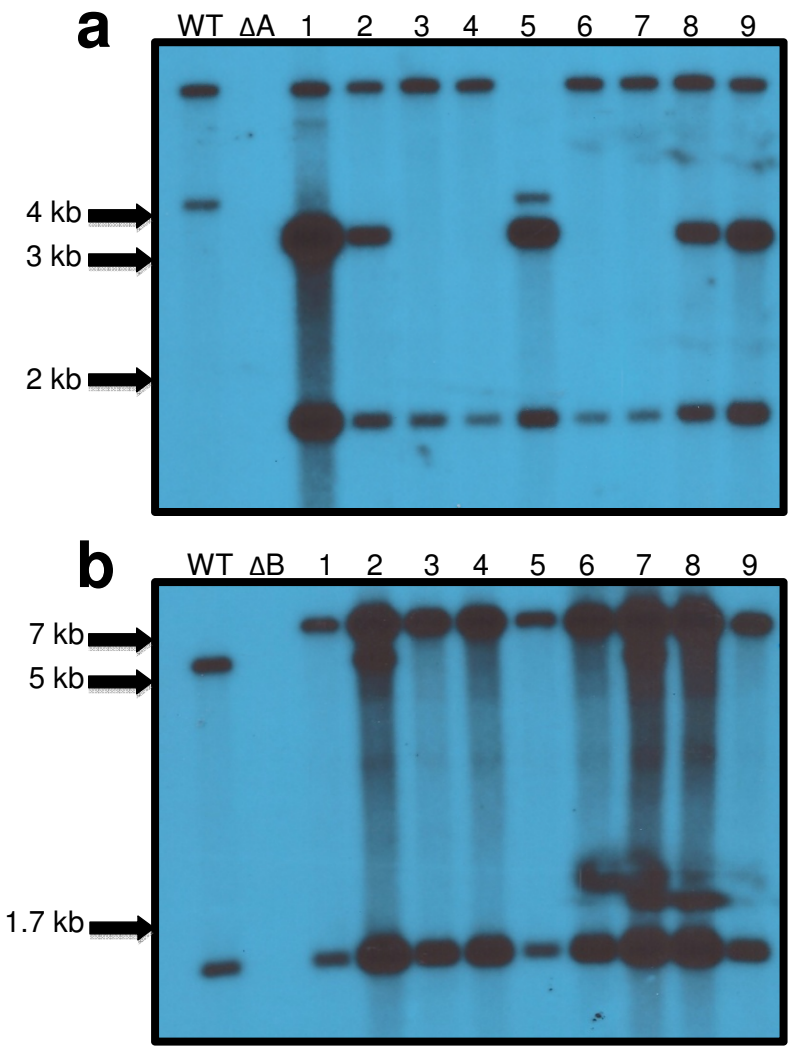


Figure 2.3. Southern hybridizations of *gipA(R)* and *gipB(R)* transformants. WT is wild-type (Af1160). (a) *gipA(R)* transformants digested with SphI. WT should have two bands, one at 4131 bps and one at 3404 bps (the lower band is extremely light). The *ΔgipA* mutant should not display any band. Correct transformants should display two bands at 3404 bps and 1967 bps, which indicates 5' integration of the complement plasmid. (b) *gipB(R)* transformants digested with EcoRI. WT should display two bands at 5423 bps and 1225 bps. The *ΔgipB* mutant should not display any band, while correct transformants should display two bands at 7793 bps and 1225 bps, indicating 5' integration of the complement plasmid.

## 2.9 Construction of *ΔgliZ/ΔgipA* and *ΔgipA/ΔgipB*

I grew *ΔgipA* on YAG supplemented with uridine and uracil (described above) + 1 mg/ml 5-Fluororotic acid (5-FOA) at 37ºC. Colonies that reverted to a *pyrG*- phenotype grew as outgrowths from the original streak. I prepared genomic DNA from these *pyrG*- fans [51] and tested them for the presence of *gipA* by Southern hybridization (Fig. 2.4a) [114]. I used the *gipA* coding region as a DNA probe. I designated this mutant as *ΔgipA.0.* I transformed pDEST R4-R3-*gliZ* 5' FR-*AnpyrG-gliZ* 3' FR into *ΔgipA.0,* as described above for *ΔgipA.* I used the *gliZ, gipA,* and *gipB* coding regions as a DNA probe for Southern hybridization (Fig. 2.5a).

I grew *ΔgipB* on 5-FOA medium, as described above for *ΔgipA.0,* and designated this strain as *ΔgipB.0.* I prepared genomic DNA from these *pyrG*- fans [51] and tested them for the presence of *gipB* by Southern hybridization (Fig. 2.4b) [114]. I used the *gipB* coding region as a DNA probe. I transformed pDEST R4-R3-*gipA* 5' FR-*AnpyrG-gipA* 3' FR into *ΔgipB.0,* as described above for *ΔgipA.* I used the *gipA* and *gipB* coding regions as a DNA probe for Southern hybridization (Fig. 2.5b).

## 2.10 Protein Binding Microarray

I amplified the $C_2H_2$ DNA binding region from *gipA* using primers gipA C2H2 F and gipA C2H2 R. I used Af293 as template and AccuPrime Pfx DNA polymerase (Life Technologies Grand Island, NY) and per manufacturer's recommendations. I cloned the PCR product into pDONR 221 using a BP recombination reaction (Invitrogen, Grand Island, NY). I transformed the reaction mix into TOP10 cells (Invitrogen, Grand Island, NY) by

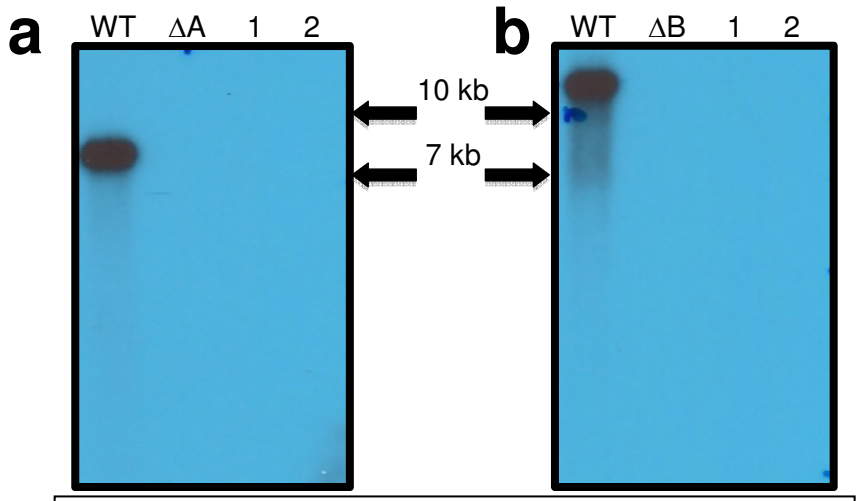


Figure 2.4. Southern hybridization of *ΔgipA* and *ΔgipB* mutants treated with 5-FOA. Samples were run on a 0.8% agarose gel. WT is wild-type (Af1160) and Δ is the untreated deletion strain. (a) *ΔgipA.0* mutants digested with EcoRV and probed with the *gipA* coding region. Only WT should display a band, which is 7616 bp. (b) *ΔgipB.0* mutants digested with ScaI and probed with the *gipB* coding region. Only WT should display a band, which is 13828 bp.

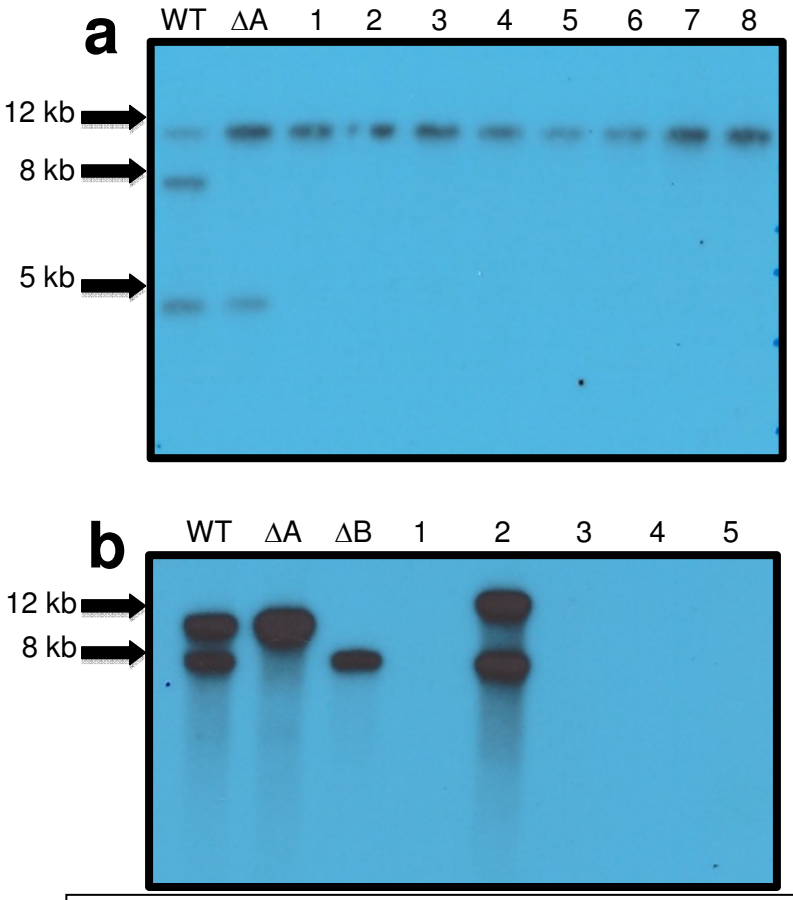


Figure 2.5. Southern hybridization of *ΔgliZ/ΔgipA* and *ΔgipA/ΔgipB* double mutants. Samples were run on a 0.8% agarose gel. WT is wild-type (Af1160). (a) *ΔgliZ/ΔgipA* transformants digested with SacI and probed with the *gliZ*, *gipA,* and *gipB* coding regions. WT should display three bands, which are 11712 bps (*gipB*), 7474 bps (*gipA*), and 4566 bps (*gliZ*). The *ΔgipA* control should display two bands, which are 11712 bps (*gipB*) and 4566 bps (*gliZ*). Correct transformants should display only one band at 11712 bps, for *gipB*. (b) *ΔgipA/ΔgipB* transformants digested with SacI and probed with the *gipA* and *gipB* coding regions. WT should display two bands, which are 11712 bps (*gipB*) and 7474 bps (*gipA*). The *ΔgipA* control should display one band at 11712 bps for *gipB* and the *ΔgipB* control should display one band at 7474 bps for *gipA*. Correct transformants should not display any bands.

electroporation, as recommended by the manufacturer. I grew the transformation mix on LB + 50 µg/ml kanamycin at 37ºC overnight. I picked colonies and transferred to 2 ml of LB liquid + 50 µg/ml kanamycin to grow overnight in a 37ºC shaking incubator. I isolated plasmid DNA from each culture using a miniprep kit (Qiagen, Hilden, Germany). I digested plasmid DNA with specific enzymes to verify the correct insertion. I recombined the *gipA* $C_2H_2$ region into pDEST 15 using an LR recombination reaction (Invitrogen, Grand Island, NY). I transformed the reaction mix into TOP10 cells (Invitrogen, Grand Island, NY) by electroporation, as recommended by the manufacturer. I grew the transformation mix on LB + 100 µg/ml ampicillin at 37ºC overnight. I picked colonies and transferred to 2 ml of LB liquid + 100 µg/ml ampicillin to grow overnight in a 37ºC shaking incubator. I isolated plasmid DNA from each culture using a miniprep kit (Qiagen, Hilden, Germany). I digested plasmid DNA with specific enzymes to verify the correct insertion. This vector, pDEST 15-gipA $C_2H_2$, was used in a protein binding microarray analysis as previously described [118].

### 2.11 Mutagenesis of the GipA DNA Binding Site in the *gliA* Promoter

I created mutated *gipA* DNA binding sites in pDHGL using a QuikChange II XL Site-Directed Mutagenesis Kit (Agilent Technologies Inc., Santa Clara, CA), as recommended by the manufacturer. I utilized primers SDMut1 F and SDMut1 R, SDMut2 F and SDMut2 R to create vectors pDHSD1 and pDHSD2, respectively. I transformed pDHGL, pDHSD1 and pDHSD2 into Af293.1, as previously described for Af293.1-GL, except I plated transformants on YAG supplemented with uridine and uracil (described above), 0.2 M sucrose, and 300 µg/ml hygromycin. I verified correct transformants by Southern hybridization using the lacZ coding region as a probe (Fig. 2.6). I designated these strains

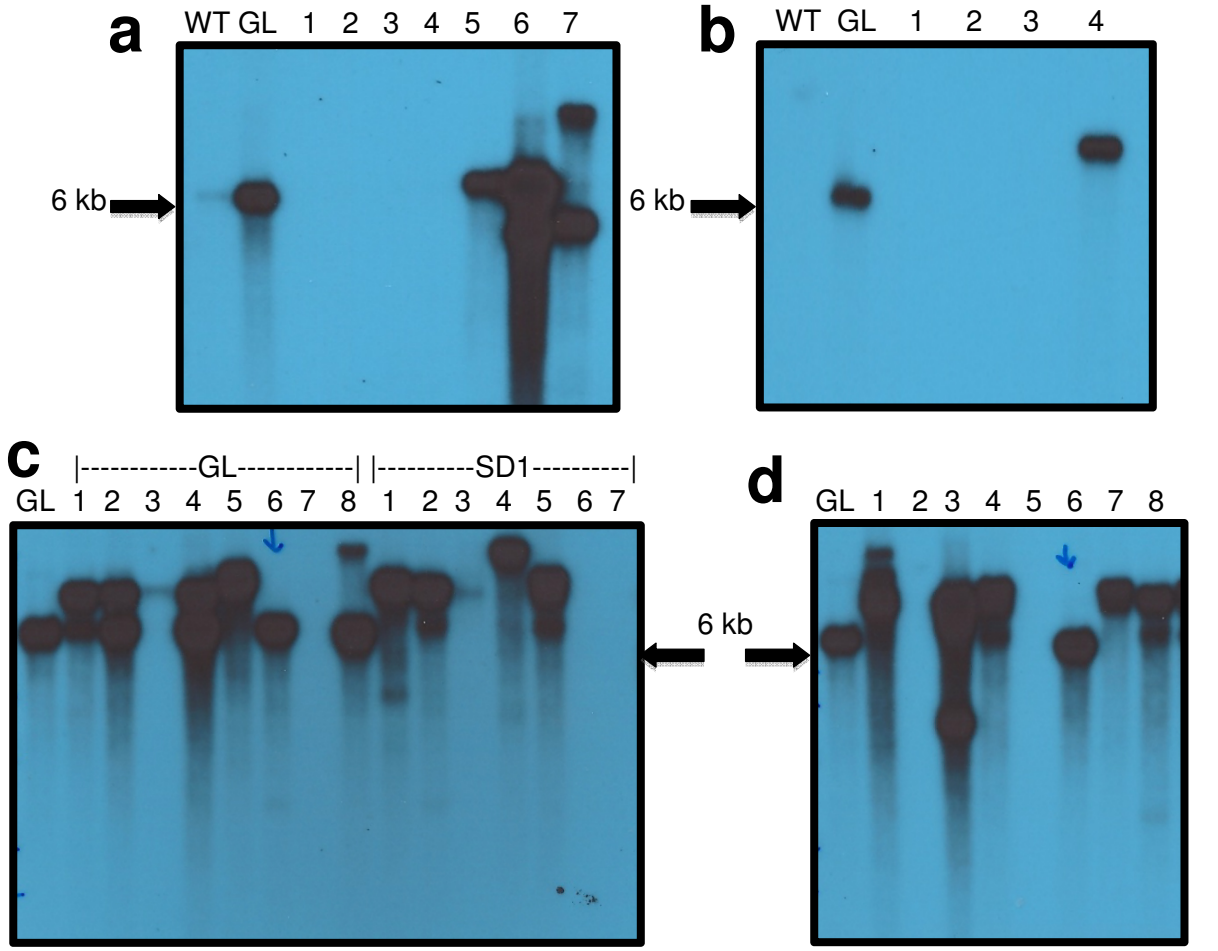


Figure 2.6. Southern hybridizations of promoter mutagenesis transformants. Samples were digested with EcoRI and run on a 0.8% agarose gel. WT is wild-type (Af293.1) and GL is Af293.1-GL. The *lacZ* coding region was used as the probe. WT should not display a band and GL should have a single band ~6500bps. Correct transformants should display a single band, any size. (a) First group of Af293.1-SD1 transformants. Isolate 5 was chosen for experiments. (b) First group of Af293.1-SD2 transformants. Isolate 4 was chosen for experiments. (c) Second group of Af293.1-GL and Af293.1-SD1 transformants. Isolate 6 and 4 were chosen for experiments, respectively. (d) Second group of Af293.1-SD2 transformants. Isolate 6 was chosen for experiments. Notice that isolates chosen for independent experiments for Af293.1-SD1 and Af293.1-SD2 display different sized bands, indicating that the pDHSD1 and pDHSD2 plasmids integrated in different places in the genome, respectively.

as Af293.1-GL, Af293.1-SD1 and Af293.1-SD2, respectively. I repeated transformations until I obtained two independent isolates for experiments, therefore, I used the AMA.GL, AMA-gliZ.GL, and AMA-gipA.GL obtained from the high-copy library screen for one set of experiments and made a new Af293.1-GL strain (Fig. 2.6c) for the second set of experiments. To test the effect of the different *gipA* binding site mutants, I transformed pDONR AMA, pDONR AMA-*gliZ*, and pDONR AMA-*gipA* into two independent isolates of Af293.1-GL, Af293.1-SD1 and Af293.1-SD2, as described above for AMA-gipA.GL, except I grew transformants on YAG supplemented with 0.2 M sucrose. I designated the promoter-mutated strains as AMA.SD1, AMA-gliZ.SD1, AMA-gipA.SD1, AMA.SD2, AMA-gliZ.SD2 and AMA-gipA.SD2.

**2.12 β-galactosidase Assays**

I ground 50 µl lyophilized mycelia to a fine powder with acid-washed glass beads (400-650 µm) (Sigma-Aldrich Corp., St. Louis, MO). I suspended the ground powder in 200 µl protein extraction buffer (PEB) (60mM $Na_2HPO_4 \cdot 7H_2O$, 40mM $NaH_2PO_4 \cdot H_2O$, 10mM KCl, 1mM $MgSO_4 \cdot 7H_2O$, 1mM EDTA, and 20µM PMSF [added fresh], pH 7.0) by vortexing and incubated the samples on ice for 15 minutes, with additional vortexing every 5 minutes. I spun tubes for 15 minutes at 15,600 x g at 4℃ to pellet cellular debris and beads. I transferred supernatants, containing total protein, to fresh tubes on ice and measured protein concentration using a Bio-Rad protein assay kit (Bio-Rad, Hercules, CA). In a 96-well plate, I added 10 µl of protein in PEB and 90 µl Z Buffer (60mM $Na_2HPO_4 \cdot 7H_2O$, 40mM $NaH_2PO_4 \cdot H_2O$, 10mM KCl, 1mM $MgSO_4 \cdot 7H_2O$, 50mM β-mercaptoethanol [added fresh], pH to 7.0). For samples grown in repressing conditions (CM), the total protein added was 1 µg. For samples grown in non-repressing conditions (CD), the total protein added was 0.1

µg. To begin the β-galactosidase assay, I added 20 µl of 2-Nitrophenyl-β-D-galactopyranoside (ONPG) (Sigma-Aldrich Corp., St. Louis, MO), at a concentration of 4 mg/ml in Z Buffer, and placed the 96-well plate in a 37°C incubator. I timed reactions and stopped samples with 50 µl 1 M $Na_2CO_3$. I measured absorbance at OD420 and calculated Units of β-galactosidase activity/mg protein with the following equation: (OD420 x TV)/(0.0045 x T x V x C), where TV is total volume of the reaction in ml, T is time in minutes, V is volume of protein added in ml, and C is concentration of protein used in µg/µl.

### 2.13 Creation of Strains for High-copy Gene Expression in Deletion Backgrounds

I grew Af293.1 in MAG supplemented with uridine and uracil (described above). I transformed pDEST R4-R3-*gliZ* 5' FR-*AnpyrG*-*gliZ* 3' FR and pDEST-*gipA* 5' FR-*AnpyrG*-*gipA* 3' FR into Af293.1, as previously described for *ΔgipA,* except I plated transformants on YAG supplemented with 0.2 M sucrose. I used *gliZ* 5' and 3' FRs and *gipA* 5' and 3' FRs for Southern hybridization and designated these strains *ΔgliZ.1* and *ΔgipA.1* (Fig. 2.7). I chose one strain from the *ΔgliZ* transformation that did not show homologous recombination at the gliZ locus, but was prototrophic for uridine and uracil. I designated this strain pyrG+. I collected total RNA and performed dot blot analysis on pyrG+, *ΔgliZ.1,* and *ΔgipA.1* to verify loss of *gliZ* and *gipA*, respectively (described above) (Fig. 2.8). I cloned *gliZ, gipA*, and *gipB* into pDONR AMA/HPH, as described above for pDONR AMA-*gliZ*, pDONR AMA-*gipA*, and pDONR AMA-*gipB*, respectively, except I used primers gipA 3kb F and 6g01910 R for the *gipA* cassette. I designated these plasmids pDONR AMA/HPH-*gliZ*, pDONR/HPH-*gipA*, and pDONR AMA/HPH-*gipB*. I transformed these plasmids, along with pDONR AMA/HPH empty vector, into pyrG+, *ΔgliZ.1,* and *ΔgipA.1,* as described above for

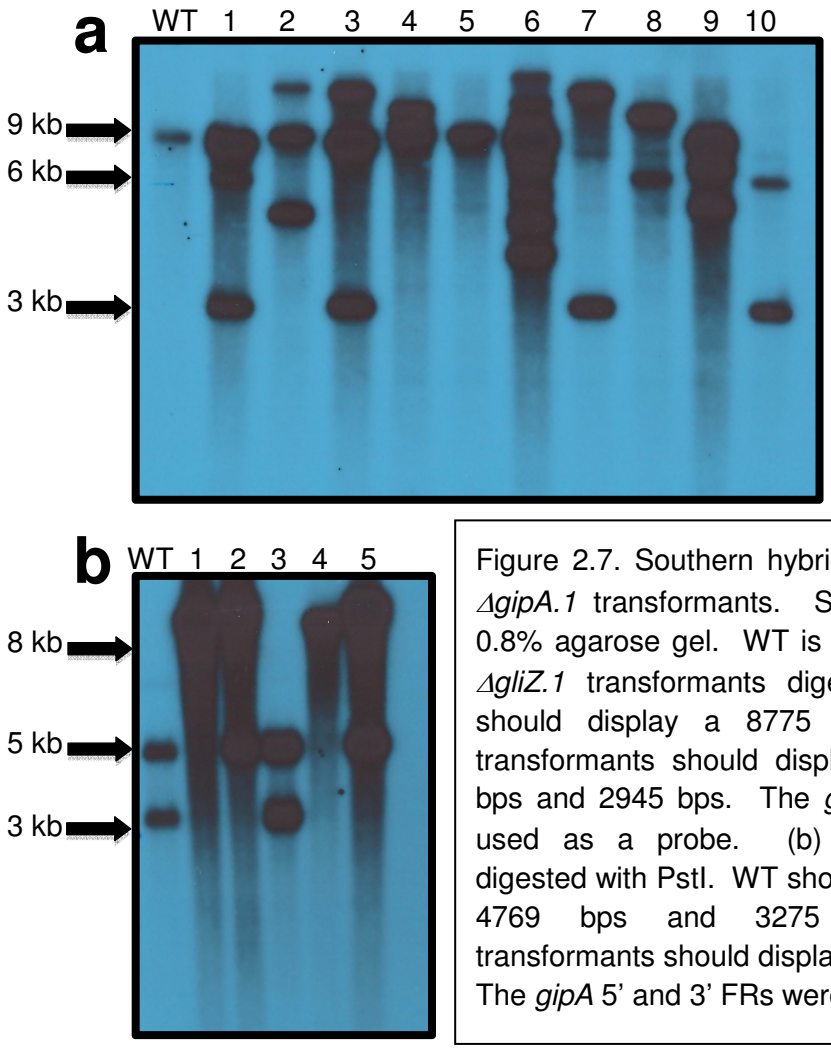


Figure 2.7. Southern hybridizations of *ΔgliZ.1* and *ΔgipA.1* transformants. Samples were run on a 0.8% agarose gel. WT is wild-type (Af293.1). (a) *ΔgliZ.1* transformants digested with KpnI. WT should display a 8775 bp band and correct transformants should display two bands at 6314 bps and 2945 bps. The *gliZ* 5' and 3' FRs were used as a probe. (b) *ΔgipA.1* transformants digested with PstI. WT should display two bands at 4769 bps and 3275 bps, while correct transformants should display one band at 8627 bps. The *gipA* 5' and 3' FRs were used as a probe.

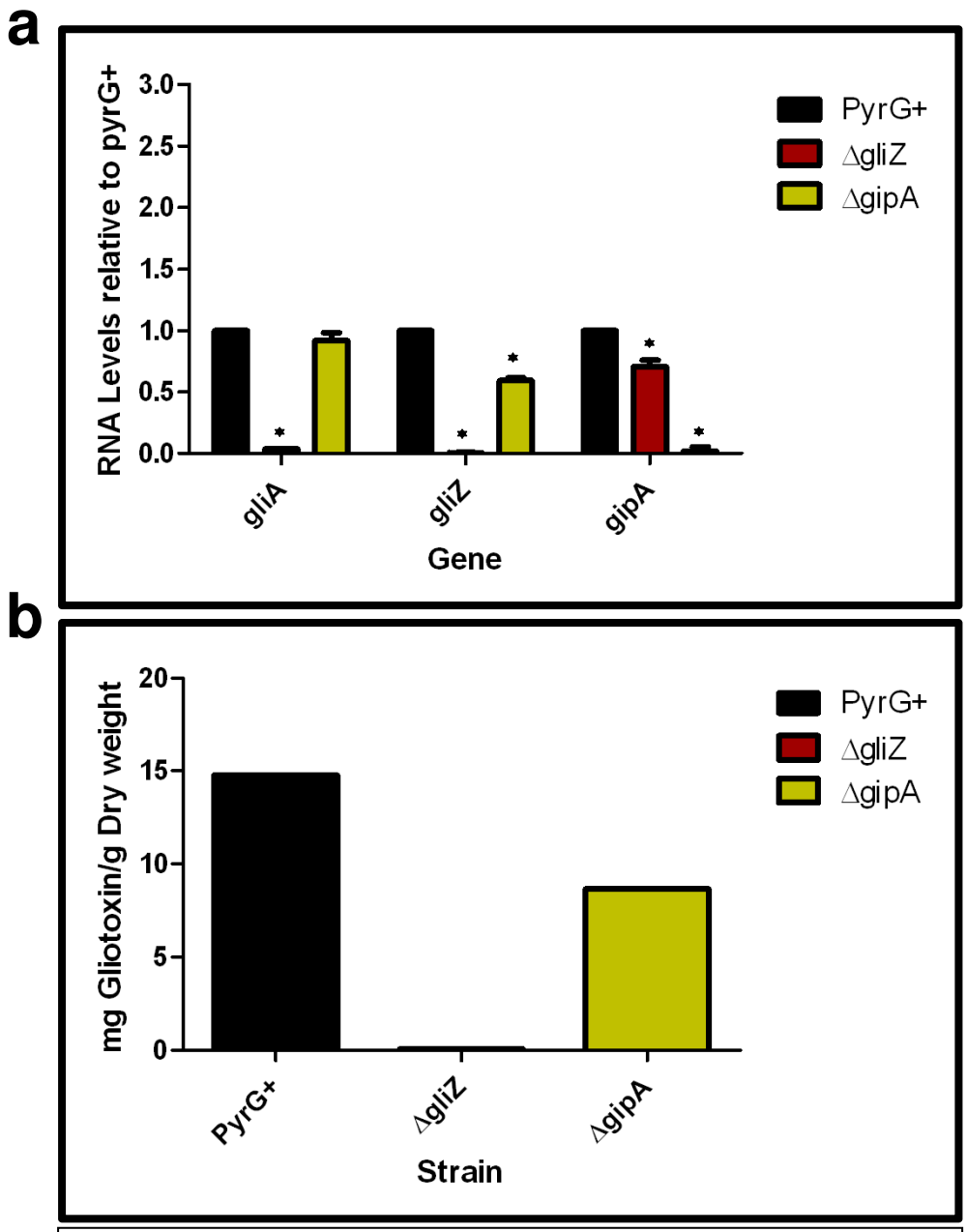


Figure 2.8. Verification of *ΔgliZ* and *ΔgipA* mutants in an Af293.1 background. (a) Cultures were grown in non-repressing conditions at 37℃ for 48 hrs. Total RNA was collected and dot blot analysis was performed in triplicate with 3 µg RNA/spot. RNA levels are relative to pyrG+. The results of one representative experiment of two biological replicates are shown. The asterisk (*) indicates a statistically significant difference (p-value <0.05), compared to PyrG+, calculated by one-way ANOVA and Tukey comparison test. (b) Gliotoxin was measured with RP-HPLC.

AMA-gipA.GL, except I grew transformants on YAG supplemented with uridine and uracil (described above), 0.2 M sucrose, and 400 µg/ml hygromycin. I designated these strains as AMA.G, AMA-gliZ.G, AMA-gipA.G, AMA-gipB.G, AMA.Z, AMA-gliZ.Z, AMA-gipA.Z, AMA-gipB.Z, AMA.A, AMA-gliZ.A, AMA-gipA.A, and AMA-gipB.A.

# Chapter 3:

# Identification of High-copy Inducers of *gliA* Expression

## 3.1 Introduction

Although a number of proteins have been shown to affect gliotoxin production in a generalized way, no direct regulation through promoter binding has been experimentally proven. Not even the cluster-specific transcription factor, GliZ, has been experimentally shown to bind to any promoter regions within the cluster [15]. To identify novel proteins that possibly directly regulate the gliotoxin biosynthesis cluster, I performed a high-copy inducer screen to identify genes that, when present in extra copies, induced the gliotoxin biosynthesis cluster in repressing conditions. I used a LacZ reporter system, under the control of the *gliA* promoter, for the screen. GliA encodes an efflux pump within the gliotoxin cluster. I chose *gliA* for several reasons. First, it has been shown that expression of *gliA* peaks when the amount of gliotoxin in surrounding medium is maximal [14, 25]. Second, experiments in the May laboratory have revealed that *gliA* is induced within 30 minutes of *A. fumigatus* germlings being exposed to human neutrophils (Fig. 3.1). These data led me to conclude that *gliA* expression would be an excellent indicator of gliotoxin cluster expression, as well as gliotoxin production.

## 3.2 Results

### *3.2.1 Creation of an Expression Cassette for the High-copy Inducer Screen*

I created a $gliA^{P}$-*lacZ*-$gliA^{T}$ cassette with fusion PCR and cloned this into pDONR HPH A, creating vector pDHGL. This cassette contained 588 base pairs (bp) of the *gliA* 5' non-coding region (NCR) ($gliA^{P}$), immediately upstream of the start codon, and 386 bp of the *gliA* 3' NCR ($gliA^{T}$), immediately downstream of the stop codon. I transformed pDHGL into Af293.1 and screened for transformants that contained only a single copy of *lacZ* by

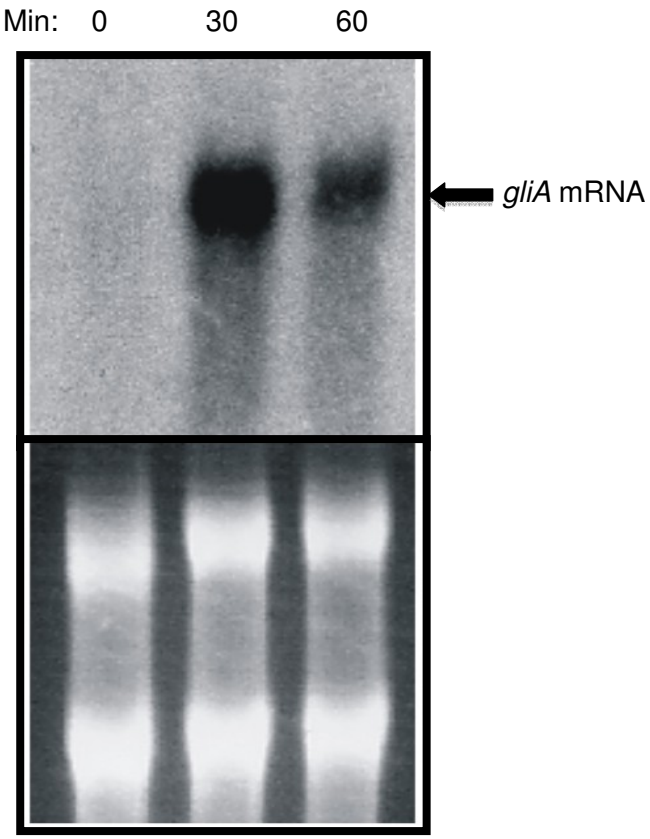


Figure 3.1. Northern analysis of gliA mRNA transcript levels in response to human neutrophils. Af293 germlings were exposed to human neutrophils (1:2) in RPMI with HEPES for 60 min. RNA was collected for each time point. The top panel is the Northern hybridization with the *gliA* coding region used as a probe. The bottom panel is an image of the RNA gel for loading control.

Southern hybridization (Fig. 2.1a). This strain was designated Af293.1-GL. I further screened transformants for the ability to produce a blue pigment when grown on non-repressing medium with X-gal (Fig. 2.1b). This indicated to us that the *lacZ* cassette was functional and responded to induction of the gliotoxin cluster.

### *3.2.2 High-copy Inducer Screen: First Round*

The first round of the high-copy inducer screen involved transforming an *A. fumigatus* genomic library into Af293.1-GL (Fig. 3.2a). This library was cloned into pRG3-AMA1-NotI, which is an autonomously replicating plasmid [115]. Due to the presence of AMA1 from *A. nidulans*, this plasmid does not insert into the genome, but remains as a circular plasmid [119, 120]. This facilitates the recovery of the plasmid by transformation of fungal genomic DNA into bacteria. This plasmid is also present in anywhere from 10 to 30 extra copies on average in each haploid genome. Therefore, this genomic library was an ideal choice for our high-copy inducer screen. I grew transformants on repressing medium with X-gal and screened for colonies that produced a blue pigment. This indicated that the AMA1-NotI plasmid within the genome was inducing the *gliA-lacZ* reporter in repressing conditions. I recovered plasmids from 70 colonies.

### *3.2.3 High-copy Inducer Screen: Second Round*

For the second round of the high-copy inducer screen, I transformed 70 individual plasmids, isolated in the first round of the high-copy inducer screen, into Af293.1-GL (Fig. 3.2b). I again grew transformants on repressing medium with X-gal and screened for

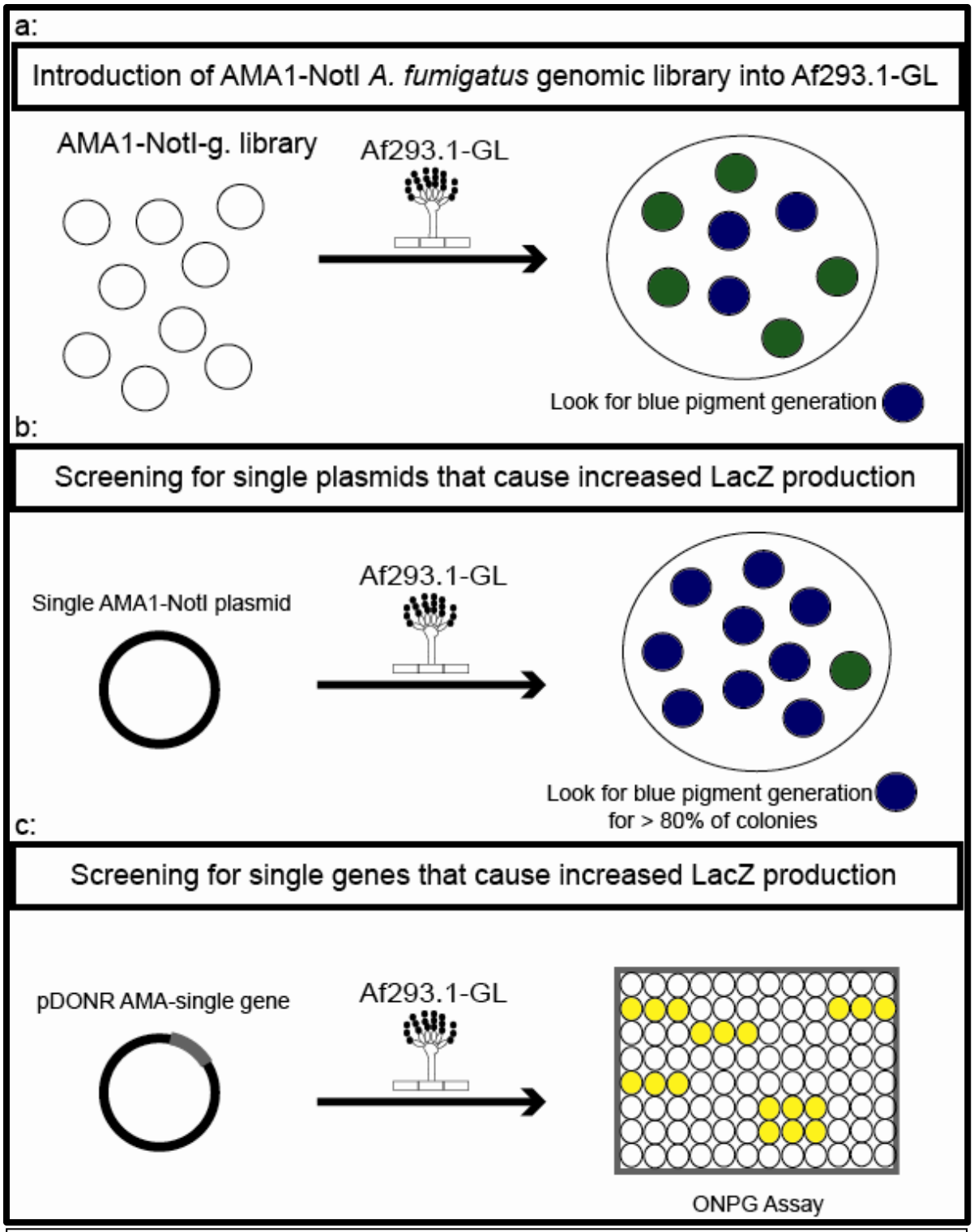


Figure 3.2. Schematic of the three rounds of the high-copy inducer screen. (a) Round one: transformation of the genomic library into Af293.1-GL. (b) Round two: transformation of single plasmids from the genomic library into Af293.1-GL. (c) Round three: transformation of single genes into Af293.1-GL.

colonies with blue pigment production. For this round, I transformed individual vectors to be sure that the effect I observed from the first round was the result of only one plasmid and not multiple plasmids. Since I transformed single plasmids, I also expected plates to contain a high number of colonies producing blue pigment. I sequenced all 70 plasmids to identify what genes were contained within the insert, using primers that flanked the insert cloning site (Ama NotI F and Ama NotI R). To measure LacZ levels in a more quantitative manner, I isolated total protein from transformants and measured β-galactosidase activity (Fig. 3.3). I transformed the pDONR AMA empty vector and pDONR AMA-*gliZ* as a negative control (AMA.GL) and positive control (AMA-gliZ.GL), respectively. Based on results, I grouped vectors into three categories: extreme inducing (>70-fold *lacZ* induction), moderate inducing (5 to 70-fold *lacZ* induction), and low inducing (<5-fold *lacZ* induction). This was based on fold change relative to the AMA.GL negative control. Of the 70 plasmids tested, 7 were in the extreme inducing category and 7 were in the moderate inducing category (Figure 3.4/Table 3.1).

### *3.2.4 High-copy Inducer Screen: Third Round*

The third round of the high-copy inducer screen entailed isolating the individual genes from each AMA1-NotI library plasmid and transforming them into Af293.1-GL (Fig. 3.2c). For this process, I decided to focus on the extreme inducing plasmids. Most plasmids had anywhere from 1 to 4 genes. I amplified each gene and cloned it into pDONR AMA. For this round, I did not screen for blue pigment formation, but rather I collected total protein from transformants and measured β-galactosidase activity (Fig. 3.5). The two genes that induced *lacZ* the most were a $C_2H_2$ transcription factor (Afu6g01910) and a

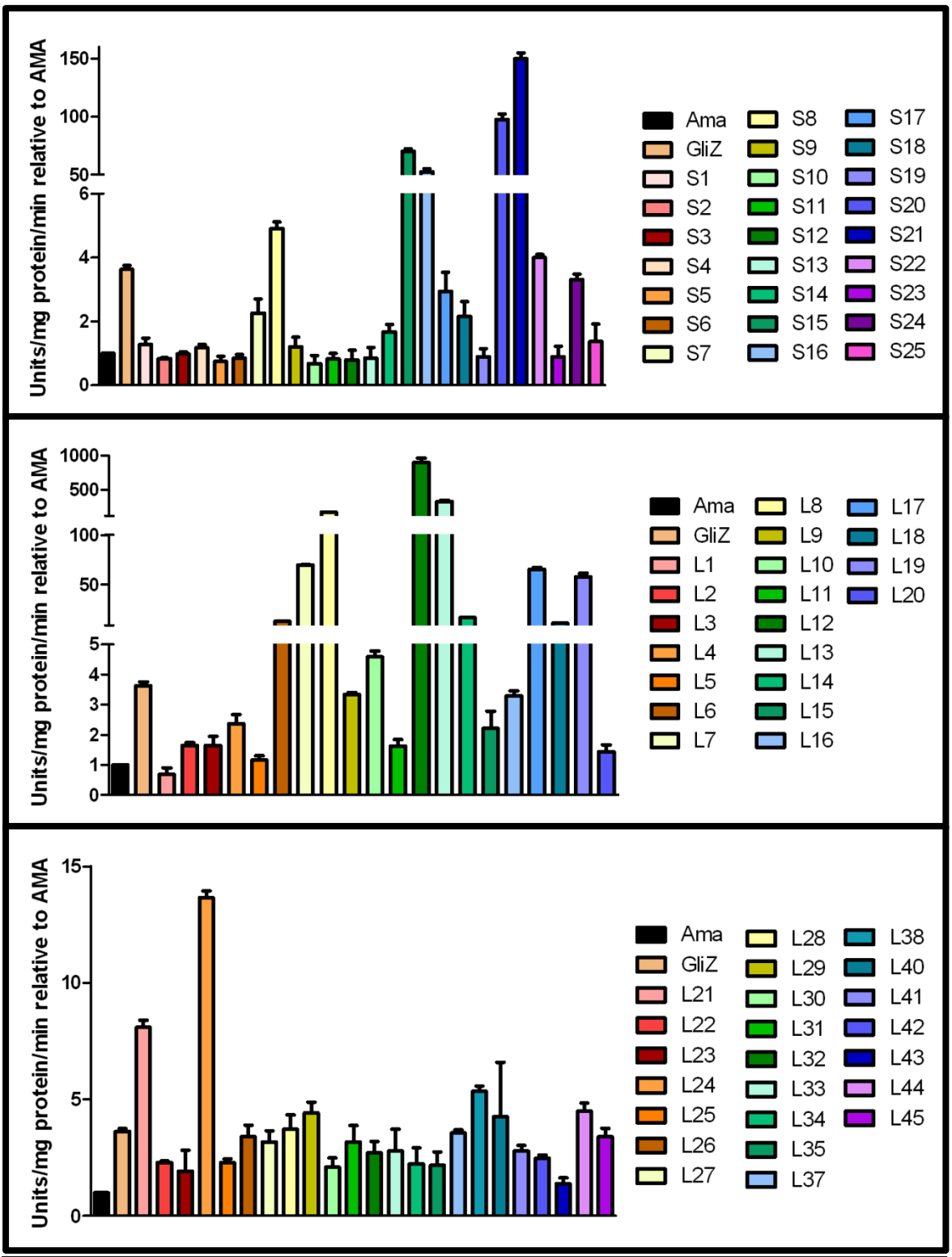


Figure 3.3. β-galactosidase assays from the second round of the high-copy inducer screen. Data is presented as fold-change relative to AMA. The results of one representative experiment of three independent experiments are shown as mean ± SD.

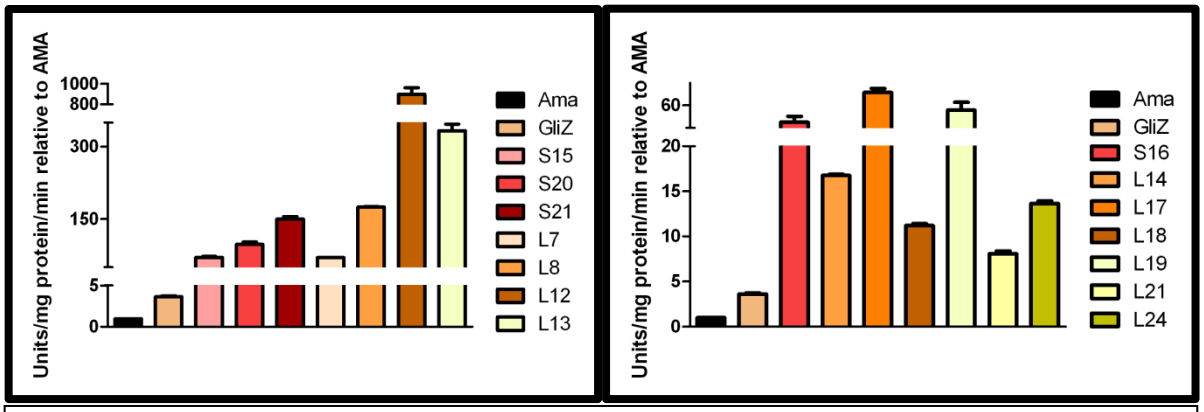


Figure 3.4. β-galactosidase assays of the extreme inducing group (left panel) and the moderate inducing group (right panel). Data is presented as fold-change relative to AMA. The results of one representative experiment of three independent experiments are shown as mean ± SD.

| **Extreme LacZ Inducing Plasmids** | | | **Moderate LacZ Inducing Plasmids** | | |
|---|---|---|---|---|---|
| **Plasmid** | **Locus** | **Gene** | **Plasmid** | **Locus** | **Gene** |
| S15 | Afu1g10860 | Hypothetical | S16 | Afu1g11890 | Serine palmitoyltransferase 2 |
| | Afu1g10870 | Cyanamide Hydratase | | Afu1g11990 | PQ Loop repeat protein |
| S20 | Afu3g11430 | Arginase | L14 | Afu6g08360 | Thiazole biosynthesis enzyme |
| | Afu3g11440 | Glutamyl-tRNA amidotransferase | | Afu6g08370 | Neutral shingomyelinase |
| S21 | Afu7g04460 | Rab geranlygeranyl transferase | | Afu6g08380 | WD Repeat protein |
| | Afu7g04470 | Hypothetical | | Afu6g08390 | Conserved hypothetical |
| | Afu7g04480 | DNA mismatch repair protein (Msh3) | L17 | Afu2g01110 | Hypothetical |
| L7 | Afu5g10940 | Conserved hypothetical | | Afu2g01120 | DNA Repair protein |
| L8 | Afu6g10650 | ATP Citrate lyase subunit 1 | | Afu2g01130 | Ubiquitin conjugating enzyme (UbcJ) |
| | Afu6g10660 | ATP Citrate lyase | | Afu2g01140 | GPI Anchored protein |
| L12 | Afu6g01900 | Hypothetical | L18 | Afu3g02560 | Hypothetical |
| | Afu6g01905 | Hypothetical | | Afu3g02570 | Polyketide synthase |
| | Afu6g01910 | $C_2H_2$ Zinc finger domain protein | L19 | Afu2g01700 | Serine/threonine protein kinase (Snf1) |
| L13 | Afu4g00300 | Hypothetical | | Afu2g01710 | GPI Anchored protein |
| | Afu4g00310 | Hypothetical | L21 | Afu6g13370 | SSU processome component (Utp10) |
| | Afu4g00320 | Sensor histidine kinase/response regulator | | Afu6g13380 | Hypothetical |
| | Afu4g00330 | Hypothetical | L24 | Afu6g06760 | Eukaryotic translation initiation factor 3 subunit (EifCj) |
| | | | | Afu6g06770 | Enolase |

Table 3.1. Genes that were represented in the extreme inducing and moderate inducing categories.

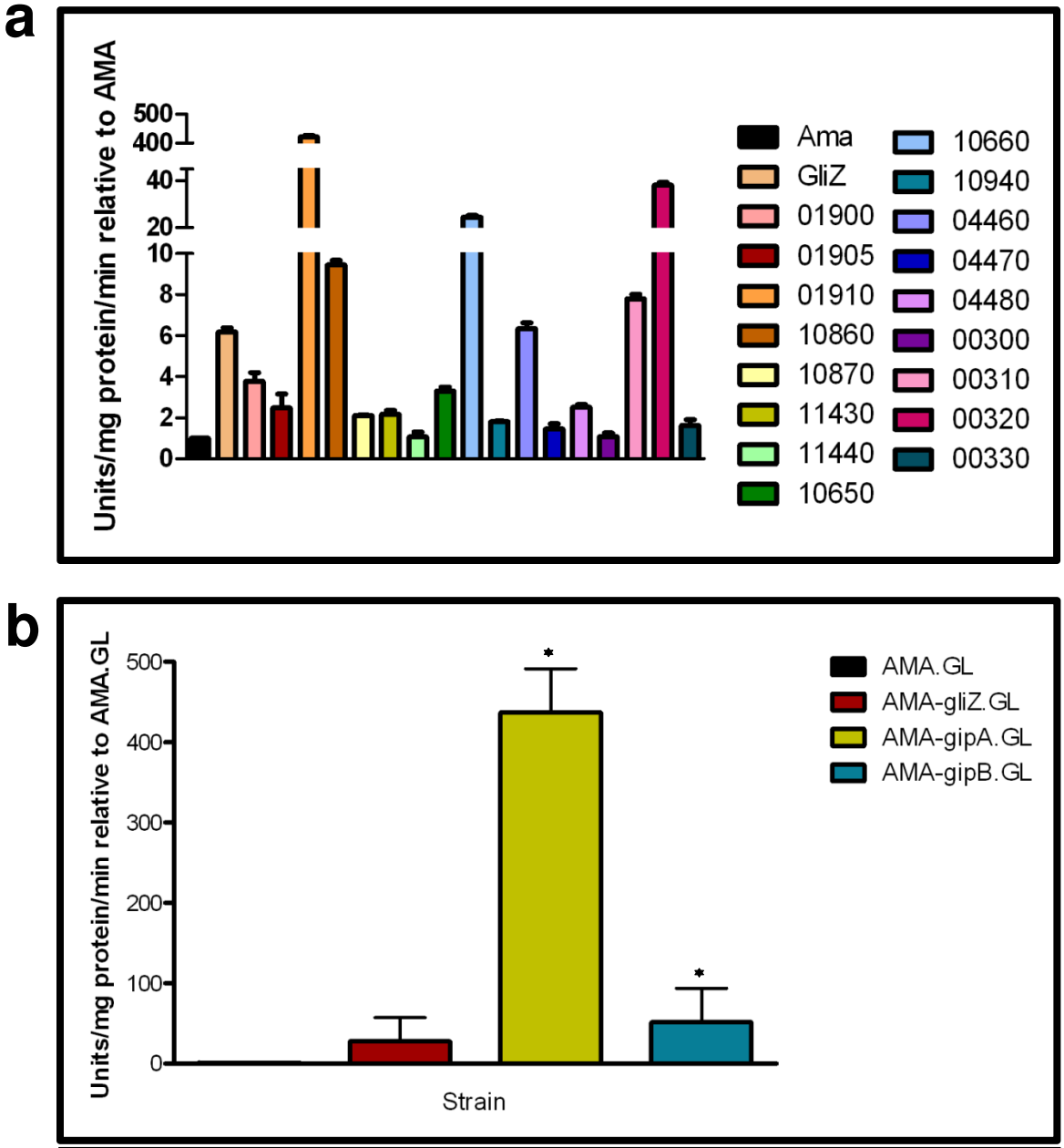


Figure 3.5. β-galactosidase assays for individual genes from extreme inducing plasmids. Data is presented as fold-change relative to AMA. (a) All genes from the extreme inducing plasmids. The results of one representative experiment of three independent experiments are shown as mean ± SD. (b) Activity of AMA-gliZ.GL, AMA-gipA.GL, and AMA-gipB.GL, relative to AMA.GL. The data presented is an average of three biological replicates. The asterisk (*) indicates a statistically significant difference (p-value <0.05), compared to AMA.GL, calculated by one-way ANOVA and Tukey comparison test.

hybrid sensor kinase (Afu4g00320); I have designated them *gipA* and *gipB*, respectively, for gliotoxin inducing protein. As shown in Figure 3.5b, AMA-gipA.GL, which has extra copies *gipA*, induced a 400-fold increase in LacZ levels and AMA-gipB.GL, which has extra copies of *gipB*, induced a 50-fold increase in LacZ levels, compared to the empty vector control. The level of *lacZ* in our positive control, AMA-gliZ.GL, was almost 30-fold higher than the empty vector control, AMA.GL, indicating that GipA and GipB positively regulate *gliA* expression, similar to GliZ.

### *3.2.5 Isolation and Sequencing of gipA and gipB cDNA*

Since *gipA* and *gipB* are novel genes, I confirmed the gene structure and protein sequence through isolation and sequencing of cDNAs for each. As shown in Figure 3.6a, *gipA* has an open reading frame (ORF) of 1314 bp with one intron and is predicted to encode a 419 amino acid protein. There are two $C_2H_2$ regions at the 3' end, the first as $X_2$-C-$X_2$-C-$X_{12}$-H-$X_3$-H and the second as $X_2$-C-$X_2$-C-$X_{12}$-H-$X_5$-C. The 5' untranslated region (UTR) of *gipA* is unusually long (at least 877 bp) with three µORFs and the 3' UTR of *gipA* consists of at least 360 bp, which indicates that *gipA* is under post-transcriptional control, possibly due to reduced translational efficiency and mRNA stability. I confirmed the length of the 5' and 3' UTR using a λ phage library screen, which does not always reveal the full length mRNA transcript, but Northern analysis of total RNA verified that the size of the *gipA* transcript is around 2.4 kb, which supports the size I predicted (3.6b). A Blastp search of the entire protein sequence revealed that there are only a few proteins that are homologous to GipA, the closest being a $C_2H_2$ transcription factor in *N. fischeri*, a close relative to *A. fumigatus* (Fig. 3.7a). The rest of the proteins from the Blastp search were from other

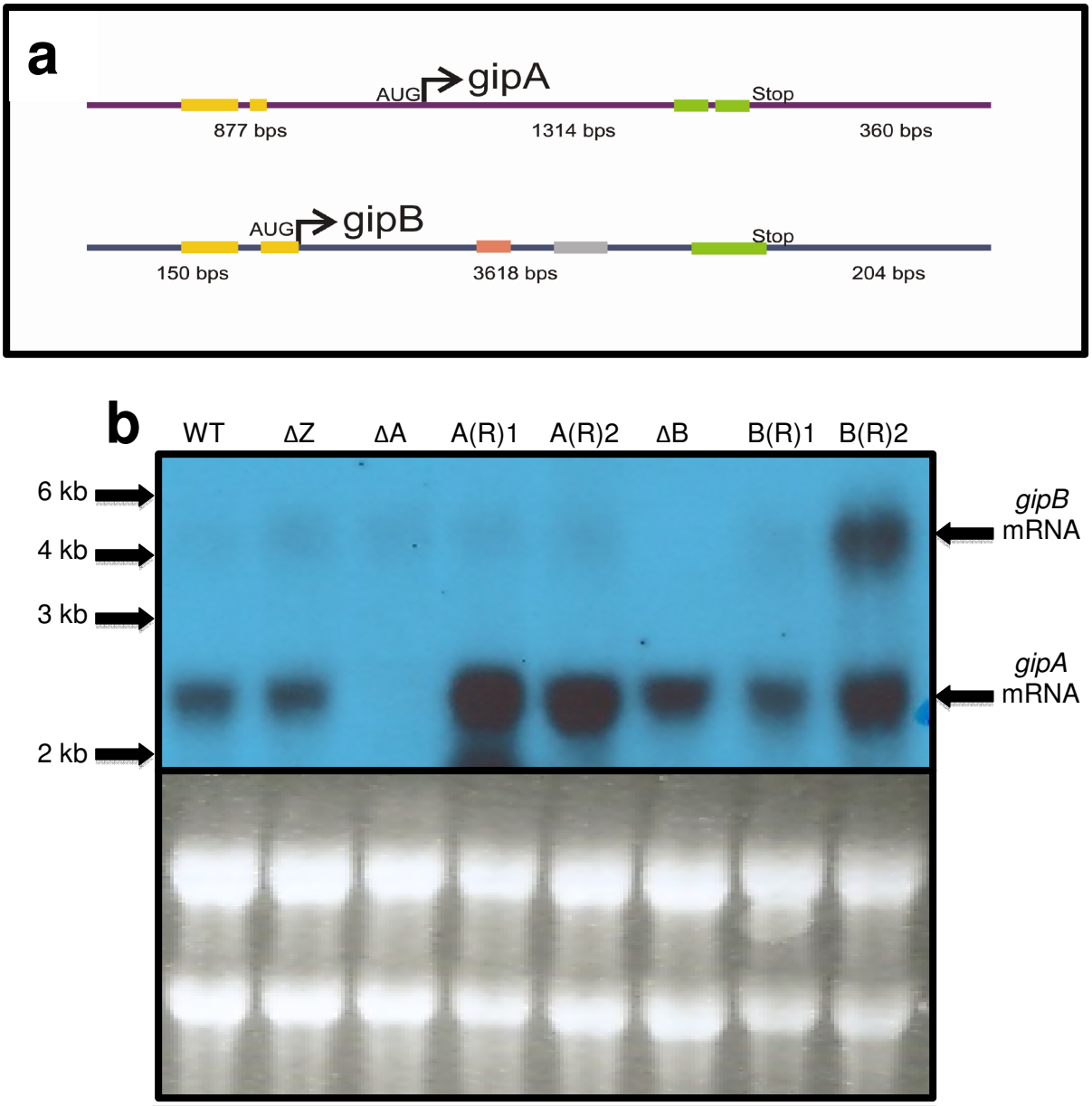


Figure 3.6. Characterization of *gipA* and *gipB* mRNA. (a) Schematic of mRNA size and composition. Yellow bars signify µORFs. For *gipA*, the green bars display the two zinc finger domains. For *gipB*, the pink bar is the histidine kinase A domain, the grey bar is the GHKL domain, and the green bar is the response regulator domain. Sizes indicated for the coding regions include introns. (b) Northern hybridization of *gipA* and *gipB* from total RNA. WT is wild-type (Af1160), Δ signifies deletion strains, and (R) signifies complemented strains.

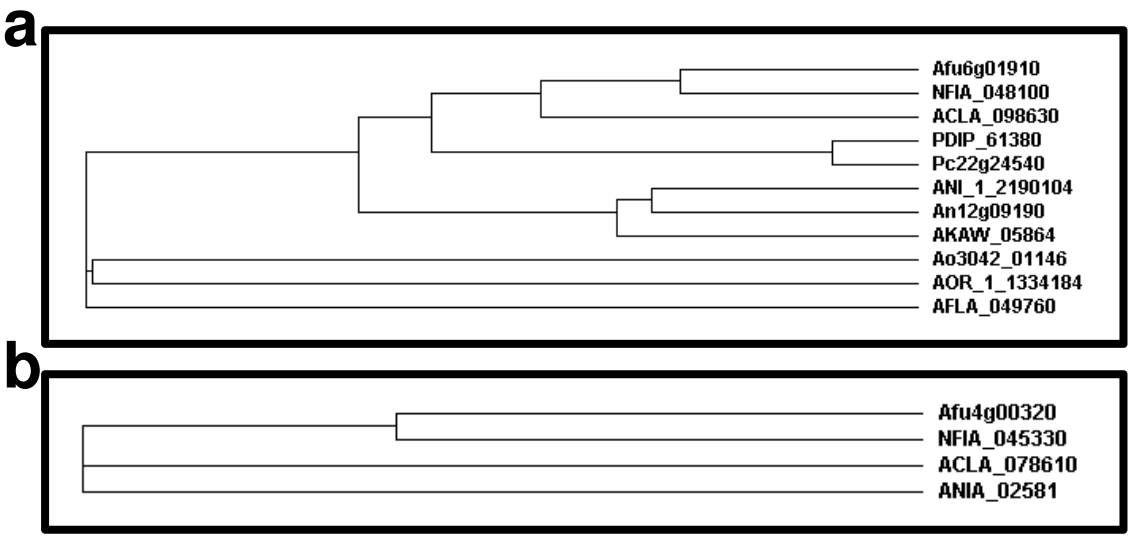


Figure 3.7. Cladograms of GipA and GipB homologues. (a) Afu6g01910 is GipA, NFIA is *N. fischeri*, ACLA is *A. clavatus*, PDIP is *P. digitatum*, Pc is *P. chrysogenum*, ANI and AN is *A. niger*, AK is *A. kawachii*, AO is *A. oryzae*, and AF is *A. flavus*. (b) Afu4g00320 is GipB, NFIA is *N. fischeri*, ACLA is *A. clavatus*, and ANIA is *A. nidulans*.

*Aspergillus* species and a few *Penicillium* species, which suggests that GipA is not highly conserved at the primary sequence. The coding region of *gipB* is 3618 bp with two introns and is predicted to encode a protein of 1170 amino acids. Within the coding region is a histidine kinase A (phospho-acceptor) domain, a GHKL (ATPase) domain, and a response regulator receiver domain. Results from the λ phage library screen indicated that the 5' UTR of *gipB* is 150 bp and contains two μORFs and the 3' UTR of *gipB* is 204 bp (Fig. 3.6a), suggesting that *gipB* is also possibly under post-transcriptional regulation. However, *gipB* mRNA appeared to be over 4 kb in size from Northern analysis, indicating that *gipB* could encode UTRs that are longer than what was predicted from the λ phage library screen (Fig. 3.6b). As with *gipA*, only a few proteins show a high level of similarity to GipB, the closest being from *N. fischeri,* suggesting that GipB is not highly conserved at the primary sequence (Fig. 3.7b).

### *3.2.6 Model of gliA Regulation*

I offer a model for *gliA* induction, involving GliZ, the $Zn_2Cys_6$ binuclear finger transcription factor located within the gliotoxin cluster, GipA, the novel $C_2H_2$ transcription factor I identified, and AreA, the positive-acting global regulator of nitrogen metabolite repression (Fig. 3.8) I propose that GliZ and GipA work together to induce *gliA* transcription, not in a linear pathway, but interdependently. I also posit that AreA acts as a co-activator of *gliA* expression in nitrogen-specific non-repressing conditions. To achieve this, AreA likely induces *gliZ*, which is required for the complete induction of the cluster. Figure 3.9a illustrates an example of the differential gene expression observed in the repressing and

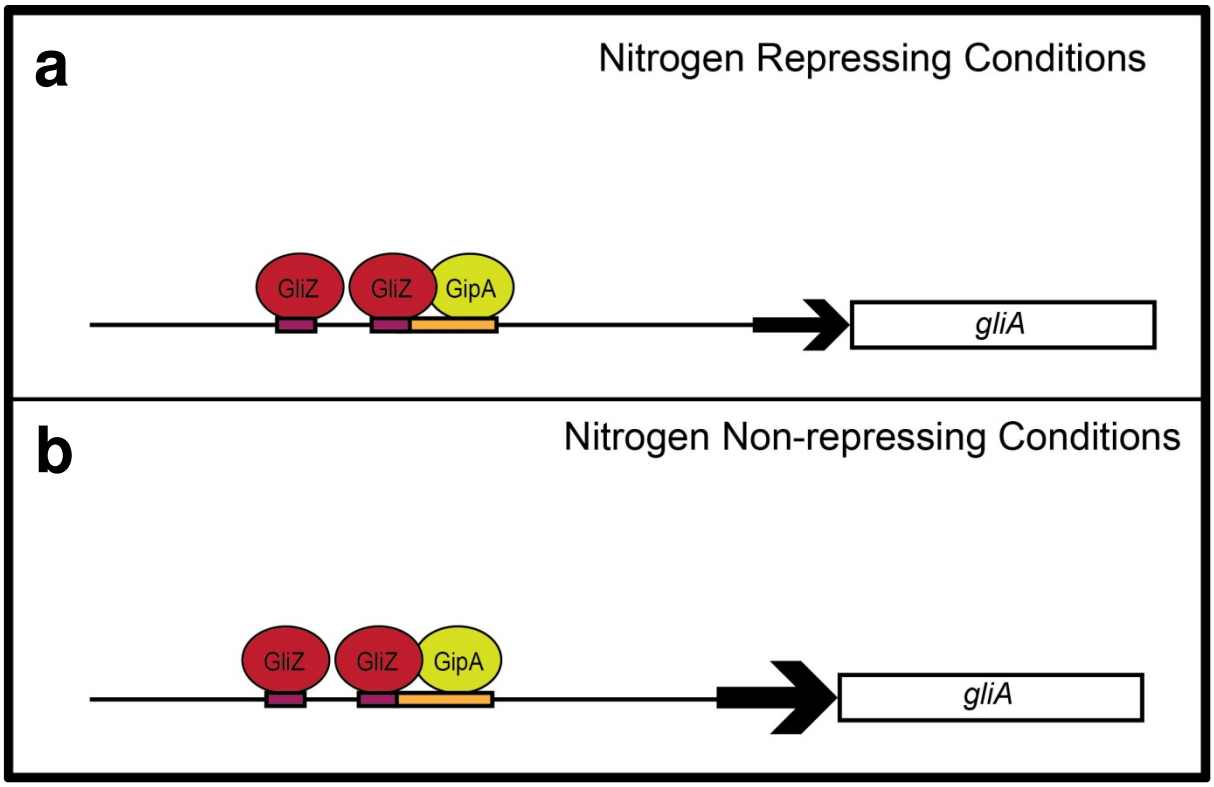


Figure 3.8. Model for *gliA* regulation involving GliZ, GipA, and AreA. (a) I propose that GliZ and GipA both work interdependently to induce *gliA*. (b) Furthermore, I propose that in nitrogen-specific non-repressing conditions, AreA acts to further enhance the expression of *gliA*, likely through induction of *gliZ*.

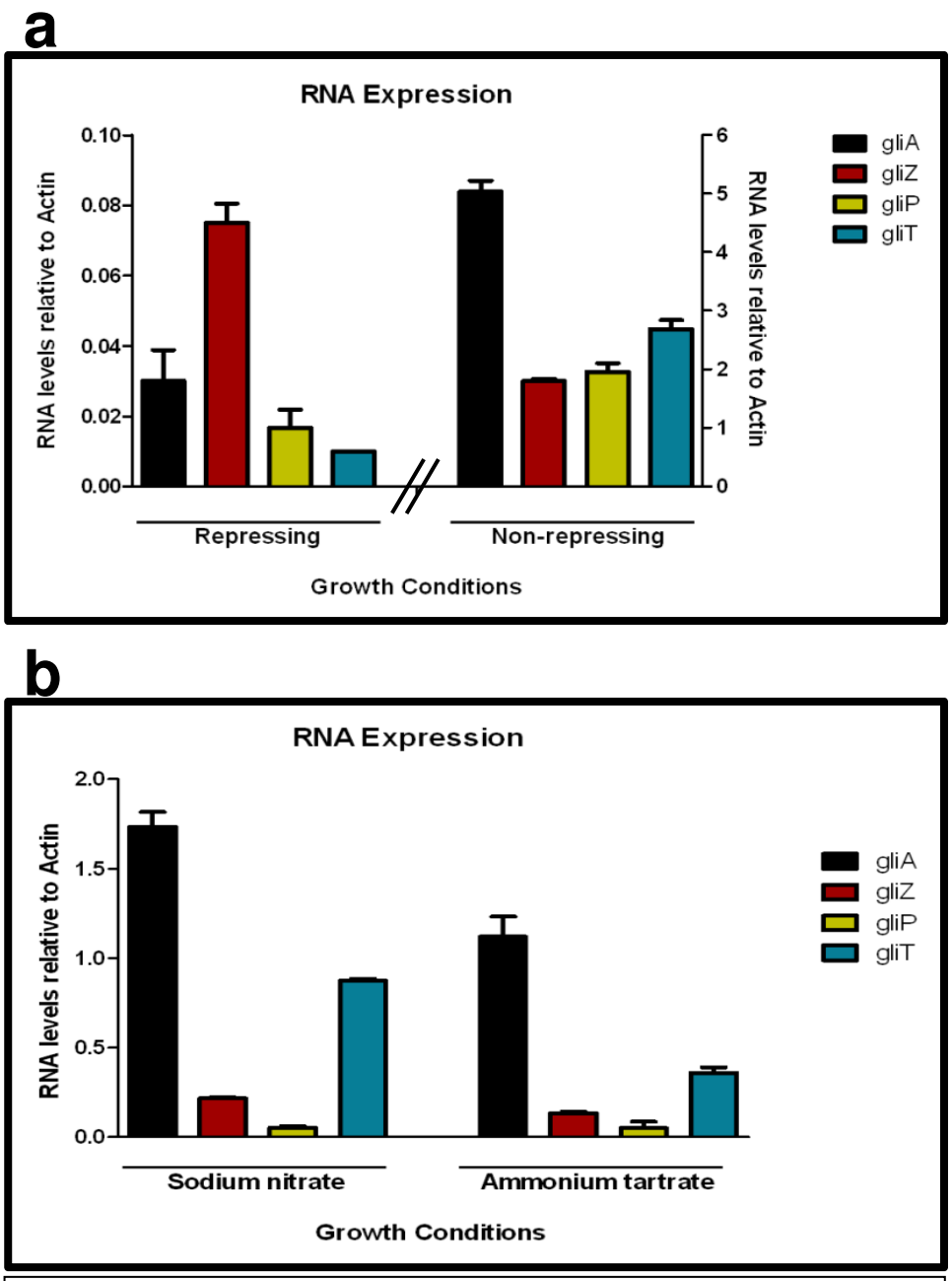


Figure 3.9. Regulation of *gliA* and other gliotoxin cluster genes. (a) Differential mRNA transcript levels of gliotoxin cluster genes in repressing (CM) and non-repressing (CD) media used in this study. (b) Differential mRNA transcript levels of gliotoxin cluster genes in nitrogen-specific non-repressing (SN) and nitrogen-specific repressing (AT) media. mRNA levels are displayed relative to actin. The results of one representative experiment of three independent experiments are shown as mean ± SD.

non-repressing conditions used in this study. Figure 3.9b shows an example of the differential gene expression when cultures are grown in nitrogen-specific repressing or nitrogen-specific non-repressing conditions, implicating AreA in the regulation of the gliotoxin cluster. I present this model as a product of the experiments I describe in the chapters to follow. Although this model does not include GipB, the hybrid sensor kinase from this study, I will discuss later how GipB could be involved in the regulation of *gliA*.

### 3.3 Summary

I performed a high-copy library screen in a strain of *A. fumigatus* that contains a *lacZ* expression plasmid under the control of the *gliA* promoter. I screened for plasmids that induce *lacZ* expression in repressing conditions. Of the 70 plasmids I recovered from the screen, 7 were extreme-inducing (>50-fold *lacZ* induction) and 7 were moderate-inducing (50 to 5-fold *lacZ* induction) (Fig. 3.4/Table 3.1). From the extreme-inducing plasmids, I chose two genes for further studies: *gipA*, a $C_2H_2$ transcription factor, and *gipB*, a hybrid sensor kinase. High-copy expression of GipA induced *lacZ* over 400-fold and high-copy expression of GipB induced *lacZ* 50-fold, compared to AMA.GL (Fig. 3.5b).

Upon sequencing, I discovered that *gipA* has an unusually long 5' UTR, which contains three μORFs. This suggests that *gipA* is under post-transcriptional control, most likely involving translational regulation through one or all of the μORFs. The 3' UTR of *gipA* is also longer than what is seen on average in fungi (200 bps). This could be involved in targeting of the *gipA* transcript for Nonsense Mediated Decay (NMD) [121]. Being a $C_2H_2$ transcription factor, *gipA* contains two DNA binding regions at the 3' end, the first as $X_2$-C-$X_2$-C-$X_{12}$-H-$X_3$-H and the second as $X_2$-C-$X_2$-C-$X_{12}$-H-$X_5$-C (Fig. 3.6). There are two μORFs in the 5' UTR of *gipB*, raising the possibility that *gipB*, like *gipA*, is under some form of post-

transcriptional regulation. As *gipB* is a hybrid sensor kinase, three domains are present that are involved in signal transduction: histidine kinase A (phospho-acceptor) domain, a GHKL (ATPase) domain, and a response regulator receiver domain (Fig. 3.6). At the protein sequence level, neither GipA nor GipB appear to be highly conserved, as only a few proteins in other fungal species showed a high level of similarity, the most conserved being in *N. fischeri* for both proteins (Fig. 3.7). This does not mean that there are not proteins in a variety of other fungal species that function similar to GipA or GipB, as research has shown that primary sequences evolve much more rapidly than tertiary sequences. Therefore, there could be a protein in another fungal organism that has a completely dissimilar sequence to GipA, but has the exact same folding pattern and consequently functions in a similar manner.

Based on experiments performed in this study, I propose a model for GipA-mediated regulation of *gliA*, involving GliZ, the $Zn(II)_2Cys_6$ transcription factor located within the gliotoxin cluster, and AreA, the global positive regulator of nitrogen metabolite repression (Fig. 3.8). My model depicts a situation where GliZ and GipA are both binding to the same site, or within close proximity, and interdependently regulating expression of *gliA*. I propose that AreA is also contributing to the overall induction of *gliA* by inducing *gliZ* in nitrogen-specific non-repressing conditions.

# Chapter 4:

# Characterization of GipA

## 4.1 Introduction

$C_2H_2$ DNA binding regions of transcription factors are the most common type of zinc finger domains, which are stabilized when bound to a zinc ion [122, 123]. The $C_2H_2$ DNA binding domain, which forms a $\beta\beta\alpha$ structure when folded, is so named for the conserved cysteine and histidine residues that bind to the zinc ion (Fig. 4.1). The consensus sequence for the zinc finger domain of these transcription factors is (F/Y)-X-C-$X_{2-5}$-C-$X_3$-(F/Y)-$X_5$-$\Psi$-$X_2$-H-$X_{3-4}$-H, where X is any amino acid and $\Psi$ is any hydrophobic residue, although natural variants that contain a cysteine instead of a histidine as the final zinc-chelating residue ($C_2HC$) produce the same structure (not to be confused with the C-$X_2$-C-$X_4$-H-$X_4$-C class of zinc finger proteins, which folds into a completely different structure) [122, 123]. One transcription factor can contain multiple zinc finger domains, which are often clustered together. $C_2H_2$ zinc finger domains, ubiquitous to all kingdoms, are one of the most commonly found domains within eukaryotes. In fact, recent reports have estimated that 3% of genes within humans contain $C_2H_2$ zinc finger domains, securing their spot as the second most common protein motif [122, 123]. Typically assumed to take part in DNA binding, $C_2H_2$ zinc finger domains have also been proposed to be capable of interacting with RNA and protein [122, 123].

## 4.2 Results

### *4.2.1 High-copy Expression of gipA and Its Effect on Gliotoxin Production*

As previously shown, high-copy expression of *gipA* induces *lacZ* expression, under the control of the *gliA* promoter, which suggests that GipA positively regulates *gliA*. Since the gliotoxin cluster is co-regulated, I predicted that the other genes within the cluster would also be induced in a high-copy *gipA* strain. To verify this, I grew AMA.GL,

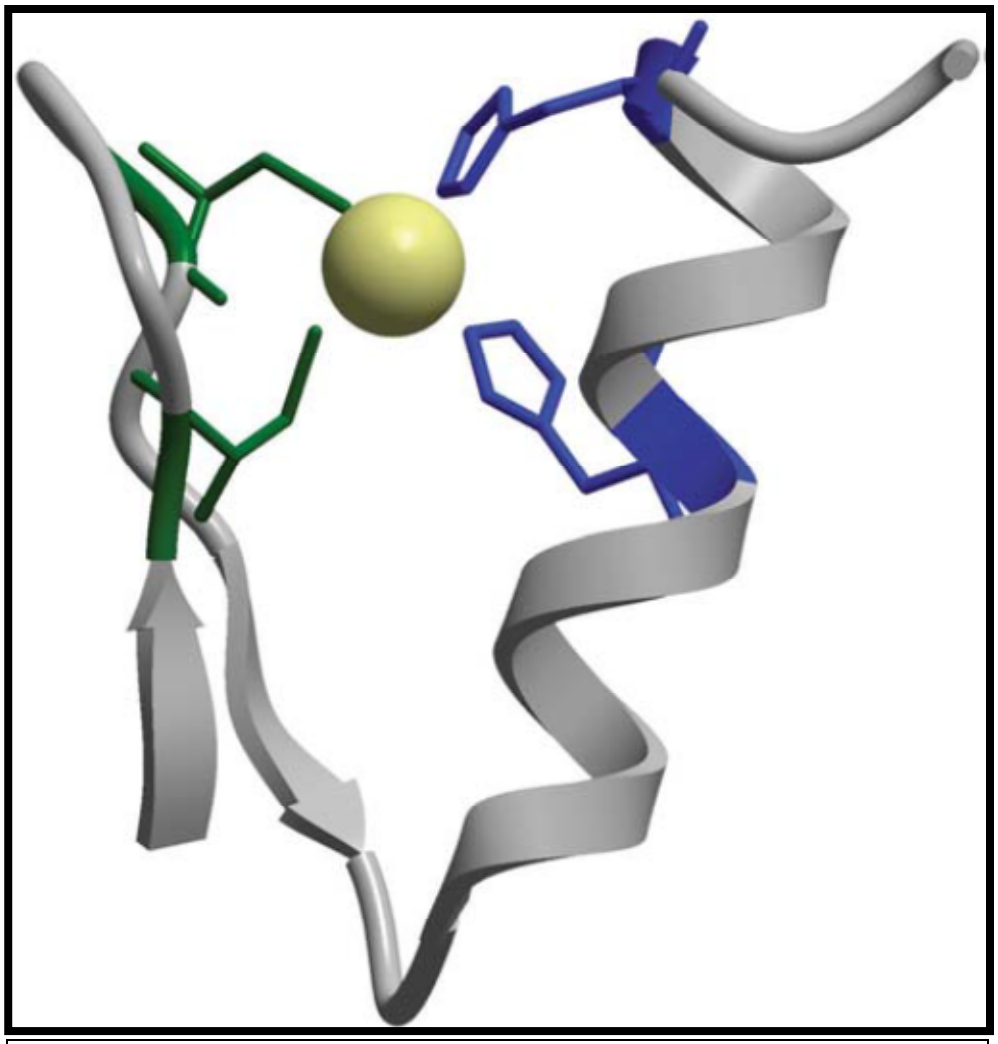

Figure 4.1. The canonical structure of the $C_2H_2$ zinc finger domain. A ribbon diagram representing the third $C_2H_2$ domain from TFIIIA in *Xenopus laevis*, which shows the stabilization of the ββα fold by the interaction of a zinc ion (yellow) with the two cysteine residues (green) and two histidine residues (blue). Reprinted with permission of Springer Science and Business Media: Cell Biochemistry and Biophysics [122], copyright 2008.

AMA-gliZ.GL, and AMA-gipA.GL in repressing conditions and isolated total RNA from mycelia. I quantified RNA levels of multiple genes within the gliotoxin biosynthesis cluster with RNA dot blot analysis. I also measured gliotoxin levels via RP-HPLC. As expected, AMA-gipA.GL had higher levels of *gliA* mRNA, compared to AMA.GL, at both 24 and 48 hours. Transcript levels of gliA in AMA-gipA.GL were 7-fold higher and 4.5-fold higher, compared to AMA.GL, at 24 and 48 hours growth, respectively (Fig. 4.2a & b). The mRNA levels of the other gliotoxin-specific genes tested were also significantly higher in AMA-gipA.GL, compared to AMA.GL, as *gliZ* was induced 2-fold and 12-fold, *gliP* was induced 4.5-fold and 5-fold, and *gliT* was induced 8-fold and 2-fold, at 24 and 48 hours of growth, respectively. Gliotoxin levels reflected what was seen with RNA, as AMA-gipA.GL produced gliotoxin at higher levels than AMA.GL (7-fold by 24 hours) (Fig. 4.2c). AMA-gliZ.GL was the positive control and showed the same pattern as AMA-gipA.GL, with respect to induction of the gliotoxin biosynthesis cluster. Therefore, high-copy expression of *gipA* causes an increase in gliotoxin production in conditions where gliotoxin production is repressed.

### *4.2.2 High-copy Expression of gipA and Its Effect on Growth and Virulence of A. fumigatus*

Producing extra gliotoxin could possibly prove advantageous to the fungus with respect to evading the immune system in a model host, although it could also have disadvantages. For instance, over-expression of *gliZ* displays a trend of increased death in an immune-suppressed murine model of infection [13], but *A. fumigatus*, if not properly protected, is sensitive to the toxic effects of this secondary metabolite, therefore too much gliotoxin could harm the fungus rather than help it [27]. Since high-copy expression of *gipA*

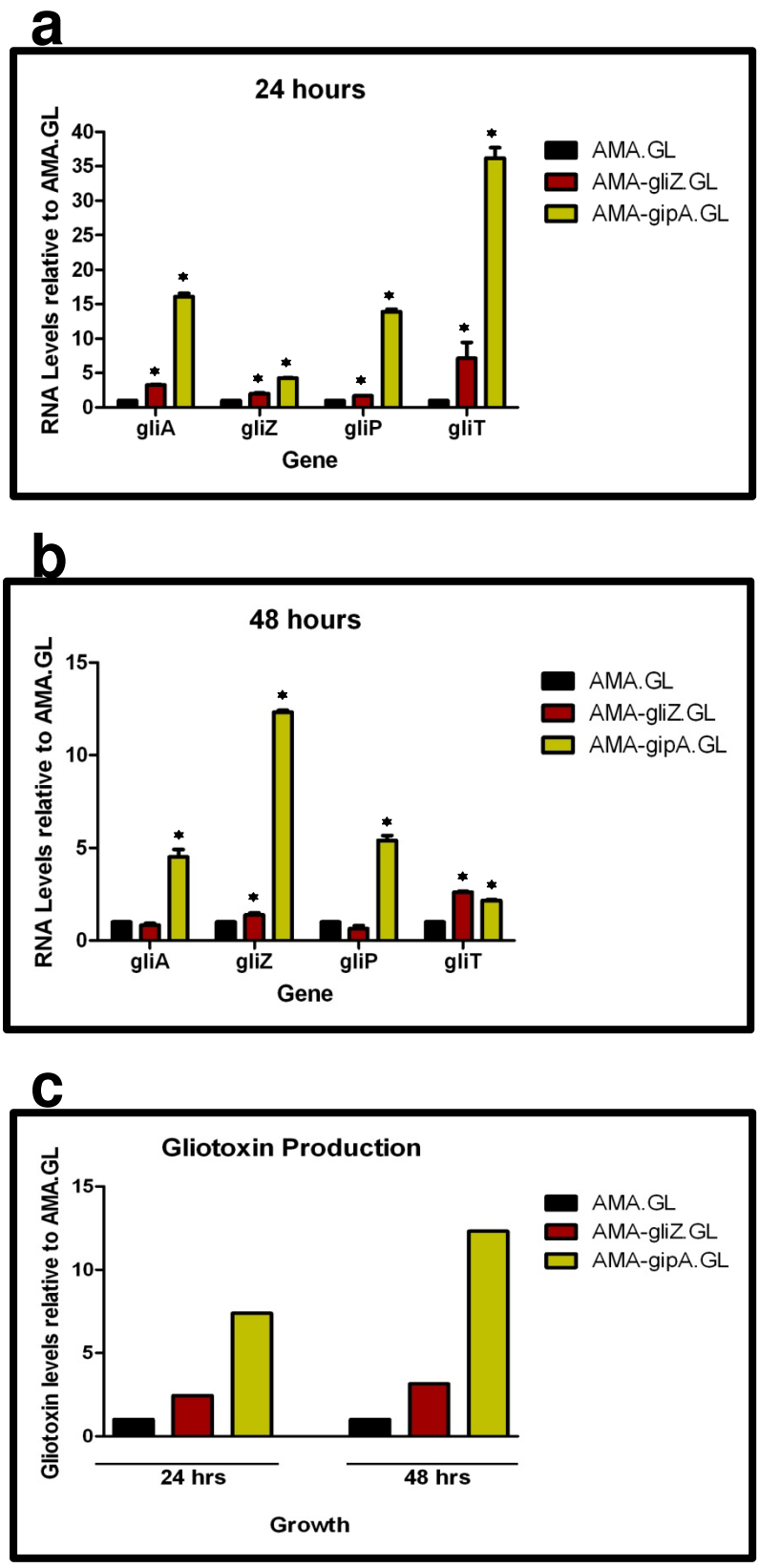


Figure 4.2. High-copy expression of *gipA* induces gliotoxin production. All cultures were grown in repressing conditions. Total RNA was isolated and quantified by dot blot analysis in triplicate. Gliotoxin levels were quantified by RP-HPLC. (a) mRNA transcript levels of several gliotoxin cluster genes after 24 hours of growth. Each data set is normalized to AMA.GL (b) mRNA transcript levels of several gliotoxin cluster genes after 48 hours of growth. Each data set is normalized to AMA.GL. (c) Gliotoxin levels in growth medium, normalized to AMA.GL. The asterisk (*) indicates a statistically significant difference (p-value <0.05), compared to AMA.GL, calculated by one-way ANOVA and Tukey comparison test. The results of one representative experiment of three independent experiments are shown as mean ± SD.

results in increased gliotoxin production, I aimed to test whether this affected growth or virulence of *A. fumigatus*. For growth assays, I inoculated spores of each strain onto rich medium (YAG) and minimal medium (MMVAT), as well as minimal medium with exogenous gliotoxin. AMA.GL, AMA-gliZ.GL, and AMA-gipA.GL all grew similarly on all medium tested, indicating that growth of the fungus is not affected by high-copy expression of *gliZ* or *gipA* (Fig. 4.3). For virulence studies, I infected Toll-deficient *D. melanogaster* fruit flies by needle puncture. This system has been suggested to mimic a steroid-treated, non-neutropenic murine model [23, 124]. Neither AMA-gipA.GL nor AMA-gliZ.GL showed a statistically significant difference in virulence in the Toll-deficient *D. melanogaster* model system, compared to AMA.GL (Fig. 4.4). These data suggest that the high-copy expression of *gipA* is not sufficient to alter the mortality in this model system.

### *4.2.3 Microarray Analysis of GipA regulation*

To expand our view of GipA regulation, a microarray analysis of AMA-gipA.GL vs. AMA.GL, grown in repressing conditions for 24 hours, was performed. Of the 9,436 total genes analyzed, 443 genes were up-regulated > 2-fold and 75 genes were down-regulated > 2-fold in the AMA-gipA.GL strain, compared to the AMA.GL control. There were several genes common to secondary metabolism clusters (e.g. transporters, oxidoreductases, methyltransferases, nonribosomal peptide synthetases and polyketide synthases) up-regulated (Table 4.1). 30 secondary metabolism clusters have been proposed using genomic mapping and microarray techniques [53, 91]. Of these 30 potential secondary metabolism clusters, 20 contained at least one gene that was up-regulated > 2-fold in

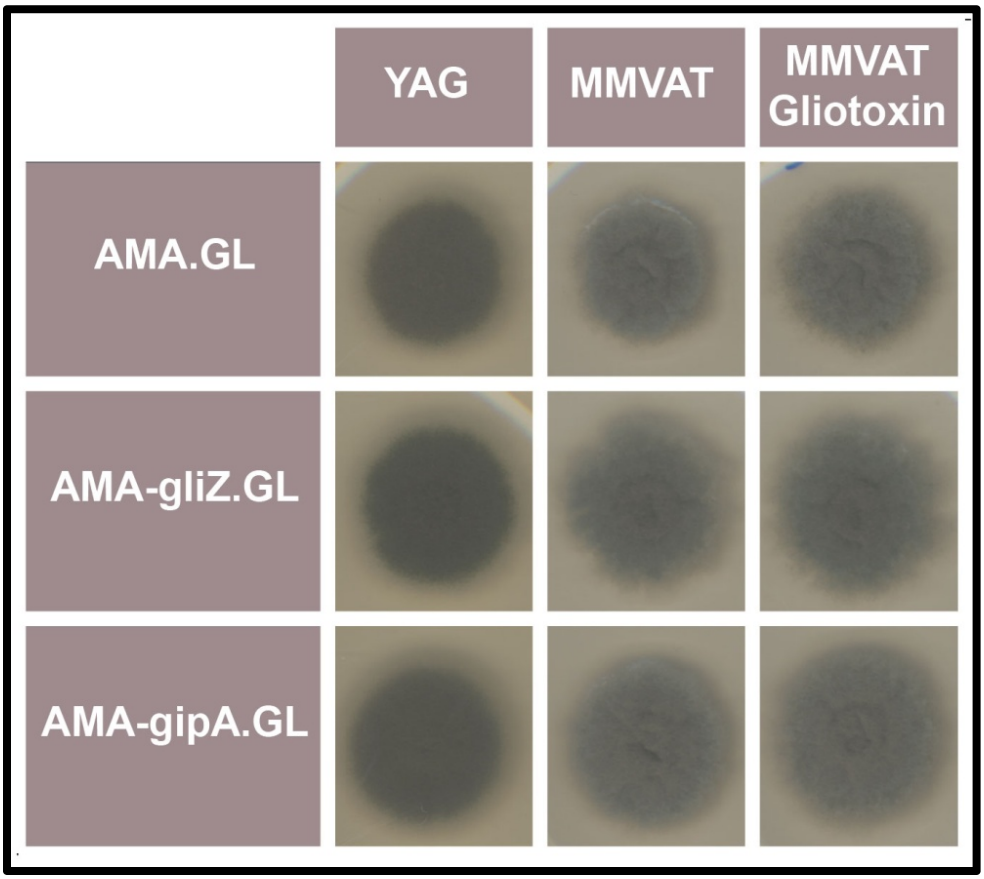


Figure 4.3. High-copy expression of *gipA* does not significantly affect growth of *A. fumigatus*. 1000 spores were spotted onto each plate and incubated at 37℃ for 48 hours (YAG) or 72 hours (MMVAT).

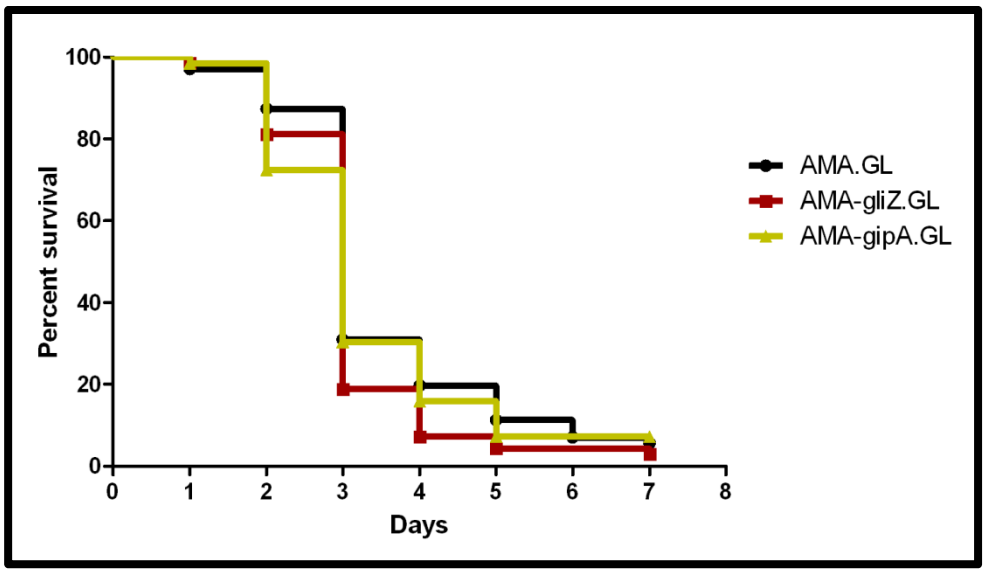


Figure 4.4. High-copy expression of *gipA* does not significantly affect virulence of *A. fumigatus*. Toll-deficient *D. melanogaster* fruit flies were infected by needle puncture and incubated at 29℃ for 7 days. This graph includes three independent virulence assays.

| Genes | Number up-regulated >2-fold |
|---|---|
| Transporters/Pumps | 20 |
| NRPS/PKS | 9 |
| Oxidoreductase | 5 |
| Methyltransferase | 4 |
| Acetyltransferase | 1 |
| C6 Transcription Factors | 8 |

Table 4.1. Genes commonly found to be involved in secondary metabolism possibly regulated by GipA.

| Cluster | Cluster range* | Product |
|---|---|---|
| 1 | Afu1g17710-Afu1g17740 | Unknown |
| 2 | Afu2g05730-Afu2g05840 | Unknown |
| 3 | Afu2g17930-Afu2g18060 | Ergot alkaloids: Festuclavine, Elymoclavine, Fumigaclavines A, B, and C |
| 4 | Afu3g01400-Afu3g01560 | Unknown |
| 5 | Afu3g02570-Afu3g02640 | Unknown |
| 6 | Afu3g02670-Afu3g02760 | Unknown |
| 7 | Afu3g03280-Afu3g03580 | Possibly two compounds: (a siderophore and a distinct toxin) |
| 8 | Afu3g12770-Afu3g13000 | Putative ETP |
| 9 | Afu3g14690-Afu3g14880 | Unknown |
| 10 | Afu3g15250-Afu3g15290 | Unknown |
| 11 | Afu4g00210-Afu4g00260 | Unknown |
| 12 | Afu4g14440-Afu4g14730 | Unknown |
| 13 | Afu5g09940-Afu5g10220 | Unknown |
| 14 | Afu5g12720-Afu5g12840 | Unknown |
| 15 | Afu6g08540-Afu6g08560 | Unknown |
| 16 | Afu6g09580-Afu6g09740 | Gliotoxin |
| 17 | Afu6g12040-Afu6g12160 | Unknown |
| 18 | Afu7g00120-Afu7g00180 | Unknown |
| 19 | Afu8g00100-Afu8g0280 | Fumitremorgen B |
| 20 | Afu8g02350-Afu8g02460 | Unknown |

Table 4.2. Secondary metabolism clusters I predict to be positively regulated by GipA. *Cluster ranges were predicted using SMURF [125] and can be found at http://jcvi.org/smurf/index.php.

AMA-gipA.GL, compared to AMA.GL (Table 4.2). Based on microarray data obtained previously [91], loss of *laeA*, a global regulator of secondary metabolism, affected 13 of 22 identified secondary metabolite clusters. This suggests that GipA is not specific to the gliotoxin cluster, but potentially acts on numerous other secondary metabolism gene clusters in *A. fumigatus*, similar to LaeA.

### *4.2.4 Deletion of gipA and Its Effect on Gliotoxin Production*

Since GipA can induce gliotoxin production, I sought to discover if loss of *gipA* has any effect on the gliotoxin cluster. I replaced the coding region of *gipA* with *pyrG* and designated this strain as *ΔgipA*. I created a complemented strain, *gipA*(R), using hygromycin (*hph*) as the selective marker. I also created a *gliZ* deletion strain as a control, since previous studies have shown that loss of *gliZ* results in a significant decrease in RNA levels of gliotoxin-specific genes [13]. As shown in Figure 4.5a, loss of *gipA* caused a significant decrease in mRNA levels of *gliA, gliZ, gliP, and gliT* in non-repressing conditions, as most genes exhibited close to a 50% reduction. The gliotoxin biosynthesis cluster is not completely dependent on *gipA*, as there was still RNA being made for the genes I tested. The *gipA* deletion mutant also produced significantly less gliotoxin than the 1160G control strain (50% reduction) (Fig. 4.5b), which suggests that *gipA* may be an important positive regulator of gliotoxin production. Gliotoxin-specific gene expression and gliotoxin production of *gipA*(R) were restored beyond wild-type levels, which demonstrates that the effect I observed with the *gipA* deletion was due to the absence of *gipA*. As expected, loss of *gliZ* caused almost a complete loss in gene expression for *gliA, gliP*, and *gliT* and abolished gliotoxin production.

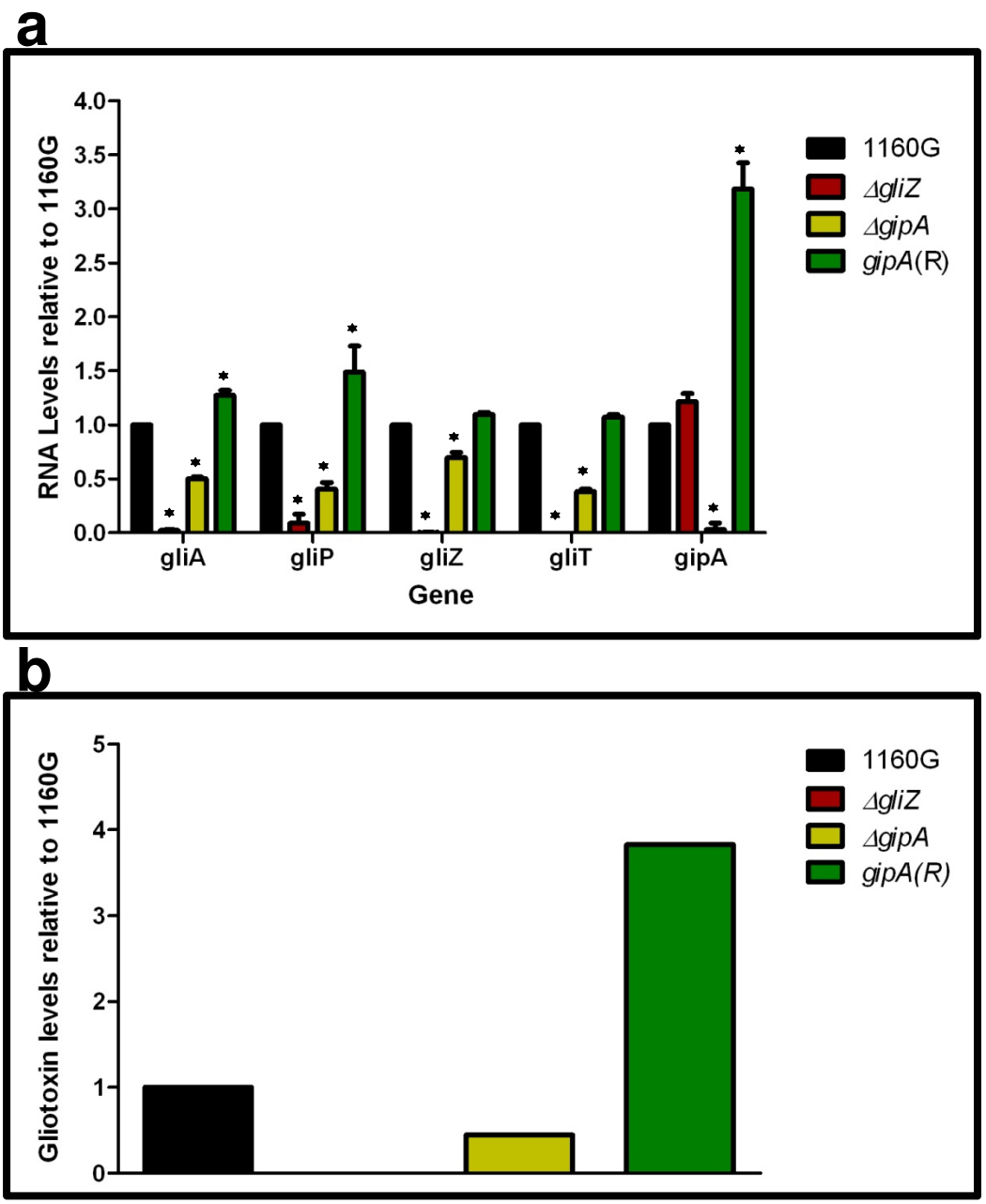


Figure 4.5. Loss of *gipA* negatively affects gliotoxin production. All cultures were grown for 48 hours in non-repressing conditions. Total RNA was isolated and quantified by dot blot analysis in triplicate. Gliotoxin levels were quantified by RP-HPLC. (a) mRNA transcript levels of several gliotoxin cluster genes. Each data set is normalized to 1160G. The results of one representative experiment of three independent experiments are shown as mean ± SD. (b) Gliotoxin levels in growth medium, normalized to 1160G. The results of one representative experiment of three independent experiments are shown. The asterisk (*) indicates a statistically significant difference (p-value <0.05), compared to 1160G, calculated by one-way ANOVA and Tukey comparison test.

*4.2.5 Deletion of gipA and Its Effect on Growth and Virulence of A. fumigatus*

As *gipA* is important for gliotoxin production, I sought to determine if loss of *gipA* would affect the growth or pathogenicity of *A. fumigatus*. Loss of *gliT*, which plays a role in self-protection of the fungus against gliotoxin, results in the inability of *A. fumigatus* to grow in the presence of exogenous gliotoxin [27]. Loss of *gipA* causes a significant decrease in *gliT* mRNA transcript levels, which could adversely affect the ability of the fungus to grow in the presence of exogenous gliotoxin. Furthermore, deletion of *gliP*, which is required for the biosynthesis of gliotoxin and consequently abolishes gliotoxin production, was found to cause a significant attenuation in virulence of *A. fumigatus* in a Toll-deficient *D. melanogaster* model system [23]. Therefore, a significant reduction in gliotoxin production from loss of *gipA* could negatively affect the virulence of *A. fumigatus* in this model system.

Growth of *ΔgliZ* and *ΔgipA* on minimal and rich media was comparable to the 1160G control, indicating that loss of either *gliZ* or *gipA* does not adversely affect radial growth or conidiation on the medium tested. Addition of exogenous gliotoxin (10 μg/ml) did not significantly affect the growth of either deletion strain, compared to the 1160G control (Fig. 4.6). These data support previous findings that *gliT* is independently regulated and does not require GliZ for self-protection [27]. Furthermore, even though gliotoxin is being produced at significantly reduced levels in both *ΔgliZ* and *ΔgipA*, there was no statistically significant difference in virulence of either deletion strain, compared to 1160G, in a Toll-deficient *D. melanogaster* model system (Fig. 4.7), suggesting neither gene is essential for *A. fumigatus* pathogenicity in this model system. This does not rule out the possibility that GipA may affect the ability of *A. fumigatus* to modulate immune-cell functions, but any effects that might be there are not enough to alter the overall mortality rate in the model system I tested.

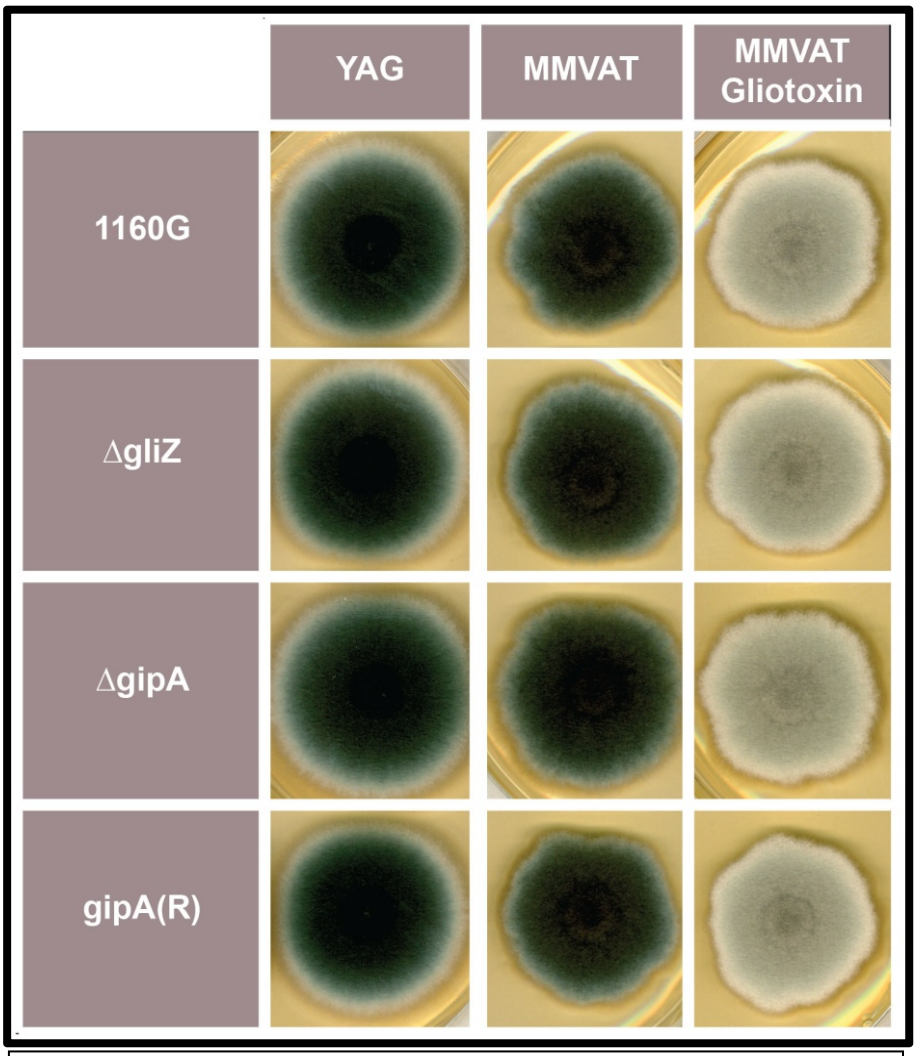


Figure 4.6. Loss of *gipA* does not significantly affect growth of *A. fumigatus*. 1000 spores were spotted onto each plate and incubated at 37℃ for 48 hours (YAG) or 72 hours (MMVAT).

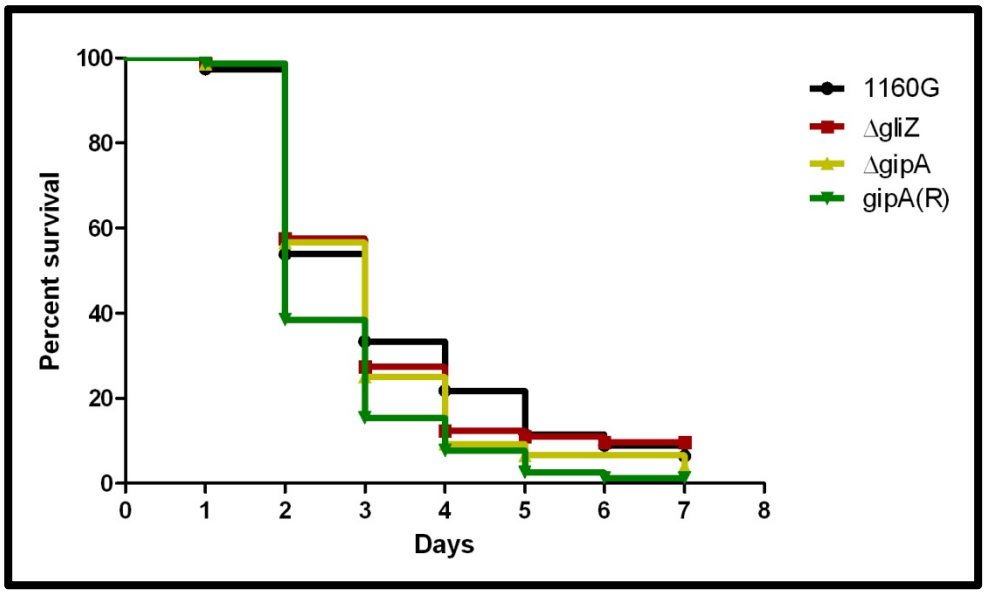


Figure 4.7. Loss of *gipA* does not significantly affect virulence of *A. fumigatus*. Toll-deficient *D. melanogaster* fruit flies were infected by needle puncture and incubated at 29℃ for 7 days. This graph includes three independent virulence assays.

*4.2.6 Identification of a DNA Binding Site for GipA*

Since GipA is a $C_2H_2$ transcription factor, it is highly likely that GipA is directly binding to DNA. I sought to identify a consensus sequence and to discover if this sequence was present within the gliotoxin biosynthesis cluster. I fused a GST tag onto the 5' end of the DNA binding region of GipA for a protein-binding microarray analysis (done by Tim Hughes' Laboratory), which identified a consensus DNA binding sequence for GipA (5'-TNNVMGCCNC-3') (Fig. 4.8). This putative sequence is 10 nucleotides, which coincides with one complete turn of the DNA double helix. The protein-binding microarray verified direct DNA binding of GipA, as the purified DNA-binding region, and not whole cell extract, was analyzed in the microarray. I analyzed the genomic sequence of the gliotoxin biosynthesis cluster to locate potential GipA binding sites. Indeed, I found variations of this consensus sequence scattered throughout the gliotoxin biosynthesis cluster. In fact, I identified a possible GipA binding site within the intergenic region of *gliA* (5'-TTGCCGCCAC-3' 315 bp upstream of the start site), as well as all other gliotoxin-specific genes, except *gliM*.

*4.2.7 gliA Promoter Mutagenesis*

To verify that GipA was in fact exerting its effects through this sequence, I mutated the GipA binding site on pDHGL, which contains *lacZ* flanked by the *gliA* 5' and 3' NCRs. I created two mutated binding sites: SD1 (**T**TGCCGCCAC → **C**TGCCGCCAC) and SD2 (TTG**CCGCCA**C → TTG**GGTGAG**C). I transformed these plasmids into an Af293.1 background and then transformed pDONR AMA, pDONR AMA-*gliZ*, and pDONR AMA-*gipA*

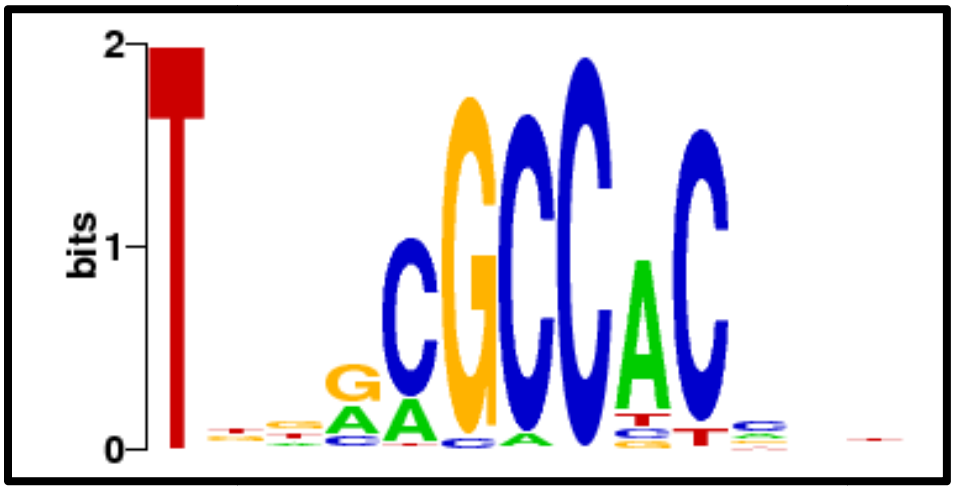


Figure 4.8. Consensus sequence representing the putative DNA binding site for GipA obtained by protein binding microarray analysis.

into each strain. Therefore, each version of the binding site was exposed to extra copies of *gliZ (*AMA-gliZ.GL, AMA-gliZ.SD1, and AMA-gliZ.SD2), extra copies of *gipA* (AMA-gipA.GL, AMA-gipA.SD1, and AMA-gipA.SD2), or a pDONR AMA empty vector control (AMA.GL, AMA.SD1, and AMA.SD2). The pDONR AMA empty vector control served as a negative control. I grew these strains in both repressing and non-repressing conditions. Under repressing conditions, expression would be based solely on extra copies of the gene within the pDONR AMA plasmid or any other transcriptional activator present, while under non-repressing conditions, expression would show induction of *lacZ* in response to the nutritional environment, as well as the pDONR AMA plasmids. Two different patterns emerged between LacZ levels that were normalized to actin and LacZ levels that were additionally normalized to the pDONR AMA control. The LacZ levels that are normalized to actin depict the overall expression of *lacZ* in each strain, which could be affected by GliZ or GipA specifically, but also any other regulatory elements. By further normalizing data to pDONR AMA, I was able to observe induction of *lacZ* based solely on extra copies of GliZ or extra copies of GipA.

In Figure 4.9a, I present *lacZ* expression levels of AMA.GL, AMA.SD1, and AMA.SD2, relative to actin. I did not include the data for the pDONR AMA-*gliZ* or pDONR AMA-*gipA* strains, because all three pDONR AMA strains followed the same pattern, regardless of which pDONR AMA vector was being expressed. In AMA.GL, which harbors the wild-type binding site, there was a moderate level of LacZ in repressing conditions. This could be due to the presence of endogenous GliZ or GipA, as well as any other endogenous inducers specific to *gliA* expression. When AMA.GL was grown in non-repressing conditions, LacZ levels increased 30-fold, compared to repressing conditions (Fig. 4.9a). This is to be expected because the gliotoxin cluster is being induced in these

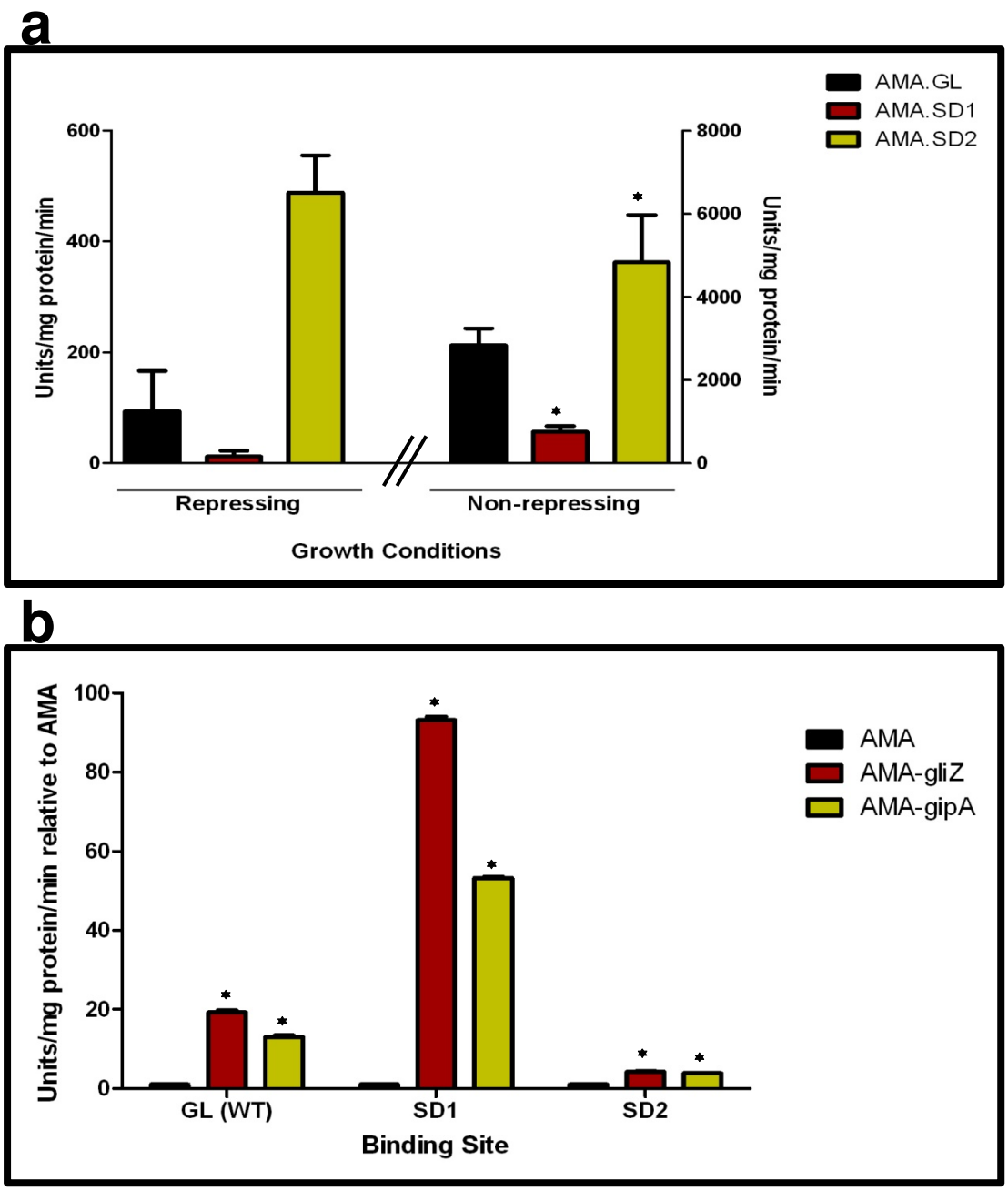


Figure 4.9. GipA and GliZ both induce *gliA* through the GipA binding site. Strains were grown in stationary cultures. Total protein was collected from lyophilized mycelia and β-galactosidase activity was measured. (a) LacZ levels of AMA.GL in both repressing and non-repressing conditions. The results of one representative experiment of three independent experiments are shown as mean ± SD. (b) LacZ levels of each strain in repressing conditions, relative to the AMA control. The results of one representative experiment of six independent experiments are shown as mean ± SD. The asterisk (*) indicates a statistically significant difference (p-value <0.05) for each data set, compared to the AMA control strain, calculated by one-way ANOVA and Tukey comparison test.

conditions. Furthermore, carbon sources used in all conditions are known to suppress endogenous β-galactosidase activity, therefore the β-galactosidase activity reported in these experiments should be specific to the *gliA*$^{P}$-*lacZ* expression plasmid. AMA.SD1 displayed decreased expression of *lacZ* (8-fold in repressing conditions and 4-fold in non-repressing conditions), compared to AMA.GL (Fig. 4.9a). This suggests that mutation of the single 5' T residue interferes with the binding of an unknown transcriptional activator. This could also be a result of a lower affinity of GipA for the binding site, instead of an unidentified transcriptional activator, however if this were the case, I would expect AMA.SD2 to have lower β-galactosidase activity, similar to AMA.SD1. In fact, LacZ levels of AMA.SD2 were higher than those of AMA.GL (5-fold in repressing conditions and almost 2-fold in non-repressing conditions), supporting my hypothesis that an unidentified transcriptional activator is being displaced by mutation of the 5' T residue (Fig. 4.9a). Since the 5' T residue is present in AMA.SD2, the binding of an unknown transcriptional activator would be restored and LacZ levels would increase. AMA.SD2 harbors a mutation in the core region of the GipA binding site, so the increased levels of LacZ in AMA.SD2, compared to AMA.GL, could be due to the loss of some form of repression. The fold changes in non-repressing conditions were not as robust as those in repressing conditions, but this is to be expected as *gliA* is also being induced in response to nutritional sources in the non-repressing medium.

Figure 4.9b depicts *lacZ* expression relative to AMA.GL in repressing conditions. With the wild-type binding site, the presence of pDONR AMA-*gipA* increased LacZ levels 13-fold, relative to the pDONR AMA control, as to be expected from previous results (Fig. 4.9b). With the SD1 binding site, pDONR AMA-*gipA* also induced *lacZ* significantly (53-fold), relative to the pDONR AMA strain (Fig. 4.9b). The magnitude of induction was enhanced with the SD1 mutation when compared to the wild-type binding site (13-fold vs.

53-fold, respectively), possibly due to background LacZ levels being lower. This difference in magnitude could also due to an increased affinity of GipA to the DNA binding site, as a result of mutating the 5' T residue to C. With the SD2 binding site, in which the core region has been mutated, the pDONR AMA-*gipA* strain only weakly induced *lacZ* (4-fold), as the fold-change relative to pDONR AMA was greatly reduced, compared to the wild-type binding site (13-fold vs. 4-fold, respectively) (Fig. 4.9b). This suggests that mutation of a core sequence in the binding site significantly reduces the ability of GipA to induce *lacZ*, likely as a result of decreased binding affinity. When grown in non-repressing conditions, LacZ levels of the pDONR AMA-*gipA* strain were comparable to the pDONR AMA empty vector control in all binding site backgrounds (data not shown). This indicates that induction of *gliA*, in response to nutrient availability, is already sufficiently robust, so extra copies of *gipA* add no further induction. Interestingly, expression of *lacZ* in the pDONR AMA-*gliZ* strains followed a similar pattern to that of the pDONR AMA-*gipA* strains (Fig. 4.9b). Therefore, *lacZ* was induced by GliZ with the wild-type binding site (19-fold) and the SD1 binding site (93-fold). The level of induction was enhanced by the SD1 binding site, compared to the wild-type binding site (19-fold vs. 93-fold, respectively). Furthermore, *lacZ* was only weakly induced by GliZ, relative to the pDONR AMA control, when exposed to the SD2 binding site (4-fold). Therefore, mutation of the GipA binding site is also affecting the ability of GliZ to induce *gliA*.

### 4.3 Summary

As a high-copy *gipA* strain was able to induce *lacZ*, under the control of the *gliA* promoter, in repressing conditions, I sought to identify what effects this transcription factor has on the gliotoxin cluster. Being a $C_2H_2$ transcription factor, I also wanted to determine if

GipA is binding to the *gliA* promoter region to elicit the response I observed. High-copy expression of *gipA* not only induced *gliA*, the efflux pump of the gliotoxin cluster, but also induced several other genes within the gliotoxin cluster and enhanced production of gliotoxin in repressing conditions at both time points, suggesting that GipA plays a positive role in regulating the cluster (Fig. 4.2). This did not significantly affect growth of *A. fumigatus*, nor did it change the virulence of the fungus in a toll-deficient *D. melanogaster* model system, indicating that artificially inducing the gliotoxin cluster through *gipA* does not render the fungus growth deficient or more virulent in the model tested (Fig. 4.3 & 4.4). Microarray data revealed that 20 out of 30 possible secondary metabolism clusters in *A. fumigatus*, including the gliotoxin cluster, are also possibly induced in a high-copy *gipA* strain, revealing the possibility that GipA is not strictly regulating the gliotoxin cluster, but may be acting as a general regulator of secondary metabolism, similar to LaeA (Table 4.2).

Furthermore, loss of *gipA* negatively affected the expression of several gliotoxin-specific genes, as mRNA transcript levels were reduced close to 50%, compared to a wild-type strain (Fig. 4.5a). Gliotoxin production was also significantly reduced in a *ΔgipA* strain in non-repressing conditions, indicating that GipA is important for full induction of the gliotoxin cluster in the conditions I tested, but not essential (Fig. 4.5b). Growth was not significantly affected by the loss of *gipA*, indicating that *gipA* is not essential to the growth rate of the fungus (Fig. 4.6). The *ΔgipA* strain did not show an alteration in virulence in a Toll-deficient *D. melanogaster* model, signifying that GipA is not essential to the virulence of *A. fumigatus,* although this does not rule out the possibility that GipA is important in the fungal virulence at the cellular level (Fig. 4.7).

A consensus sequence was identified for GipA *in vitro* (5'-TNNVMGCCNC-3'), and verified *in vivo* using a *gliA*$^{P}$*-lacZ* expression plasmid and mutagenesis of the GipA DNA binding site (Figs. 4.8 & 4.9). Mutation of the 5' T residue did not eliminate GipA-mediated

*lacZ* expression, however, mutation of a core region almost completely abolished the ability of GipA to induce *lacZ*. Interestingly, GliZ-mediated induction of *lacZ* was also dependent on the core region, suggesting that GliZ and GipA signal through the same binding site, or at least in close proximity. Even though the mutation of the 5' T residue did not negatively affect the ability of GipA or GliZ to induce *lacZ*, it did reduce background levels of *lacZ* expression, suggesting that disrupting the T residue altered binding of an unidentified activator. Cultures were grown in conditions that promote suppression of endogenous β-galactosidase activity, indicating that my observations were based on *lacZ* expression specifically from the *gliA*$^{P}$*-lacZ* plasmid.

# Chapter 5:

# Characterization of GipB

## 5.1 Introduction

Hybrid sensor kinases are involved in two-component signaling in response to external stimuli. These proteins are termed hybrid sensor kinases because they contain both a histidine kinase domain and a response regulator domain [126, 127]. Two-component systems were first discovered in prokaryotes and entail two elements: (1) a sensor histidine kinase that is autophosphorylated, in response to external signals, at a conserved histidine residue and (2) a response regulator that obtains the activation signal from the sensor histidine kinase via phosphorylation of a conserved aspartate residue [126, 127]. Although these two-component systems remain highly similar in different genera, fungal two-component systems are different, in that they involve three elements: (1) a hybrid sensor kinase, which is composed of a histidine kinase domain and a response regulator domain, (2) a histidine-containing phosphotransfer (HPt) domain, and (3) a separate response regulator [126, 127].

As with bacterial two-component systems, the histidine kinase domain autophosphorylates at a conserved histidine residue, after which the phosphate is relayed to an aspartate residue located in the response regulator domain of the same protein [126, 127]. The phosphate is then relocated to the HPt protein, at a conserved histidine residue, and is subsequently transferred to the second response regulator, again to an aspartate residue. Downstream targets of this two-component signaling network can either be directly modulated by the second response regulator protein or they can be activated by a signaling cascade, oftentimes a MAPK pathway, responding to the response regulator protein [126, 127] (Fig. 5.1). This system of two-component phosphorelay has been reported in prokaryotes and lower eukaryotes, but not the animal kingdom, as sensor-type histidine kinases have not been discovered, making these proteins unique targets for antimicrobial therapies [126, 127].

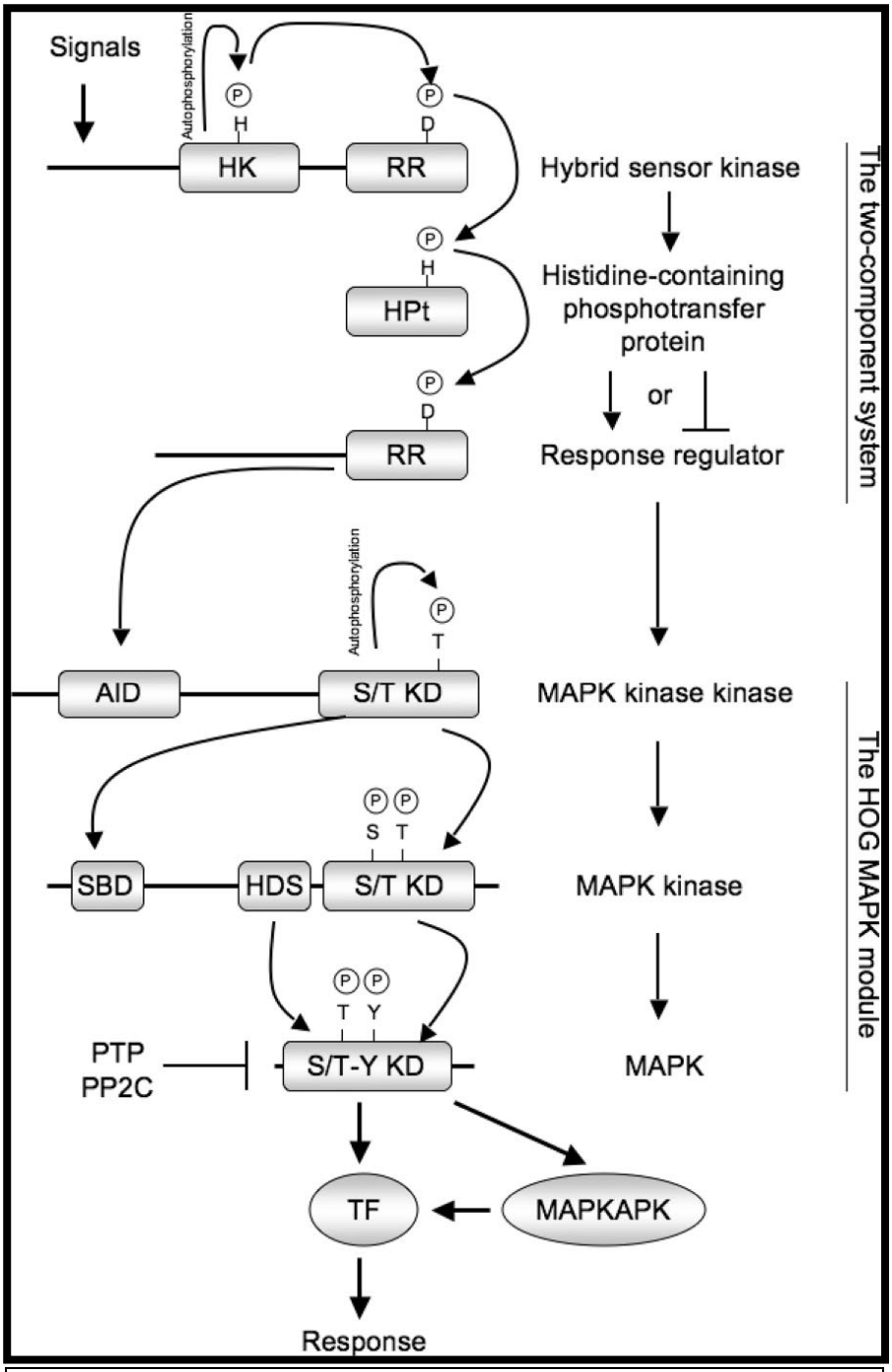


Figure 5.1. General regulatory mechanism of a fungal hybrid sensor kinase, involving the HOG MAPK pathway. Abbreviations: HK, histidine KD; RR, response regulator receiver domain; S/T kinase, Ser/Thr protein KD; SBD, Ssk2/Ssk22 binding domain; HDS, Hog1 docking site; S/T-Y KD, Ser/Thr and Tyr dual-protein KD. Reprinted with permission of American Society for Microbiology: Eukaryotic Cell [127], copyright 2008.

One of the best-characterized fungal two-component systems is the Sln1-Ypd1-Ssk1 phosphorelay system in *S. cerevisiae*. Sln1, a transmembrane hybrid sensor kinase that serves as an osmosensor, transfers a phosphoryl group to Ypd1, the HPt protein [55, 126, 127]. Under normal conditions, Ssk1, the response regulator, remains constitutively phosphorylated via Sln1 and Ypd1, which renders it inactive. However, under hyperosmotic shock, Ssk1 becomes dephosphorylated, through down-regulation of the Sln1-Ypd1-dependent phosphorylation, which allows Ssk1 to activate the HOG pathway via interaction with the MAPKKK, Ssk2 [55, 126, 127]. Some hybrid sensor kinases are transmembrane domains, while others lack transmembrane regions and therefore remain cytosolic. Of the cytosolic hybrid sensor kinases that have been studied so far in filamentous fungi, most appear to be more important in regulating morphogenesis and developmental processes than the transmembrane histidine kinases [127].

## 5.2 Results

### *5.2.1 High-Copy Expression of gipB and Its Effect on Gliotoxin Production*

Similar to what is seen with *gipA*, high-copy expression of *gipB* induces *lacZ* expression, under the control of the *gliA* promoter, which suggests that GipB positively regulates *gliA*. Since the gliotoxin cluster is co-regulated, I predicted that the other genes within the cluster would also be induced in a high-copy *gipB* strain. To test the effect of *gipB* on the gliotoxin cluster, I performed RNA dot blot analysis and measured gliotoxin production as described for *gipA*. Comparable to what I observed with *gipA*, extra copies of *gipB* (AMA-gipB.GL) caused an increase in transcription of several genes within the gliotoxin cluster at 24 hours, but not after 48 hours of growth (Fig. 5.2a). Furthermore,

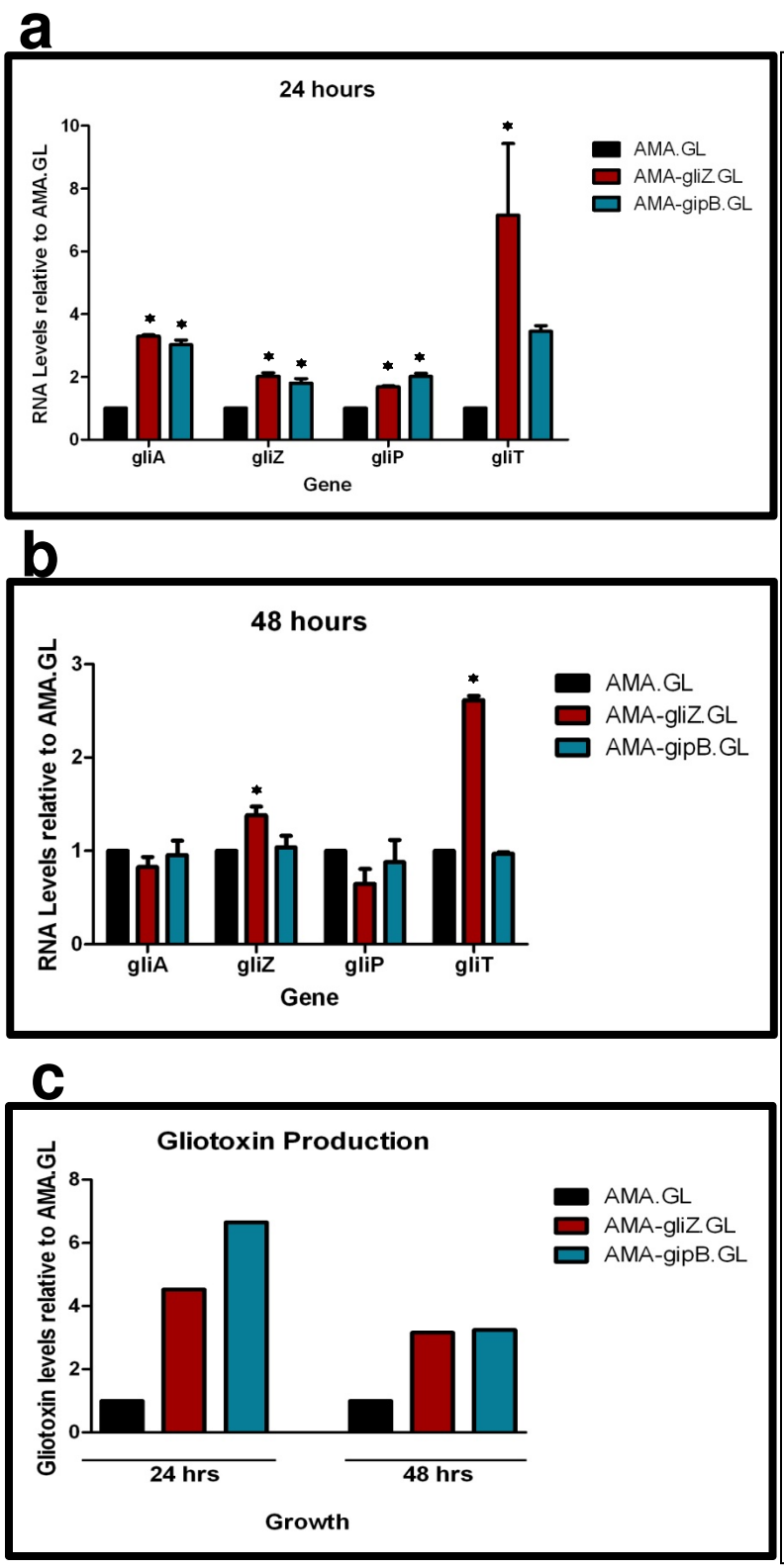


Figure 5.2. High-copy expression of *gipB* induces gliotoxin production at 24 hours growth, but not 48 hours growth. All cultures were grown in repressing conditions. Total RNA was isolated and quantified by dot blot analysis in triplicate. Gliotoxin levels were quantified by RP-HPLC. (a) mRNA transcript levels of several gliotoxin cluster genes after 24 hours of growth. (b) mRNA transcript levels of several gliotoxin cluster genes after 48 hours of growth. Each data set for (a) and (b) is normalized to AMA.GL. The results of one representative experiment of three independent experiments are shown as mean ± SD. (c) Gliotoxin levels in growth medium, normalized to AMA.GL. The results of one representative experiment of three independent experiments are shown. The asterisk (*) indicates a statistically significant difference (p-value <0.05), compared to AMA.GL, calculated by one-way ANOVA and Tukey comparison test.

gliotoxin was made at higher levels in AMA-gipB.GL at both time points, compared to the AMA.GL control (Fig. 5.2b). The lack of induction of gliotoxin-specific genes after 48 hours growth suggests that GipB is not activated during the later phase of asexual development. Although gene expression was not affected by high-copy expression of *gipB* after 48 hours growth, a higher amount of gliotoxin was detected in the surrounding medium, compared to the AMA.GL strain (Fig. 5.2c). This is not surprising as high-copy expression of *gipB* did induce gliotoxin production after 24 hours growth, therefore the gliotoxin detected at 48 hours growth was likely produced at an earlier time point. The level of induction was not as robust as in AMA-gipA.GL, which is to be expected, as GipB is a hybrid sensor kinase possibly acting upstream of several proteins.

### *5.2.2 High-copy Expression of gipB and Its Effect on Growth and Virulence of A. fumigatus*

Since high-copy expression of *gipB* results in increased gliotoxin production at 24 hours, I aimed to test whether this affected growth or virulence of *A. fumigatus,* as dysregulation of the gliotoxin cluster could cause adverse effects. Furthermore, over-expression of *gliZ* displays a trend towards increased death in an immune-suppressed murine model of infection [13]. For growth assays, I inoculated 1000 spores of each strain onto rich medium (YAG) and minimal medium (MMVAT), as well as minimal medium with exogenous gliotoxin. AMA-gipB.GL grew similarly on all medium tested, indicating that high-copy expression of *gipB* does not affect radial growth of *A. fumigatus* (Fig. 5.3). For virulence studies, I infected Toll-deficient *D. melanogaster* fruit flies by needle puncture. This system has been suggested to mimic a steroid-treated, non-neutropenic murine model [23, 124]. There was no statistically significant difference in virulence between

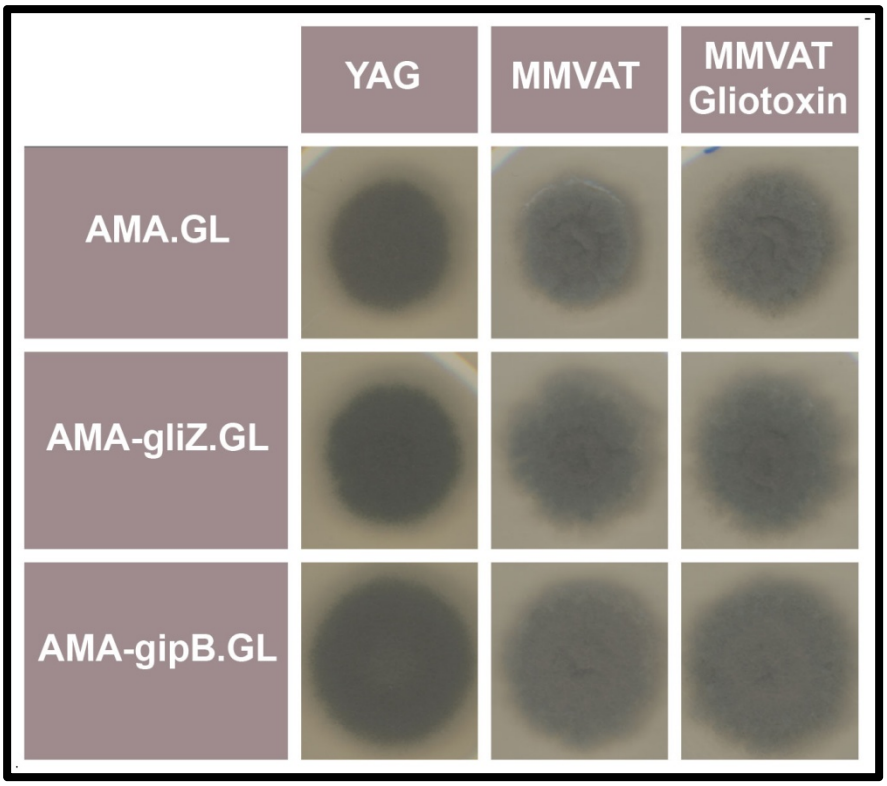


Figure 5.3. High-copy expression of *gipB* does not significantly affect growth of *A. fumigatus*. 1000 spores were spotted onto each plate and incubated at 37℃ for 48 hours (YAG) or 72 hours (MMVAT).

AMA-gipB.GL and AMA.GL, which suggests that *gipB* does not contribute to the virulence of *A. fumigatus* in this model system (Fig. 5.4).

### *5.2.3 Deletion of gipB and Its Effect on Gliotoxin Production*

I also wanted to test the effects of *gipB* deletion on gliotoxin production. As with *gipA*, I created a *gipB* deletion strain by replacing the coding region of *gipB* with *pyrG*. I designated this mutant as *ΔgipB*. I also created a strain complemented for *gipB* expression, *gipB*(R). As shown in Figure 5.5a, loss of *gipB* did not drastically reduce the RNA levels of the gliotoxin cluster genes I tested. There was a 10% reduction for *gliA* and *gliZ* mRNA, a 30% reduction for *gliT* mRNA, and almost a 2-fold increase in *gliP* mRNA. Gene expression was restored to 1160G control levels in the *gipB*(R) strain, indicating that the effects I observed were specific to the loss of *gipB*. Furthermore, gliotoxin levels were reduced by 10% in the *ΔgipB* mutant, compared to the 1160G parent strain and the *gipB*(R) complement (Fig. 5.5b). These data suggest that *gipB* is important for full induction of the gliotoxin cluster, but not essential. The minor level of reduction observed with the genes tested is not surprising as GipB is likely acting upstream of several proteins and could possibly be redundant for another hybrid sensor kinase. Furthermore, GipB is possibly only activated during earlier phases of conidiation, making it likely that its activity is not essential to gliotoxin production in later phases of conidiation or other conditions.

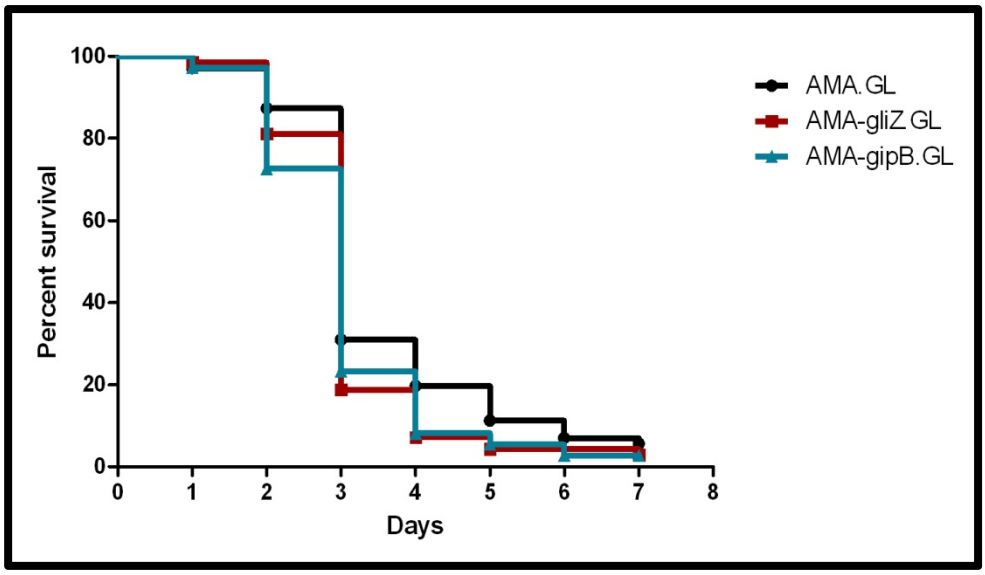


Figure 5.4. High-copy expression of *gipB* does not significantly affect virulence of *A. fumigatus*. Toll-deficient *D. melanogaster* fruit flies were infected by needle puncture and incubated at 29℃ for 7 days. This graph includes three independent virulence assays.

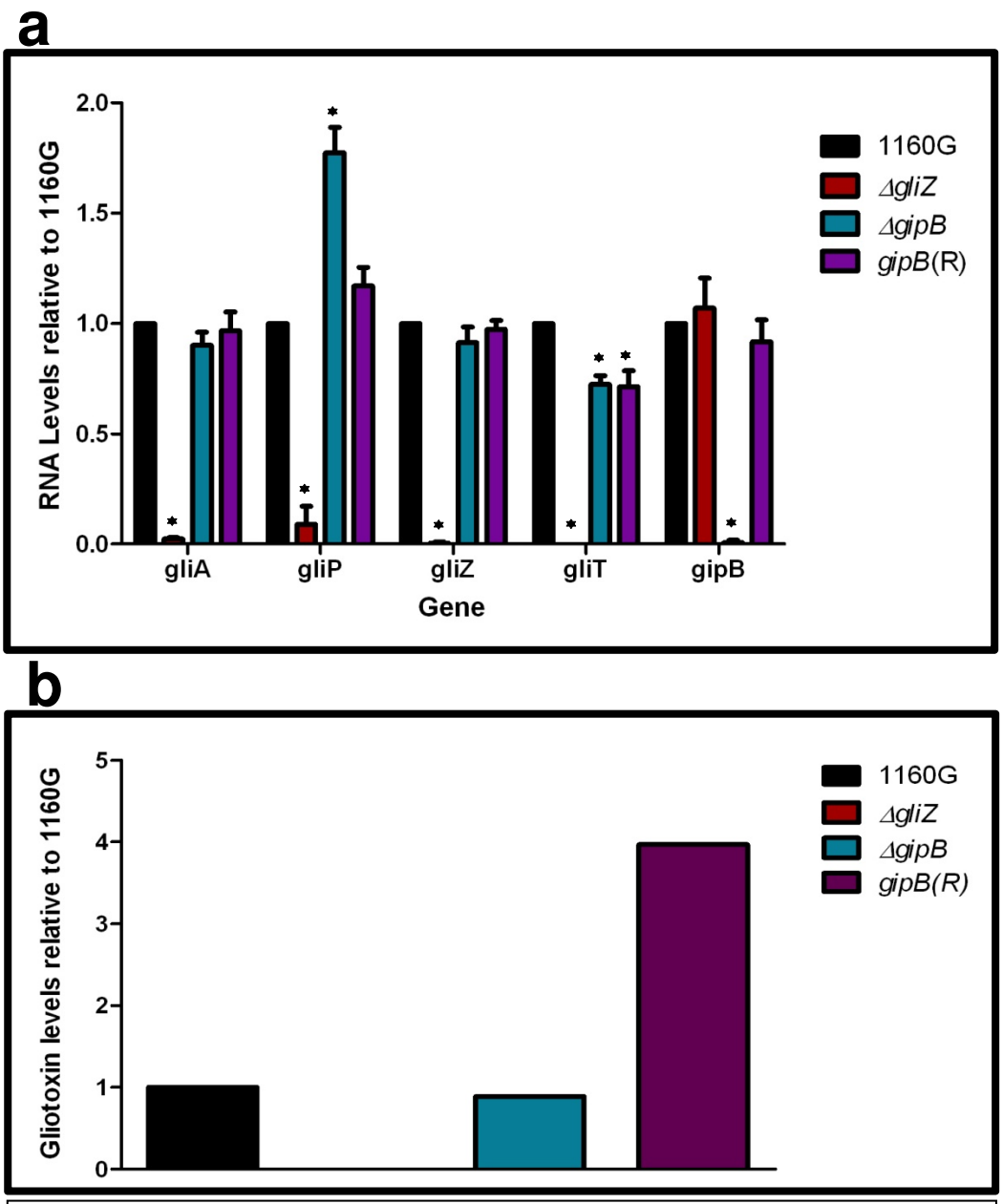


Figure 5.5. Loss of *gipB* does not significantly affect gliotoxin production. All cultures were grown for 48 hours in non-repressing conditions. Total RNA was isolated and quantified by dot blot analysis in triplicate. Gliotoxin levels were quantified by RP-HPLC. (a) mRNA transcript levels of several gliotoxin cluster genes. Each data set is normalized to 1160G. The results of one representative experiment of three independent experiments are shown as mean ± SD. (b) Gliotoxin levels in growth medium, normalized to 1160G. The results of one representative experiment of three biological replicates are shown. The asterisk ( ) indicates a statistically significant difference (p-value <0.05), compared to 1160G, calculated by one-way ANOVA and Tukey comparison test.

*5.2.4 Deletion of gipB and Its Effect on Growth and Virulence of A. fumigatus*

Even though loss of *gipB* did not exhibit a dramatic effect on gliotoxin production, I aimed to determine if GipB is important for growth and virulence of *A. fumigatus*. I inoculated 1000 spores of 1160G, *ΔgliZ*, *ΔgipB*, and *gipB*(R) onto rich medium (YAG), minimal medium (MMVAT), and MMVAT with exogenous gliotoxin. Deletion of *gipB* did not drastically affect growth of *A. fumigatus*, which suggests that GipB does not play a major role in growth of the fungus (Fig. 5.6). For virulence studies, I infected Toll-deficient *D. melanogaster* fruit flies by needle puncture, as described previously. Loss of *gipB* did not affect virulence of *A. fumigatus* in a Toll-deficient *D. melanogaster* model system, compared to the 1160G parent strain, indicating that loss of *gipB* does not attenuate the virulence of this fungus (Fig. 5.7). This does not rule out the possibility that loss of *gipB* could be affecting the ability of *A. fumigatus* to effectively combat host immune cells.

**5.3 Summary**

To uncover the effects of GipB on gene regulation of the gliotoxin cluster and gliotoxin production, I measured mRNA transcript levels of several genes within the cluster, as well as gliotoxin levels in the surrounding medium. High-copy expression of *gipB* increased mRNA levels of several genes in the gliotoxin cluster after 24 hours growth in repressing conditions, compared to the control strain, although this effect was not observed after 48 hours growth (Fig. 5.2a). Furthermore, gliotoxin was produced at higher levels with high-copy expression of *gipB*, compared to the control strain (Fig. 5.2b). This indicates that GipB does act to induce the gliotoxin biosynthetic cluster, but not as strongly as GipA, which is not surprising as GipB is a hybrid sensor kinase likely acting upstream of other

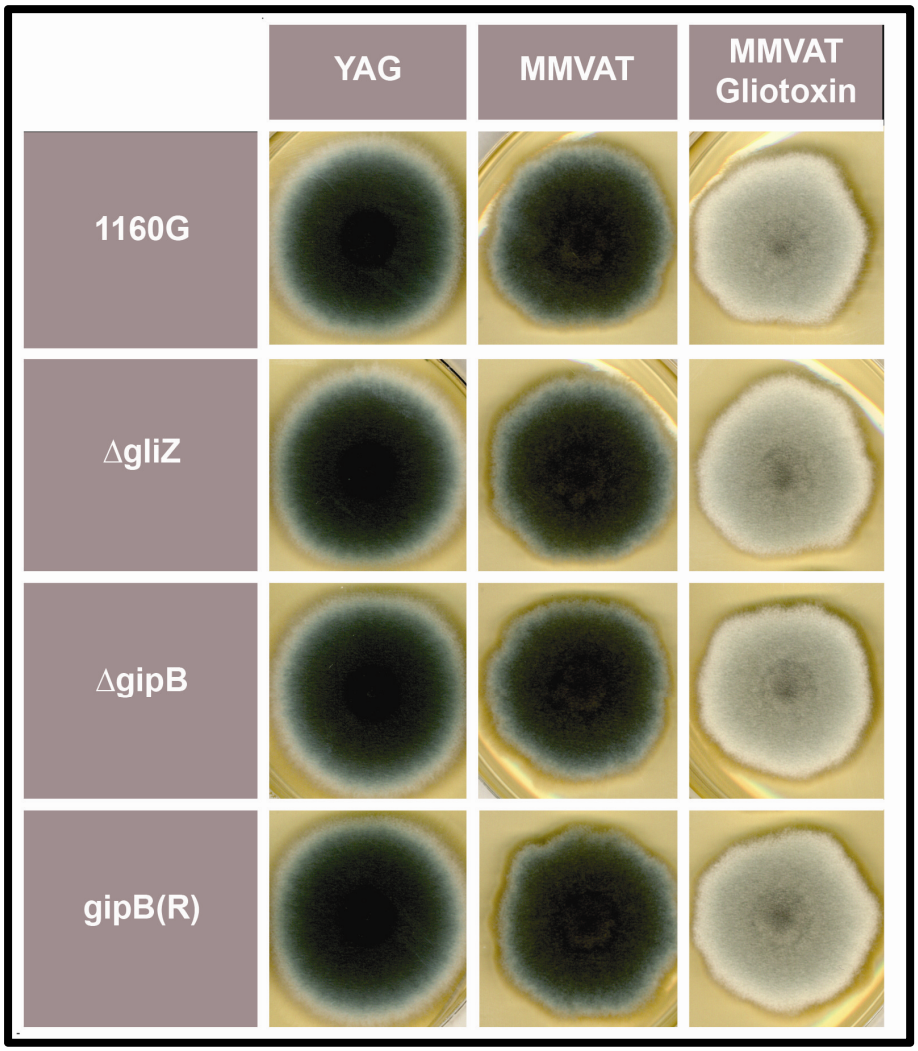


Figure 5.6. Loss of *gipB* does not significantly affect growth of *A. fumigatus*. 1000 spores were spotted onto each plate and incubated at 37℃ for 48 hours (YAG) or 72 hours (MMVAT).

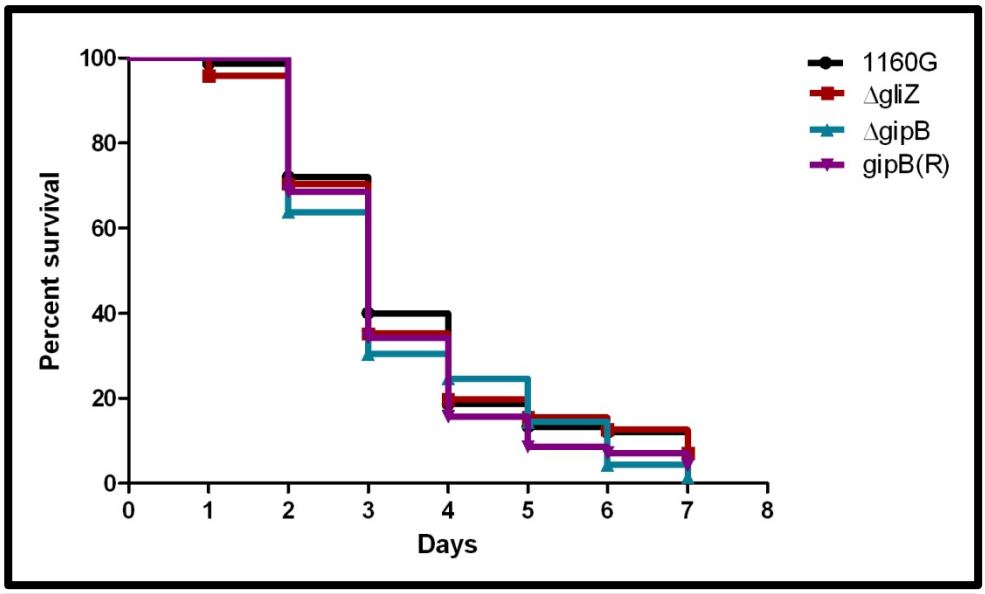


Figure 5.7. Loss of *gipB* does not significantly affect virulence of *A. fumigatus*. Toll-deficient *D. melanogaster* fruit flies were infected by needle puncture and incubated at 29℃ for 7 days. This graph includes three independent virulence assays.

proteins. This could also indicate that GipB is only activated during specific stages of development, as high-copy expression during the later phase of conidiation did not induce the gliotoxin cluster.

Deletion of *gipB* had a slight negative effect on the gliotoxin cluster, as gliotoxin levels were reduced by 10% in the *ΔgipB* mutant in non-repressing conditions, compared to the control strain (Fig. 5.5b). These data suggest that GipB activity is not essential to gliotoxin production in the conditions tested. Neither the high-copy *gipB* strain nor the *ΔgipB* grew differently than the control strain on rich or minimal medium (Fig. 5.3 & 5.6). Therefore differential expression of *gipB* does not affect normal growth in *A. fumigatus*. In addition, all strains tested were not significantly different in virulence, compared to the control strain. This indicates that alterations in *gipB* expression do not make *A. fumigatus* significantly more or less virulent in the Toll-deficient *D. melanogaster* model (Fig. 5.4 & 5.7).

# Chapter 6:

# GliZ, GipA, and GipB: Independent or Interdependent?

## 6.1 Introduction

In chapter 3, I presented a model for *gliA* regulation, involving GliZ, GipA, and AreA (Fig. 3.8a). In this model, I propose that GliZ and GipA are both binding to the promoter region of *gliA* to induce gene expression, not in an independent fashion, but interdependently, in which both proteins bind in close proximity and require the presence of the other for signaling. In the conditions tested, non-repressing medium contained sodium nitrate, instead of ammonium tartrate, releasing nitrogen metabolite repression. As shown in Figure 3.9b, a non-preferred nitrogen source causes induction of the gliotoxin cluster, indicating that AreA is acting on the gliotoxin cluster to induce gene expression. This most likely occurs via AreA-mediated induction of *gliZ* first, possibly followed by direct binding of AreA to promoter regions of other genes in the cluster. There is an AreA recognition sequence in the *gliA* promoter, 37 base pairs upstream of the ATG start site, which could indicate that AreA is directly binding to the promoter of *gliA,* although this may not be likely as the recognition element is so close to the ATG start site for *gliA* (Fig. 6.1). This model was proposed based on the experiments performed for this project.

As discussed in Chapter 4, mutation of the core region within the GipA recognition sequence in the *gliA* promoter drastically reduced both GliZ- and GipA-dependent *lacZ* expression, indicating that both proteins rely on this binding site for activity. Upon further examination, I discovered that the GipA recognition sequence is embedded within a potential GliZ binding site, which supports my proposed model that both proteins are binding in close proximity (Fig. 6.1). This does not, however, give evidence of an interdependent relationship between GliZ and GipA, as these two proteins could possibly be binding at separate times and inducing *gliA* independently.

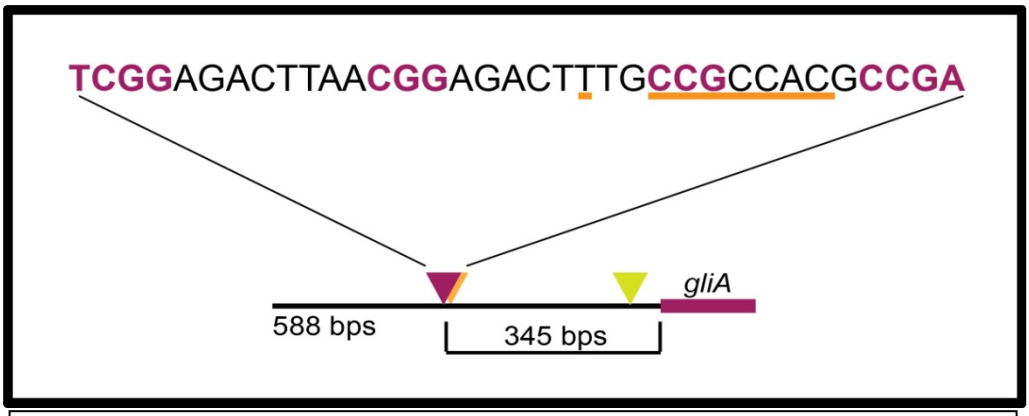


Figure 6.1. Layout of the GipA/GliZ binding sites in the *gliA* promoter region, relative to the *gliA* start site. GliZ tandem repeats are purple and the GipA DNA binding site is underlined in orange. The AreA recognition element is signified by the yellow triangle.

## 6.2 Results

### *6.2.1 A ΔgliZ/ΔgipA Double Mutant and Its Effect on Gliotoxin Production*

I created a double deletion mutant, Δ*gliZ/ΔgipA* and measured RNA levels via dot blot analysis and gliotoxin production via RP-HPLC in non-repressing conditions. I sought to determine if GipA and GliZ signal independently of each other or work together within a pathway. The *gliZ/gipA* double deletion mutant revealed a pattern of gene expression similar to the *gliZ* single deletion mutant (Fig. 6.2a). Furthermore, gliotoxin production in the double mutant was abolished, similar to what I observed in the *gliZ* single deletion strain (Fig. 6.2b). These results indicate that GipA is signaling cooperatively with GliZ and not independently, but it's not completely clear from these data. RNA levels and gliotoxin levels were already so low with the *gliZ* deletion strain, an additive effect could be difficult to identify for the *gliZ/gipA* double mutant.

### *6.2.2 A ΔgliZ/ΔgipA Double Mutant and Its Effect on Growth and Virulence of A. fumigatus*

Both *ΔgliZ* and *ΔgipA* single deletion mutants grew comparable to the control strain, so I tested the growth of the *ΔgliZ/ΔgipA* mutant by inoculating 1000 spores onto YAG, MMVAT, and MMVAT with exogenous gliotoxin. The growth of *ΔgliZ/ΔgipA* appeared comparable to 1160G, signifying that loss of both *gliZ* and *gipA* does not adversely affect growth of *A. fumigatus*, even in the presence of exogenous gliotoxin (Fig. 6.3). Furthermore, neither *ΔgliZ* nor *ΔgipA* display a statistically significant difference in virulence, compared to 1160G, so I sought to verify if this would be the same case with a Δ*gliZ/ΔgipA* double mutant. Indeed, the Δ*gliZ/ΔgipA* mutant did not show statistically significant

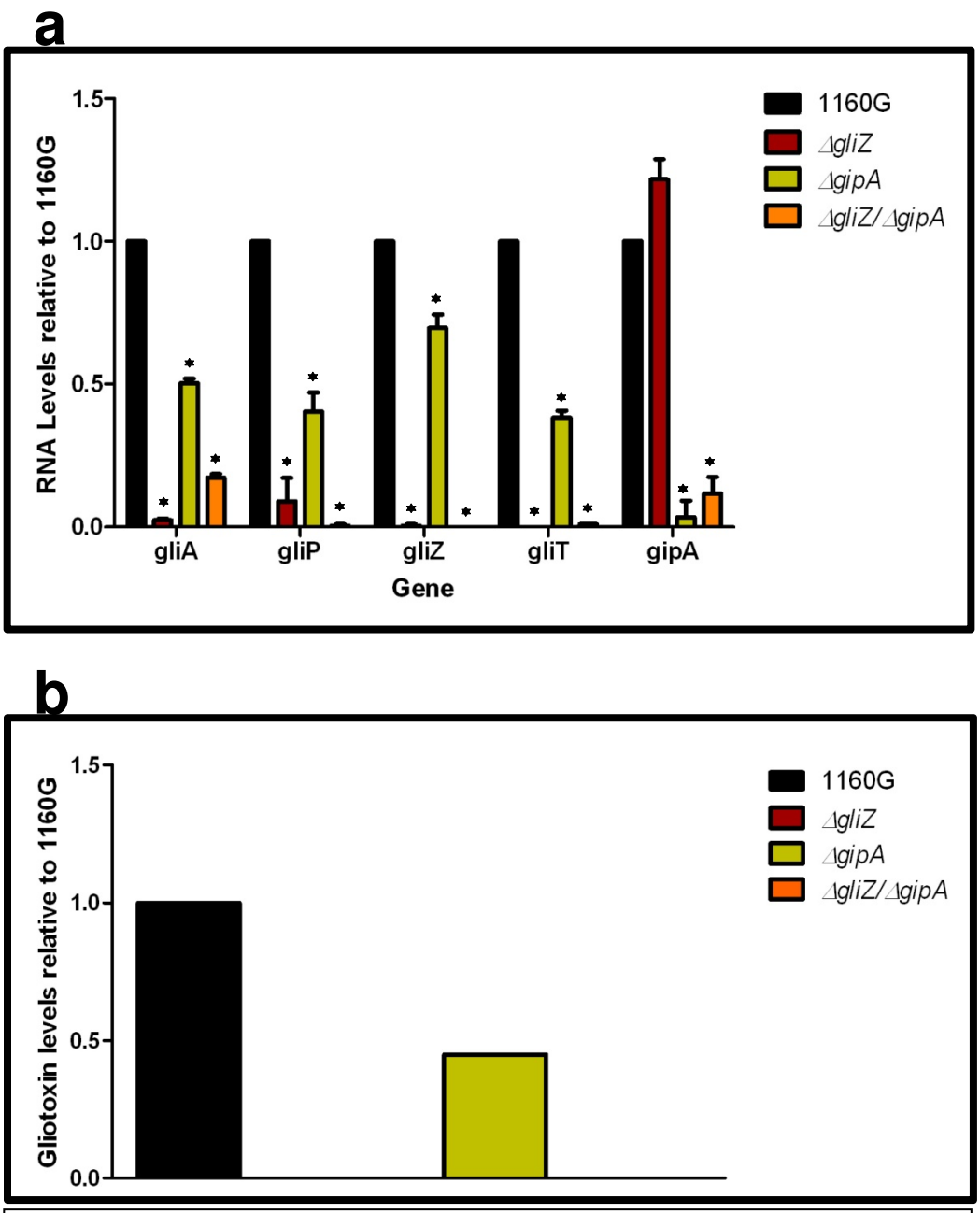


Figure 6.2. Loss of *gliZ* and *gipA* negatively affects gliotoxin production. All cultures were grown for 48 hours in non-repressing conditions. Total RNA was isolated and quantified by dot blot analysis in triplicate. Gliotoxin levels were quantified by RP-HPLC. (a) mRNA transcript levels of several gliotoxin cluster genes. Each data set is normalized to 1160G. The results of one representative experiment of three independent experiments are shown as mean ± SD. (b) Gliotoxin levels in growth medium, normalized to 1160G. The results of one representative experiment of three biological replicates are shown. The asterisk (*) indicates a statistically significant difference (p-value <0.05), compared to 1160G, calculated by one-way ANOVA and Tukey comparison test.

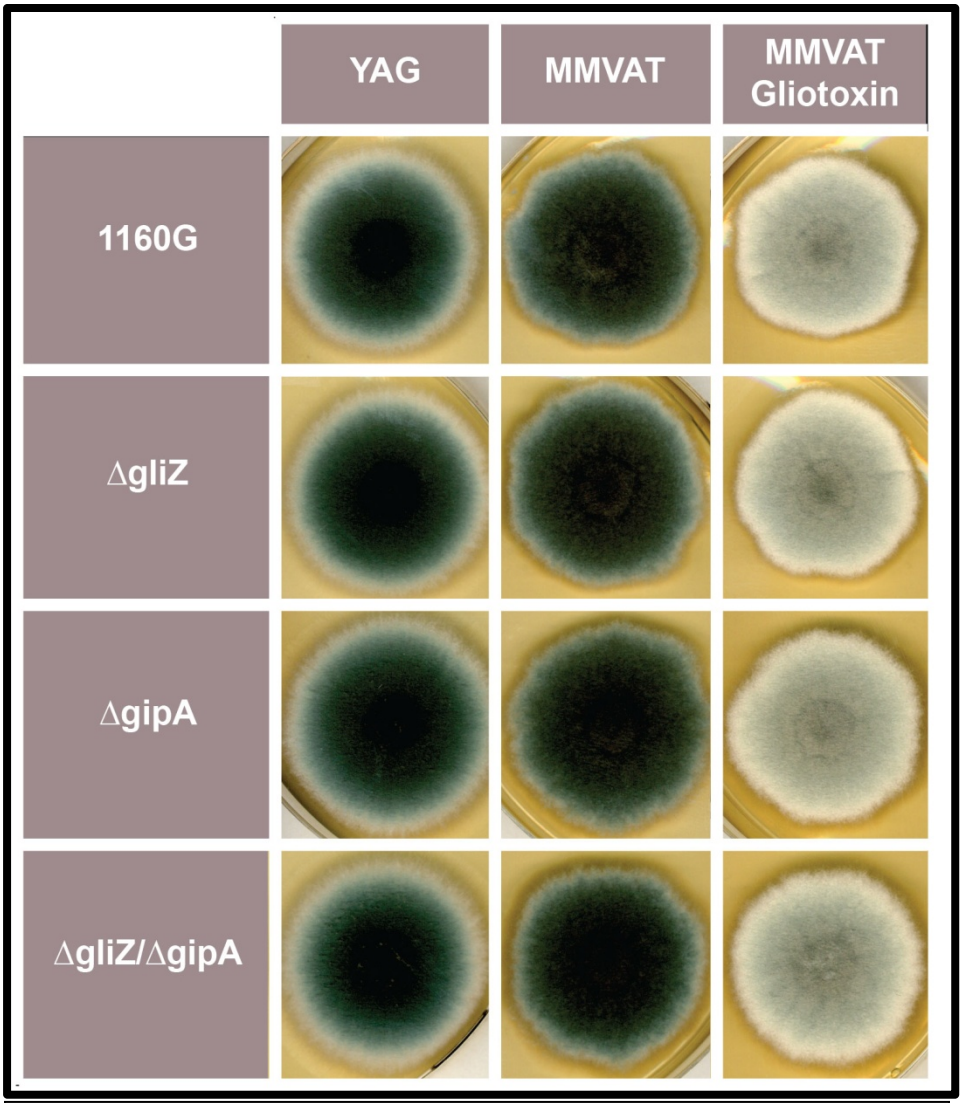


Figure 6.3. Loss of *gliZ* and *gipA* does not significantly affect growth of *A. fumigatus*. 1000 spores were spotted onto each plate and incubated at 37℃ for 48 hours (YAG) or 72 hours (MMVAT).

attenuation of virulence in a Toll-deficient *D. melanogaster* model system (Fig. 6.4). Therefore, no adverse additive effects were observed with respect to virulence in the model I tested.

### *6.2.3 A ΔgipA/ΔgipB double mutant and Its Effect on Gliotoxin Production*

I created a *ΔgipA/ΔgipB* double deletion mutant and grew this strain, along with controls, in non-repressing conditions. I measured RNA levels via dot blot analysis and gliotoxin levels via RP-HPLC to determine if GipA and GipB are signaling independently of each other or in a linear pathway. RNA levels of the gliotoxin-specific genes in the *gipA/gipB* double deletion mutant were similar to what I observed in the *ΔgipA* single mutant (Fig. 6.5a). Gliotoxin was also being produced in Δ*gipA/ΔgipB* at an amount comparable to the *ΔgipA* single mutant (50% reduction compared to 1160G) (Fig. 6.5b). These data suggest that there is no additive effect when removing both GipA and GipB from the genome, although loss of *gipB* alone does not produce a significant decrease in gliotoxin production. Therefore, these two proteins possibly work in a pathway and do not signal independent of each other.

### *6.2.4 A ΔgipA/ΔgipB double mutant and Its Effect on Growth and Virulence of A. fumigatus*

I sought to determine if the Δ*gipA/ΔgipB* double mutant would have an abnormal phenotype on rich or minimal medium. The Δ*gipA/ΔgipB* mutant grew at a similar rate to the 1160G control, but loss of both *gipA* and *gipB* appeared to negatively affect condiation

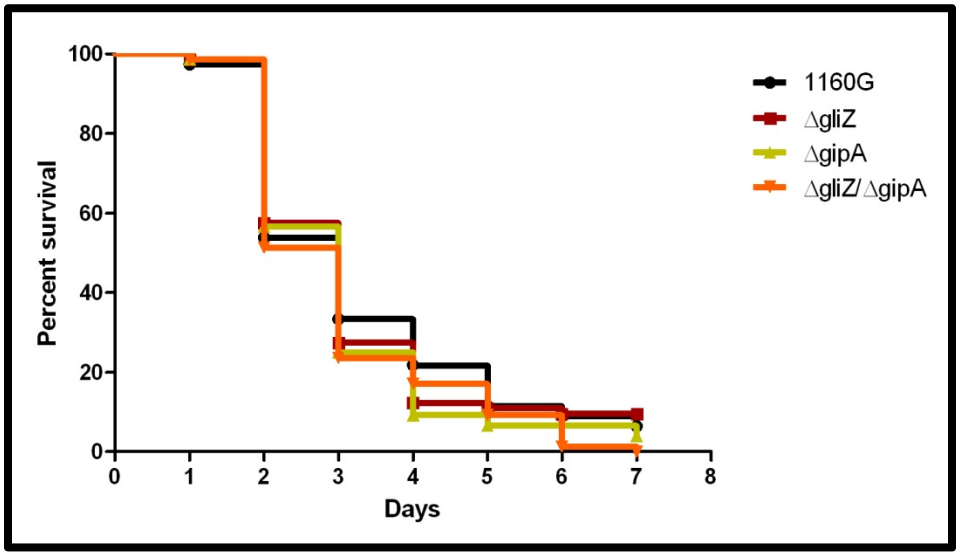


Figure 6.4. Loss of *gliZ* and *gipA* does not significantly affect virulence of *A. fumigatus*. Toll-deficient *D. melanogaster* fruit flies were infected by needle puncture and incubated at 29℃ for 7 days. This graph includes three independent virulence assays.

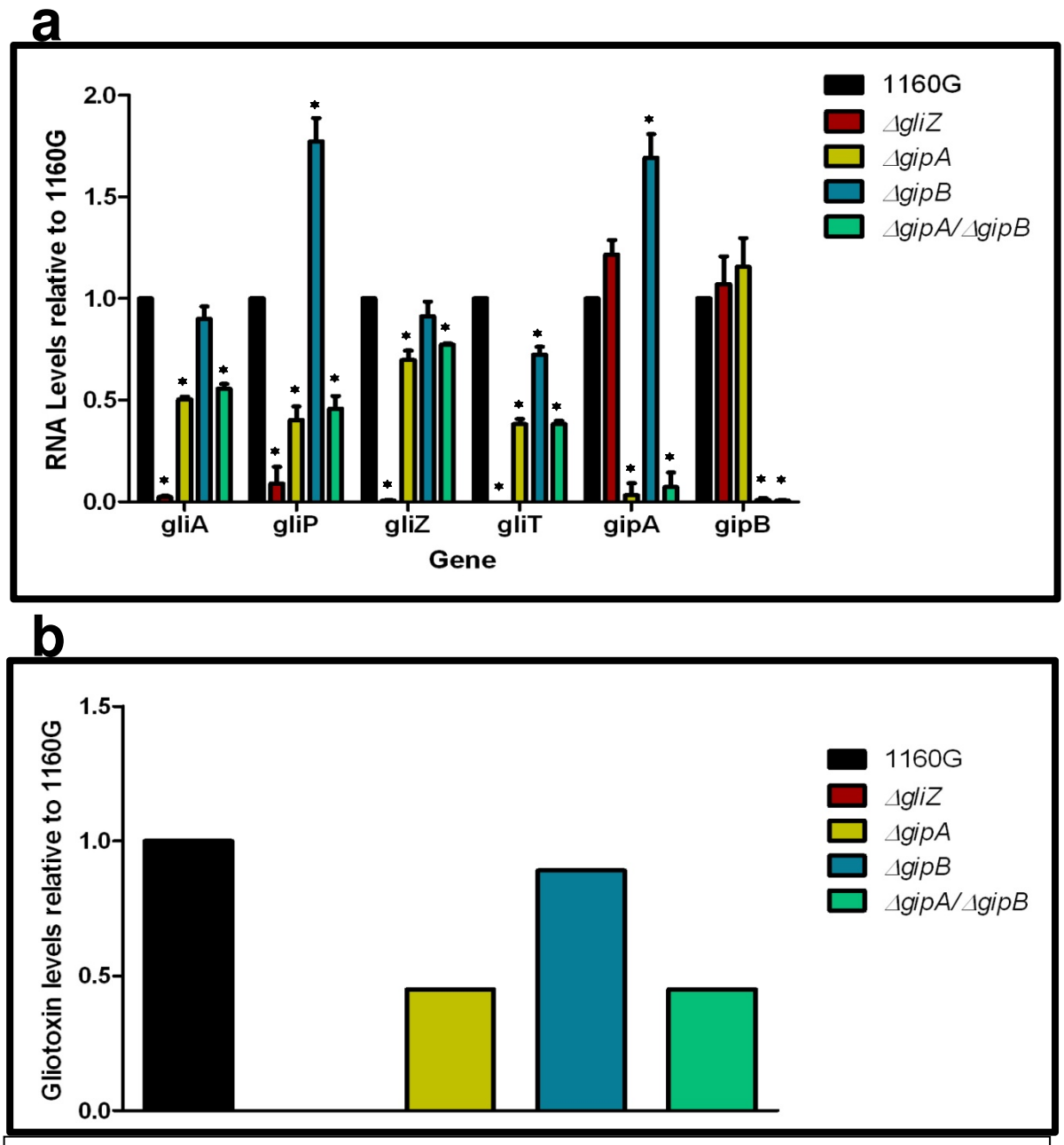


Figure 6.5. Loss of *gipA* and *gipB* negatively affects gliotoxin production. All cultures were grown for 48 hours in non-repressing conditions. Total RNA was isolated and quantified by dot blot analysis in triplicate. Gliotoxin levels were quantified by RP-HPLC. (a) mRNA transcript levels of several gliotoxin cluster genes. Each data set is normalized to 1160G. The results of one representative experiment of three independent experiments are shown as mean ± SD. (b) Gliotoxin levels in growth medium, normalized to 1160G. The results of one representative experiment of three biological replicates are shown. The asterisk (*) indicates a statistically significant difference (p-value <0.05), compared to 1160G, calculated by one-way ANOVA and Tukey comparison test.

(Fig. 6.6). Indeed, when spores/cm$^2$ was calculated, the Δ*gipA/ΔgipB* mutant poduced approximately 50% less spores than the 1160G control when grown on rich medium. This significant reduction in spore number was not observed for either the *ΔgipA* or *ΔgipB* single deletion mutants, suggesting that in regards to conidiation, *gipA* and *gipB* are possibly involved in separate pathways. Furthermore, I performed a virulence assay with the Δ*gipA/ΔgipB* mutant to establish if loss of both genes affected virulence of *A. fumigatus*. The Δ*gipA/ΔgipB* double mutant did not show a statistically significant attenuation in virulence in a Toll-deficient *D. melanogaster* model system, compared to the 1160G control, indicating that the compound loss of both GipA and GipB does not alter the ability of the fungus to kill Toll-deficient fruit flies (Fig. 6.7).

### *6.2.5 High-copy Expression of GipA and GipB in a gliZ deletion background*

I performed a series of experiments to determine if GipB or GipA are dependent on GliZ for signaling. I created two strains in Af293.1: (1) pyrG+ (wild-type background) and (2) *ΔgliZ.1* (*ΔgliZ* background). Into each of these strains, I transformed pDONR AMA (AMA.G, AMA.Z), pDONR AMA-*gliZ* (AMA-gliZ.G, AMA-gliZ.Z), pDONR AMA-*gipA* (AMA-gipA.G, AMA-gipA.Z), and pDONR AMA-*gipB* (AMA-gipB.G, AMA-gipB.Z) to produce strains with extra copies of GliZ, GipA, or GipB in a wild-type or *gliZ* deletion background (strains and genotypes are listed in Table 2.2). High-copy expression of *gliZ* served as a control, as extra copies of GliZ would rescue for loss of *gliZ*. I grew all strains in non-repressing conditions for 48 hours and quantified RNA levels of gliotoxin-specific genes (*gliA* and *gliP*) by RNA dot blot analysis. For this experiment, I present data that is normalized to AMA.G, as this strain is the empty vector control in the wild-type background.

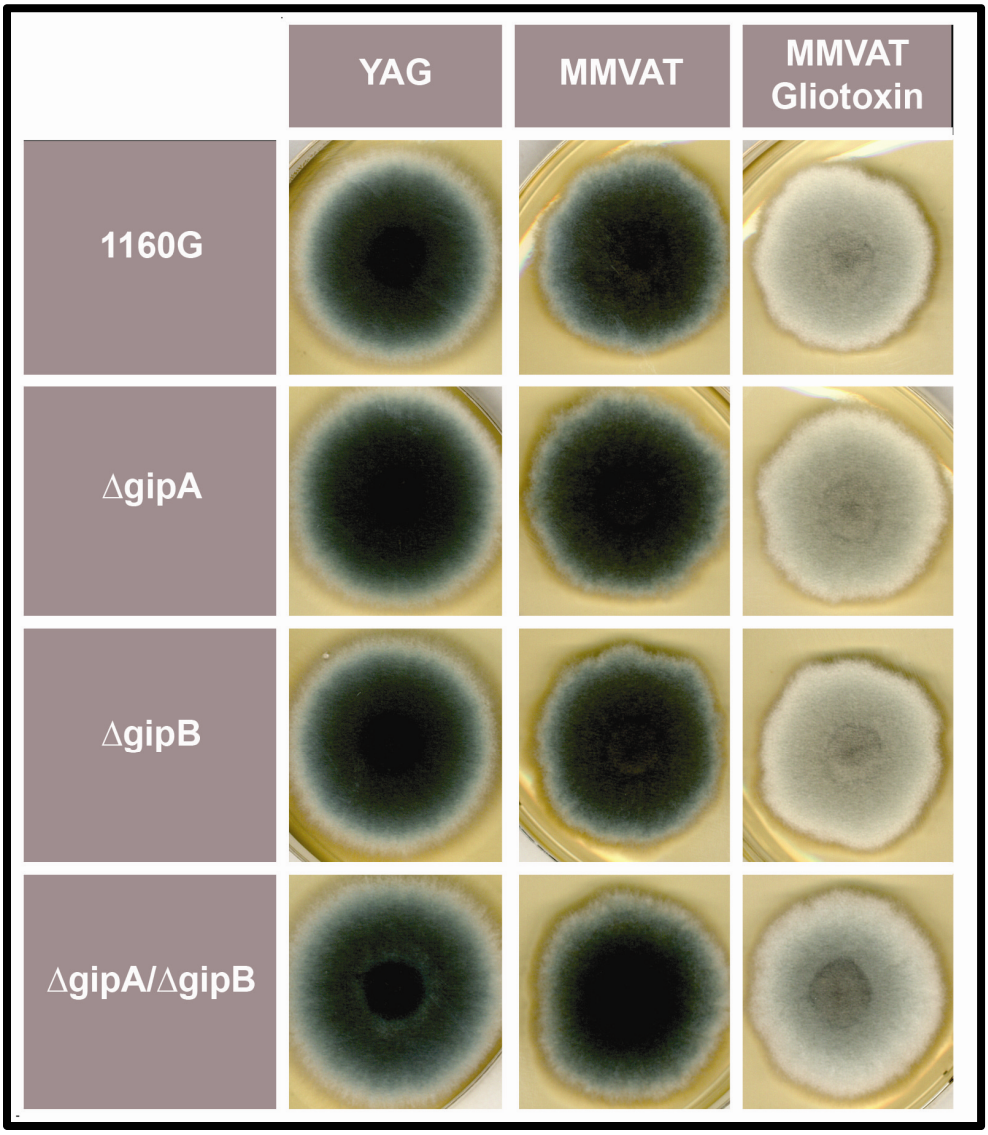


Figure 6.6. Loss of *gipA* and *gipB* negatively affects conidiation in *A. fumigatus*. 1000 spores were spotted onto each plate and incubated at 37℃ for 48 hours (YAG) or 72 hours (MMVAT).

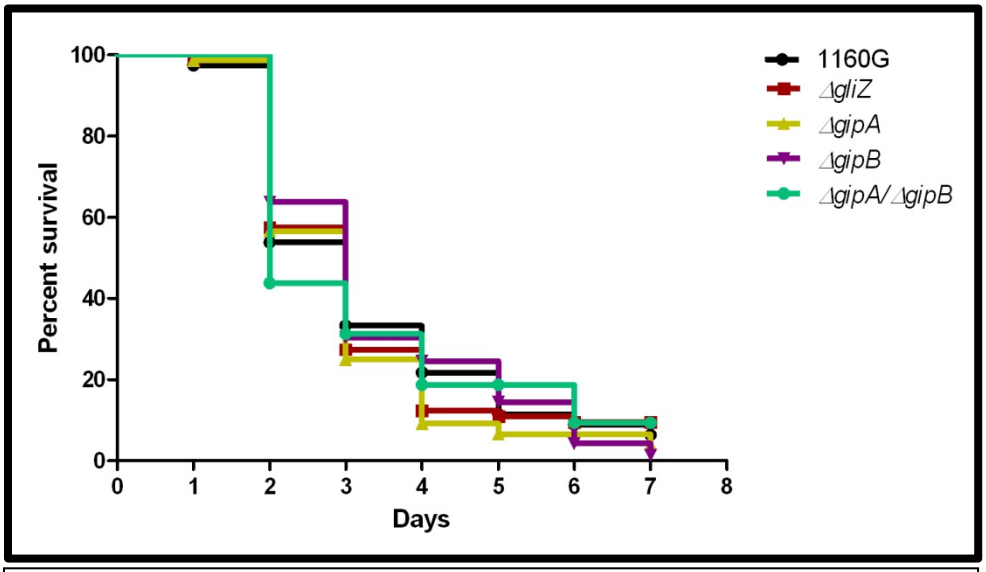


Figure 6.7. Loss of *gipA* and *gipB* does not significantly affect virulence of *A. fumigatus*. Toll-deficient *D. melanogaster* fruit flies were infected by needle puncture and incubated at 29℃ for 7 days. This graph includes three independent virulence assays.

In the pyrG+ background, AMA-gliZ.G, AMA-gipA.G, and AMA-gipB.G had increased mRNA levels for *gliP*, while only AMA-gipA.G had increased mRNA levels for *gliA,* compared to AMA.G (Fig. 6.8). These changes were slight because growth in non-repressing conditions already induced these genes to high levels, so having extra copies of GipA or GipB did not greatly contribute to gene expression. In AMA.Z, mRNA levels for both *gliA* and *gliP* were almost completely undetectable, as to be expected from previous experiments. High-copy expression of *gliZ* brought transcript levels of both genes back to AMA.G levels (Fig. 6.8). AMA-gipA.Z displayed a reduction in mRNA levels similar to AMA.Z. For *gliA*, the level of mRNA present in AMA-gipA.Z was slightly higher (close to 5-fold) than what was observed for AMA.Z. However, the level of *gliP* RNA did not exceed that of the AMA.Z empty vector control. Therefore, GipA was not able to induce *gliA* or *gliP* in the absence of GliZ. Additionally, transcription of both *gliA* and *gliP* in AMA-gipB.Z did not reach levels above AMA.Z (Fig. 6.8). This suggests that GliZ is required for GipA to induce both *gliP* and *gliA*. Furthermore, the lack of *gliA* and *gliP* induction in AMA-gipB.Z indicates that GliZ is required for GipB-mediated signaling for both genes.

### *6.2.6 High-copy expression of GliZ and GipB in a gipA deletion background*

I created two strains in Af293.1: (1) pyrG+ (wild-type background), and (2) *ΔgipA.1* (*ΔgipA* background). Into each of these strains, I transformed pDONR AMA (AMA.G, AMA.A), pDONR AMA-*gliZ* (AMA-gliZ.G, AMA-gliZ.A), pDONR AMA-*gipA* (AMA-gipA.G, AMA-gipA.A), and pDONR AMA-*gipB* (AMA-gipB.G, AMA-gipB.A). AMA-gipA served as a control, as high-copy expression of *gipA* should rescue for loss of *gipA*. As described above, strains were grown in non-repressing conditions and RNA was quantified by RNA dot blot analysis. Data presented are normalized to AMA.G.

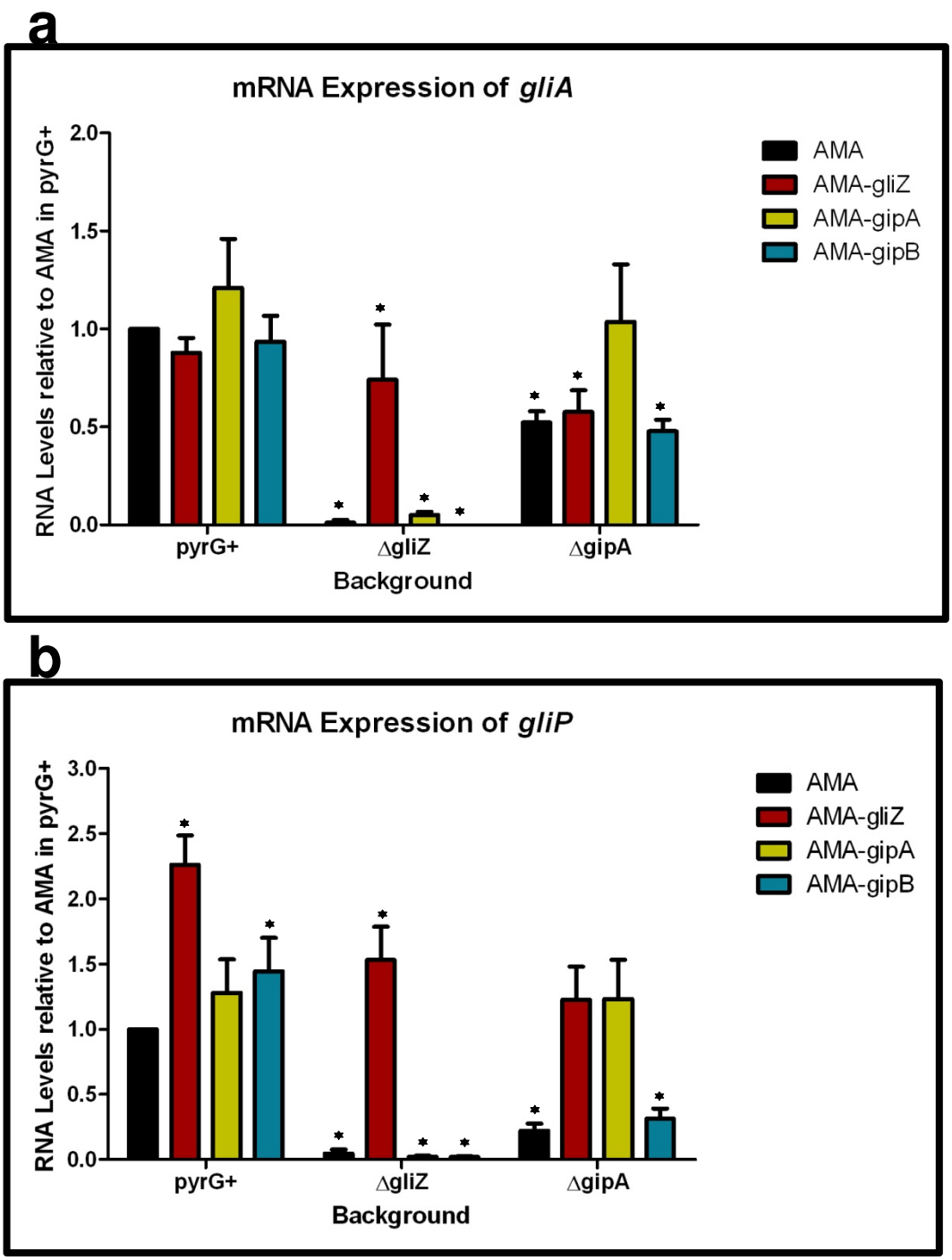


Figure 6.8. GliZ and GipA are dependent on each other for *gliA* induction. Cultures were grown in non-repressing conditions and RNA was quantified by dot blot analysis in triplicate. Data are normalized to AMA.G (pyrG+ background). These graphs are an average of three biological replicates. (a) mRNA levels of *gliA* in all backgrounds. (b) mRNA levels of *gliP* in all backgrounds. The asterisk (*) indicates a statistically significant difference (p-value <0.05), compared to AMA.G, calculated by one-way ANOVA and Tukey comparison test.

As expected from previous experiments, mRNA levels in AMA.A of both *gliA* and *gliP* were reduced significantly, 50% and 80%, respectively. RNA levels of *gliP* in AMA-gliZ.A were comparable to those of AMA.G; however RNA levels of *gliA* were not significantly higher than background levels (AMA.A) (Fig. 6.8). This indicates that GliZ is not dependent on GipA for induction of *gliP*, however induction of *gliA* by GliZ does appear to be dependent on GipA. Moreover, RNA levels of both *gliA* and *gliP* in AMA-gipB.A were not significantly higher than those in AMA.A. Although *gliP* did have a slight increase in gene expression in AMA-gipB.A (1.5-fold), it did not reach the level of *gliP* in the wild-type background (Fig. 6.8b). Therefore, GipB appears to be dependent on GipA for full *gliA* and *gliP* induction. An alternative interpretation of the high-copy *gipB* results are discussed in the next chapter.

### 6.3 Summary

To determine if GliZ, GipA, and GipB are part of a single pathway, I performed a series of epistasis and bypass suppression experiments. Transcript levels of several gliotoxin-specific genes were reduced in the *ΔgliZ/ΔgipA* mutant to the level of the single *ΔgliZ* strain, as were gliotoxin levels in the surrounding medium (Fig. 6.2). This suggests that deletion of both *gliZ* and *gipA* does not produce an additive effect in gene expression or gliotoxin production and that signaling of both proteins is through GliZ, although loss of *gliZ* causes such as severe reduction in gliotoxin production that an additive effect from the additional deletion of *gipA* might be difficult to discern. No additive effects were observed with regards to the growth of the fungus on different media or with the virulence of the fungus in a Toll-deficient *D. melanogaster* model system, further supporting the idea of GliZ and GipA working interdependently and not separately (Fig. 6.3 & 6.4). In the *ΔgipA/ΔgipB*

mutant, mRNA transcript levels of the gliotoxin-specific genes tested were comparable to the single *ΔgipA* strain, as were gliotoxin levels in the surrounding medium (Fig. 6.5). This indicates that deletion of both *gipA* and *gipB* does not cause an additive effect in gene expression or gliotoxin production and that GipB acts upstream of GipA, supporting the idea that they are both involved in a linear pathway with regards to gliotoxin production. Even though the *ΔgipA/ΔgipB* double mutant grew at a rate similar to the 1160G control strain on all media tested, sporulation appeared to be negatively affected by loss of both genes on rich medium (Fig. 6.6). The *ΔgipA/ΔgipB* mutant exhibited a mortality rate similar to the 1160G control in the Toll-deficient *D. melanogaster* model system, suggesting that virulence of the fungus is not affected by loss of both genes (Fig. 6.7).

The *gliA* promoter mutagenesis experiments revealed that both GliZ and GipA are dependent on a single binding site for induction of *gliA* expression. Therefore, I sought to determine if GliZ is dependent on GipA for induction of *gliA* and vice versa. I also measured *gliP* mRNA transcript levels to determine if what I have observed is unique to *gliA* regulation or also affected other genes of the gliotoxin cluster. In a *ΔgliZ* background, high-copy expression of *gipA* did not raise mRNA transcript levels of *gliP* above basal levels, although it did slightly increase (almost 5-fold) mRNA transcript levels of *gliA* (Fig. 6.8). This suggests that GliZ is required for GipA-mediated induction of both *gliP* and *gliA*, although it appears that GipA can stimulate a slight elevation in *gliA* expression independent of GliZ. Furthermore, high-copy expression of *gipB* in a *ΔgliZ* background did not result in an increase in *gliP* or *gliA* mRNA above basal levels, indicating that GliZ is required for GipB-mediated induction of both *gliP* and *gliA* (Fig. 6.8). These results are not entirely surprising, as in-cluster transcription factors are usually essential for expression of other genes in the cluster.

In a *ΔgipA* background, high-copy expression of *gliZ* caused an increase in *gliP* mRNA transcript to wild-type levels. Surprisingly, *gliA* mRNA transcript levels in the high-copy *gliZ* strain were comparable to basal levels, suggesting that GliZ induces *gliP* independent of GipA, but cannot induce *gliA* in the absence of GipA (Fig. 6.8). Furthermore, high-copy expression of *gipB* in a *ΔgipA* background only slightly increased *gliP* mRNA levels above basal levels (1.5-fold) and *gliA* mRNA levels did not exceed basal levels, indicating that GipB-mediated induction of both *gliP* and *gliA* is dependent on GipA (Fig. 6.8).

# Chapter 7:

# General Discussion

Although recent studies have revealed gliotoxin intermediates, which have led to a better understanding of the biosynthesis of gliotoxin, information on regulation of the genes involved in the biosynthesis pathway is lacking [92]. There have been a number of proteins shown to affect gliotoxin production, but these have only been studied in a general way [13, 22, 23, 32, 50, 64, 91, 107-109, 128, 129]. No proteins have been demonstrated to bind directly to the gliotoxin cluster, not even GliZ, the in-cluster transcription factor [15]. The goal of this project was to uncover novel proteins that regulate gliotoxin production in *A. fumigatus* and to possibly piece together a signaling pathway that responds to external or internal signals. I have performed a high-copy inducer screen and uncovered two proteins, GipA and GipB, which appear to be involved in the regulation of the gliotoxin cluster.

### 7.1 Characterization of GipA

GipA is a $C_2H_2$ transcription factor, which harbors a long 5' UTR (at least 877 bps) and a moderate 3' UTR (at least 360 bps). Furthermore, there are three μORFs within the 5' UTR, which suggests that *gipA* could be under post-transcriptional regulation (Fig. 3.6a). The length of 5' UTRs appears to remain invariable between taxonomic classes, ranging from 100 to 200 nucleotides on average, however 3' UTRs can be more variable, ranging from 200 nucleotides in plants and fungi to 800 nucleotides in vertebrates [130]. Many proteins that are tightly regulated, such as growth factors, transcription factors, or proto-oncogenes, are encoded by messenger RNAs containing 5' UTRs that are longer than average, with μORFs and stable secondary structures that negatively affect translation efficiency and mRNA stability [130]. RNA levels of *gipA* remained relatively low in all growth conditions tested, which further supports controlled regulation of this gene (data not shown). μORFs can affect translation efficiency in several ways, such as preemptively

initiating translation, affecting ribosome reinitiation, or causing arrest of translational machinery [80]. For instance, reinitiation of translation is reduced as the μORF length is increased, as shown in mammalian systems. In addition, one group demonstrated a linear relationship between μORF length and translation of downstream ORFs, whereas longer μORFs decreased translation of the downstream ORFs in human immunodeficiency virus type 1 [131].

Of the three μORFs within the 5' UTR of *gipA*, the first is 7 codons, the second is 33 codons, and the third is 4 codons. Interestingly, the first μORF overlaps with the second, longer μORF (Fig. 3.6a). Perhaps in certain situations where *gipA* translation is favorable, the translational machinery targets the first μORF, causing the second μORF to be passed over and favoring reinitiation at the *gipA* start codon, whereas in situations where *gipA* translation is unfavorable, the translational machinery targets the second μORF, preventing reinitiation downstream. This could possibly be tested through mutational analysis of each μORF in the *gipA* 5' UTR, involving either complete deletion of each μORF or mutation of the AUG of each μORF. Differential μORF translation has been demonstrated for many genes, one of the most studied being Gcn4 in *Saccharomyces cerevisiae*. The 5' UTR of *gcn4* contains 4 μORFs, which modify translation of Gcn4 based on amino acid levels [78-80]. Studies have shown that under normal conditions, the translation complex will initiate translation at μORF1 and then reinitiate at μORF4, which prevents translation of *gcn4*. However, in conditions of amino acid limitation, scanning of the translation complex is leakier and will scan past μORF4 to reinitiate at the *gcn4* start site [78-80]. It would also be advantageous to analyze the mRNA stability of *gipA*, as both μORFs and 3' UTR sequences have been shown to affect mRNA stability through NMD [121]. The mRNA half-life of *areA*, which is tightly regulated in response to nitrogen source, is 40 minutes in

nitrogen-non-repressing conditions, but is only 7 minutes in nitrogen-repressing conditions [60, 63].

GipA positively regulates the gliotoxin cluster, as high-copy expression of *gipA* in repressing conditions resulted in increased mRNA levels of several genes within the gliotoxin cluster, compared to the empty vector control (*gliA* was induced 7-fold and 4.5-fold, *gliZ* was induced 2-fold and 12-fold, *gliP* was induced 4.5-fold and 5-fold, and *gliT* was induced 8-fold and 2-fold, at 24 and 48 hours of growth, respectively) (Fig. 4.2a). In addition, I observed higher levels of gliotoxin in the surrounding medium, compared to an empty vector control (7-fold higher by 24 hours) (Fig. 4.2b). Although high-copy expression of *gipA* did enhance gliotoxin production, neither growth nor virulence in a Toll-deficient *D. melanogaster* model was significantly affected (Fig. 4.3 & 4.4). This does not rule out the fact that high-copy expression of *gipA* could be enhancing the ability of *A. fumigatus* to fight host immune cells, which could be verified by measuring phagocytosis of spores, cytokine production, apoptosis of immune cells, and neutrophil infiltration at the site of infection.

Based on microarray data, out of 30 potential secondary metabolism clusters, 20 contain at least one gene that was up-regulated >2-fold in a high-copy *gipA* strain, compared to an empty vector control (Table 4.2). LaeA, widely accepted as a general regulator of secondary metabolism in numerous fungal species, has been shown to regulate 13 out of 22 identified secondary metabolism clusters in *A. fumigatus* [91]. This indicates that GipA could possibly also be acting in a general fashion to regulate secondary metabolism and not specifically on the gliotoxin biosynthetic cluster. Interestingly, LaeA, a proposed methyltransferase, has been suggested to affect chromatin remodeling when regulating secondary metabolism. This is supported by studies conducted in *A. nidulans* on the sterigmatocystin biosynthesis cluster. During active growth, histone H3 lysine 9 trimethylation (H3K9me3) and high levels of heterochromatin protein 1 (HepA) are

detectable at the sterigmatocystin cluster. Upon growth arrest and sterigmatocystin cluster induction, the levels of H3K9me3 and HepA decrease concurrently with increasing levels of acetylated histone H3 associated with sterigmatocystin cluster genes. Furthermore, in a *ΔlaeA* background, HepA occupancy in the promoter *aflR*, the sterigmatocystin in-cluster transcription factor, is significantly increased [3]. These data suggest that the sterigmatocystin cluster is subject to a repressive chromatin structure through H3K9 trimethylation and HepA binding and that LaeA is involved in the derepression of this heterochromatic signature inside the cluster. It would be interesting to study the chromatin structure of the gliotoxin cluster and how it contributes to gene expression. For instance, nucleosome displacement upon gliotoxin cluster derepression could contribute to higher gene expression.

As mentioned earlier, AreA is proposed to exhibit chromatin remodeling in connection to the nitrate assimilation pathway. In 1999, Claudio Scazzocchio's group showed through DNase I and micrococcal nuclease (MNase) digestion that the intergenic region between two divergently transcribed genes within the nitrate assimilation cluster is occupied by six nucleosomes in nitrogen-repressing conditions [132]. Therefore, in the presence of ammonium, these six nucleosomes occupy the intergenic region between the two genes (*niiA* and *niaD*) and contribute to the repression of cluster gene expression. Upon derepression of the cluster, in response to the loss of ammonium and the addition of nitrate, multiple nucleosomes in this intergenic region are displaced, creating an "open" region to facilitate binding of AreA and the in-cluster transcription factor, NirA, followed by induction of cluster gene expression. The group reported that this nucleosome rearrangement is dependent on AreA, as a *ΔareA* strain did not show the same pattern of chromatin remodeling at the nitrate assimilation cluster, even in nitrogen-derepressing conditions [132]. Since nitrogen metabolite repression does affect the gliotoxin gene

cluster, it would be interesting to test if AreA specifically contributes to any nucleosome remodeling within the gliotoxin cluster to induce gene expression.

GipA appears to play a considerable role in gliotoxin production, but is not essential, as mRNA levels of several gliotoxin-specific genes were significantly decreased in a *ΔgipA* mutant in non-repressing conditions (Fig. 4.5a). Most genes I tested experienced at least 50% reduction in mRNA levels, compared to the wild-type control. Furthermore, gliotoxin levels in the surrounding medium were reduced by 50% (Fig. 4.5b). Even though gliotoxin was drastically reduced in the *ΔgipA* mutant, loss of *gipA* did not cause a significant difference in growth of the fungus, even in the presence of exogenous gliotoxin (Fig. 4.6). This indicates that loss of *gipA* does not affect growth or sporulation of *A. fumigatus*. Loss of *gipA* did not affect virulence of *A. fumigatus* in a Toll-deficient *D. melanogaster* model, signifying that *gipA* is dispensable for virulence of the fungus in the model system I tested (Fig. 4.7). It is possible that GipA serves to enhance expression of the gliotoxin cluster in certain environmental conditions. Both high-copy expression and loss of *gipA* affects *gliZ* expression, so the effects I see for the entire cluster could be the direct consequence of GipA binding to each promoter region, or an indirect consequence of GipA partially regulating *gliZ*, which in turn regulates other genes within the cluster.

Interestingly, GipA does not appear to be highly conserved at the protein level, as only a few proteins showing high similarity were identified, the closest being a hypothetical protein in *N. fisheri* that shares 96% identity (Fig. 3.7a). There are also a few other *Aspergillus* species and some *Penicillium* species that contain a protein relatively similar to GipA. Although the gliotoxin biosynthetic cluster is not conserved throughout all *Aspergilli*, most of the *Aspergillus* species that came out of the query are gliotoxin-producing or contain homologues to gliotoxin genes (e.g. *A. niger, A. flavus, A. terreus*, *A. oryzae and A. kawachii*). Interestingly, *A. clavatus* also contains a $C_2H_2$ protein with sequence similarity to

GipA. Although a putative gliotoxin cluster has not been identified in *A. clavatus*, it is possible that gliotoxin is produced in this fungus. For proteins, primary sequences evolve and change much more rapidly than do the tertiary structures. There have been numerous examples where two proteins have low sequence similarity, but once crystallized, exhibit almost identical folding patterns and subsequently share similar functions [133]. For example, Gcn4 of *S. cerevisiae* and CpcA of *A. niger* share a 35% identity, yet they both function in amino acid biosynthesis. Furthermore, CpcA is able to complement a *Δgcn4* mutant in *S. cerevisiae* [134]. When solely comparing the putative DNA binding domain of *cpcA*, the identity between CpcA and Gcn4 increases to 70% [134]. Therefore, the lack of homologous counterparts to GipA in other organisms does not necessarily mean that there is not a protein present in other fungi that functions similarly to GipA. In addition, a search for homologues to the region containing the $C_2H_2$ DNA binding domains of GipA greatly increases the number of fungal organisms that contain a protein with high similarity (data not shown).

### 7.2 Characterization of GipB

GipB is a hybrid sensor kinase, containing a histidine kinase A (phospho-acceptor) domain, a GHKL (ATPase) domain, and a response regulator receiver domain. Hybrid sensor kinases are common in fungi, in contrast to bacterial systems, which have mainly separate sensor kinases and response regulators [126, 127]. Hybrid sensor kinases will autophosphorylate a Histidine (His) residue in the histidine kinase domain, in response to external stimuli, followed by a transfer of the phosphate to an Aspartic Acid (Asp) residue in the response regulator domain [126, 127]. Within the 5' UTR of *gipB* are two μORFs, which implies that *gipB* may also be under post-transcriptional regulation, as suggested for *gipA*

(Fig. 3.6a). Similar to what was observed with *gipA*, RNA levels of *gipB* remained low throughout all growth conditions I tested. Investigation of the protein sequence of GipB did not reveal any transmembrane domains, thereby presenting GipB as a cytosolic hybrid sensor kinase. In filamentous fungi, these cytosolic hybrid sensor kinases appear to play more of a role in controlling morphogenesis and differentiation, compared to transmembrane histidine kinases [127]. The first cytosolic hybrid sensor kinase identified in filamentous fungi was Nik-1/Os-1 of *Neurospora crassa*. Nik-1 is exclusively expressed during vegetative growth and is nonexistent in the sexual phase of growth. Aberrant hyphal development is observed when *nik-1* is deleted from *N. crassa*, thereby demonstrating that Nik-1 positively regulates vegetative growth [127].

GipB positively regulates the gliotoxin cluster, as high-copy expression of *gipB* resulted in an increase in mRNA levels for *gliA* and *gliT* at 24 hours growth (Fig. 5.2a). In addition, gliotoxin levels were higher than the empty vector control in repressing conditions at 24 hours (Fig. 5.2b). At 48 hours, however, mRNA levels of all genes tested in the high-copy *gipB* strain were comparable to the empty vector control. Gliotoxin was still detectable in the surrounding medium at levels higher than the AMA.GL control, but this is likely a result of activation of GipB earlier in the growth phase. This indicates that activity of GipB may be specific to certain phases of development. The growth conditions I employed (stationary cultures) were conducive to asexual development and conidiation, as strains grew heavily at the air interface and conidiated robustly. Therefore, the fact that high-copy expression of *gipB* did not induce the gliotoxin cluster at 48 hours of growth suggests that GipB is not activated through phosphorylation in the later stages of conidiation (Fig. 5.2b).

GipB does not appear to be essential for gliotoxin production, as loss of *gipB* only caused a decrease in *gliT* mRNA levels in non-repressing conditions, compared to the wild-type control, as well as a 10% decrease in gliotoxin levels (Fig. 5.5). Although cytosolic

hybrid sensor kinases have often been found to regulate fungal morphology and differentiation, I did not observe any significant growth abnormalities in the *ΔgipB* mutant or the high-copy *gipB* strain, suggesting that either GipB does not regulate vegetative growth or conidiophore development or that another hybrid sensor kinase shares a redundant role with GipB (Fig. 5.3 & 5.6). Similarly, I did not observe a significant effect on virulence of *A. fumigatus* in a Toll-deficient *D. melanogaster* model with either the *ΔgipB* mutant or the high-copy *gipB* strain, although the high-copy *gipB* strain displayed a trend towards increased death of the fruit flies (Fig. 5.4 & 5.7). It would be interesting to test a constitutively-active mutant and a constitutively-inactive mutant of GipB, which might prove more helpful in uncovering a clear role for GipB activity.

### 7.3 Model for *gliA* Regulation

I have devised a model for regulation of *gliA* that involves GliZ, GipA, and AreA (Fig. 7.1a). I propose that GliZ and GipA work together at the same binding site to induce *gliA*. In this model, GipA and GliZ are dependent on each other for inducing gene expression of *gliA*. I further posit that AreA contributes to the overall induction of *gliA* in the presence of non-preferred nitrogen sources. As shown in Figure 3.8b, a non-preferred nitrogen source causes increased expression of several genes within the gliotoxin cluster, indicating that AreA is acting on the gliotoxin cluster to induce gene expression. This most likely occurs via AreA-mediated induction of *gliZ* first, possibly followed by direct binding of AreA to promoter regions of other genes in the cluster. There is an AreA recognition sequence in the *gliA* promoter, 37 base pairs upstream of the ATG start site, but the close proximity of the recognition element in relation to the ATG likely means that AreA does not induce *gliA*

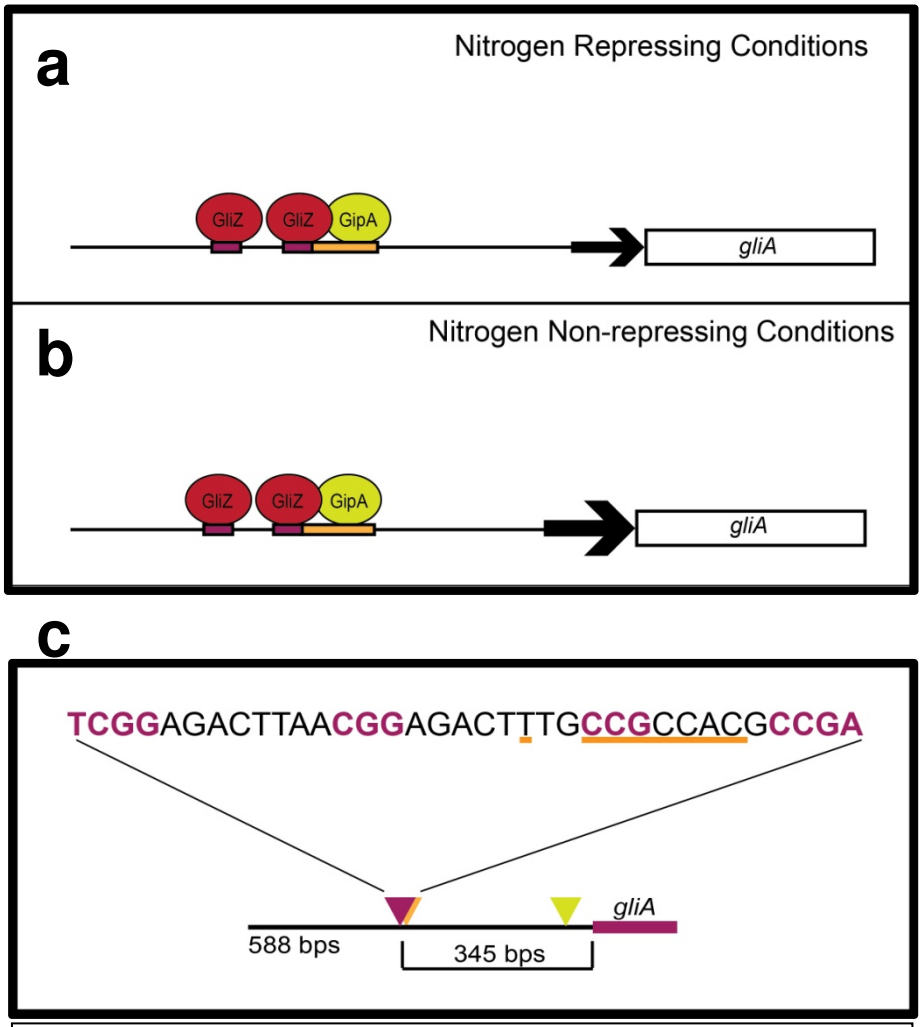


Figure 7.1. Model for *gliA* regulation. (a) I propose that both GliZ and GipA work together to induce *gliA*. (b) Furthermore, I propose that AreA acts to enhance *gliA* expression in nitrogen-specific non-repressing conditions. (c) Layout of the GipA/GliZ binding sites in the *gliA* promoter region, relative to the *gliA* start site. GliZ tandem repeats are purple and the GipA DNA binding site is underlined in orange. The AreA binding site is signified by the yellow triangle.

expression from that site (Fig. 7.1b). Although GipB is not included in this model, there are several possible models that involve GipB in the regulation of *gliA*, which are discussed below.

### 7.4 GliZ, GipA, and GipB: Independent or Interdependent?

I created two double deletion mutants to verify that either GliZ and GipA or GipA and GipB are signaling within a pathway and not independently. The *ΔgliZ/ΔgipA* double mutant appeared comparable to the *ΔgliZ* single mutant, with respect to gliotoxin biosynthesis (Fig. 6.2). I did not observe an additive effect, indicating that these two proteins do not signal through independent pathways and that GipA may signal cooperatively with GliZ. This supports my model of *gliA* regulation, in which GliZ and GipA are not independently activating *gliA* expression. These data are not completely clear, though, as the decrease in mRNA levels and gliotoxin production in a *ΔgliZ* mutant were already so low, there may not be any possibility of an additive effect, even if GipA and GliZ are independent of one another. The possibility of GliZ and GipA acting independently, although not entirely impossible, is highly unlikely, as transcription factors located within biosynthetic clusters are often required for induction of other genes within the cluster. There have been examples of independent gene regulation, though. For instance, *gliT* is positively regulated by GliZ, as are all the other genes within the gliotoxin cluster. However, when *A. fumigatus* was exposed to exogenous gliotoxin, *gliT* was induced, even in the absence of *gliZ* [27]. This raises the possibility that based on the toxic nature of some secondary metabolites, alternative regulation of certain genes within these clusters may have evolved to ensure protection of the organism from the toxin itself or possibly other toxins with similar structures that are produced by competing organisms. I did not create a *ΔgliZ/ΔgipB* double

mutant, as I hypothesized that the results would not show an additive effect, again because loss of *gliZ* already affects gene expression so drastically.

In the *ΔgipA/ΔgipB* double mutant, mRNA levels of gliotoxin-specific genes were comparable to the *gipA* single deletion mutant (Fig. 6.5). Loss of *gipA* does not reduce mRNA levels as drastically as *ΔgliZ,* so I was able to discern if an additive effect was present in the *ΔgipA/ΔgipB* strain. Since there was in fact no additive effect, it is possible that GipA and GipB are part of a linear pathway and that GipA is downstream of GipB. However, the effect of the *gipB* single mutant on the gliotoxin cluster was so mild, that an additive effect may not be possible. One explanation is that there are other hybrid sensor kinases that are redundant for GipB with respect to gliotoxin production. Neither double mutant displayed abnormal growth or virulence in a Toll-deficient *D. melanogaster* model, indicating that there is not an additive effect with respect to growth rate or virulence of *A. fumigatus* (Fig. 6.3, 6.4, 6.6 & 6.7). However, although conidiation was not drastically affected by loss of either *gipA* or *gipB*, the *ΔgipA/ΔgipB* double mutant displayed a 50% reduction in spores/cm$^2$ on rich medium, suggesting that GipA and GipB may be involved in independent signaling pathways in regards to conidiation (Fig. 6.6b). This raises the possibility that GipB and GipA are signaling independent of each other for gliotoxin cluster expression as well.

A possible consensus DNA binding site for GipA was identified through protein binding microarray (Fig. 4.8), which I verified using *in vivo* mutagenesis of the *gliA* promoter (Fig. 4.9). A few interesting discoveries came out of the *in vivo* promoter mutagenesis experiments. First is the possibility of an unknown transcriptional activator binding to a sequence near the GipA binding site. I propose this based on the fact that mutation of the single 5' T residue resulted in a significant decrease (8-fold in repressing conditions and 4-fold in non-repressing conditions) in *lacZ* expression in AMA.SD1 (background LacZ) (Fig.

4.9a), yet GipA-specific *lacZ* expression was significantly induced (53-fold), compared to the empty vector control (Fig. 4.9b). This observation could also be explained by weaker GipA binding, which is rescued by high-copy expression of GipA. However, when a core region of the GipA binding site was mutated, I discovered that basal *lacZ* expression not only increased, but exceeded the basal levels of the wild-type binding site (5-fold in repressing conditions and 2-fold in non-repressing conditions) (Fig. 4.9b), yet GipA-specific *lacZ* induction was significantly reduced, almost to the level of the empty vector control (Fig. 4.7b). This supports my hypothesis that an unknown transcriptional activator is binding in close proximity to the GipA binding site and that mutation of the single T residue negatively affects this. If there was not an additional transcriptional activator present and both mutations were only affecting GipA binding, I would expect the basal LacZ levels to remain low for both binding site mutants. The fact that mutation of the core sequence in the binding site raised basal LacZ levels higher than they were with the wild-type binding site suggests two possibilities: (1) GipA and this unknown transcriptional activator are competing for binding or (2) GipA and this unknown transcriptional activator play antagonistic roles in *gliA* expression. This is further supported by the fact that GipA-specific induction of *lacZ* was higher when the single T residue was mutated than it was when exposed to the wild-type binding site.

The second interesting discovery was the fact that GliZ-specific *lacZ* induction was similar to that observed with GipA-specific induction (Fig. 4.9). I expected GliZ-specific induction of *lacZ* to be independent of the GipA binding site, but this was not the case. Upon further examination, I realized that the GipA binding site is embedded within possible GliZ binding sites (Fig. 7.1c). Although a GliZ binding site has not yet been tested, one has been predicted ($TCGGN_3CCGA$). This sequence is present in the intergenic region of every gene within the gliotoxin cluster, except *gliZ* and *gliA* [15]. Studies have shown that

recognition of these sequences by $Zn_2Cys_6$ binuclear finger transcription factors is very specific and even a slight change to the length or base composition of the linker sequence can result in reduced binding *in vivo* [16, 18, 19]. Within the *gliA* promoter region, there are four sequences commonly found to be recognized by $Zn_2Cys_6$ transcription factors (Fig. 7.1c). The innermost two are inverted repeats with an 8 bp linker sequence, while the outer two, which are also inverted repeats, contain a 27 bp linker sequence, although the longer linker sequence seems less likely to be recognized by a $Zn_2Cys_6$ transcription factor. Furthermore, the core sequence of the GipA binding site that I mutated contains the CCG of the smaller GliZ-like binding site (Fig. 7.1c). Therefore, mutation of the core sequence changed one of the inverted repeats, likely abolishing GliZ-mediated *lacZ* induction. From these data, I cannot distinguish whether GliZ binding is independent of GipA or dependent, because in the process of mutating the GipA binding site, I also inadvertently mutated an essential part of a possible GliZ binding site.

To test this, I expressed high-copy plasmids in various deletion backgrounds and measured RNA levels of *gliA*, as well as *gliP*. For *gliP* regulation, GipA was dependent on GliZ but GliZ did not require the presence of GipA (Fig. 6.8b). Furthermore, GipB appeared dependent on both GliZ and GipA to induce *gliP* (Fig. 6.8b). For *gliA* regulation, I observed a different pattern, as GliZ and GipA were dependent on each other to induce *gliA* (Fig. 6.8a). Dependent dual regulation of two transcription factors has been uncovered in other organisms. For example, *in A. nidulans*, FlbB and FlbD both bind in close proximity to the *brlA* promoter to regulate asexual development through *brlA* activation [39, 135]. FlbB, in a complex with FlbE, induces *flbD* expression by direct binding to the *flbD* promoter [135-137]. Once FlbD is translated, FlbD and FlbB are both necessary to activate *brlA*. Furthermore, FlbB does not bind to the *brlA* promoter in the absence of FlbD, indicating that these two transcription factors are dependent on each other for DNA binding and activation

of *brlA* [135]. GipB also appeared dependent on both GliZ and GipA for *gliA* induction (Fig. 6.8a). I did not test the high-copy plasmids in a *ΔgipB* deletion background. I attempted to isolate this mutant, but experienced issues that led us to focus on the *gliZ* and *gipA* deletion backgrounds. I created a *gipB* deletion mutant for earlier experiments, but these were done in an *nkuB* deletion background to facilitate homologous recombination. I suspect that in a *ΔgipB* background, GliZ and GipA are both able to induce *gliA* and *gliP*, as GipB encodes a hybrid sensor kinase that is likely acting upstream of both proteins.

These data support a model in which GliZ and GipA are working together to regulate *gliA* (Fig. 7.1). There appears to be a dependency with regards to *gliA* expression that I demonstrated in my experiments. I cannot say if GliZ and GipA are physically interacting by forming a complex, but the intimate nature of the DNA binding sites suggests this may be the case. $C_2H_2$ transcription factors have been shown to be involved in protein-protein interactions [138]. One well characterized example of these protein-protein interactions is that of FOG-1 and GATA-1. FOG-1 is a $C_2H_2$ zinc finger transcription factor containing nine zinc finger domains, only four of which carry the classical $C_2H_2$ motif. The other five motifs harbor the natural variant $C_2HC$ motif [139]. Studies have demonstrated that zinc finger motifs 1, 5, 6, and 9, which all contain the $C_2HC$ variant, are involved in the protein-protein interaction of FOG-1 with GATA-1 [122, 138, 139]. Interestingly, despite the fact that $C_2H_2$ domains and $C_2HC$ domains display an almost identical folding pattern, these domains are not interchangeable. This was demonstrated by the fact that mutation of the third cysteine residue in zinc finger domains 1 and 9 to histidine ($C_2HC \rightarrow C_2H_2$) in FOG-1 did not disrupt their folding, but abolished their ability to interact with GATA-1 in a yeast two-hybrid assay [122, 138]. This pattern may not apply to all protein-protein interactions involving $C_2H_2$ zinc finger transcription factors, but it does support the possibility that these natural $C_2HC$ variants are involved in protein-protein interactions.

GipA contains two zinc finger binding domains, one of which is the classical $C_2H_2$ motif and the other is the variant $C_2HC$ motif. Perhaps GipA and GliZ form a protein-protein complex, involving the $C_2HC$ motif of GipA, to facilitate DNA binding and activation of *gliA*. Mutational analysis of the $C_2HC$ motif and pull-down assays would possibly be able to elucidate the presence of such a complex. It would also be interesting to see if mutation of the GipA binding site, without mutating the GliZ palindromic sequence, would reinstate GliZ-mediated expression of *lacZ*, although I suspect this would not be the case as GipA is required for GliZ-mediated expression of *gliA* and loss of GipA binding might negatively affect GliZ binding. This model does not apply to every gene within the gliotoxin cluster, as no other genes have a GipA binding site embedded within a possible GliZ binding site, except *gliZ,* although these sequence are located farther upstream of the *gliZ* start site (Fig. 7.2). Perhaps GipA serves to aid GliZ in binding to the *gliA* promoter region, as this binding site is different from the others present in the gliotoxin cluster.

Although there are possible GipA binding sites in all gliotoxin gene promoters, except *gliM*, I cannot say with certainty whether GipA is directly binding to these other promoter regions or if GipA is simply binding in the *gliA* promoter in conjunction with GliZ. This adds to mounting evidence that genes within a gene cluster are typically coordinately regulated, but can also be individually expressed in response to certain stimuli. It is possible that *gliT* and *gliA* are both independently regulated to protect the fungus from exogenous gliotoxin, although *gliA* was not induced in a *ΔgliZ* mutant in the presence of exogenous gliotoxin as *gliT* was [27]. Another possibility is that *gliA* is independently regulated to aid in the transport and/or expression of other secondary metabolism clusters in *A. fumigatus*. There has been evidence in other fungal species that crosstalk between these gene clusters exists [140]. For instance, in *A. nidulans*, biosynthesis of asperthecin is enhanced in a strain over-expressing RsmA, a bZIP transcription factor [84]. Interestingly,

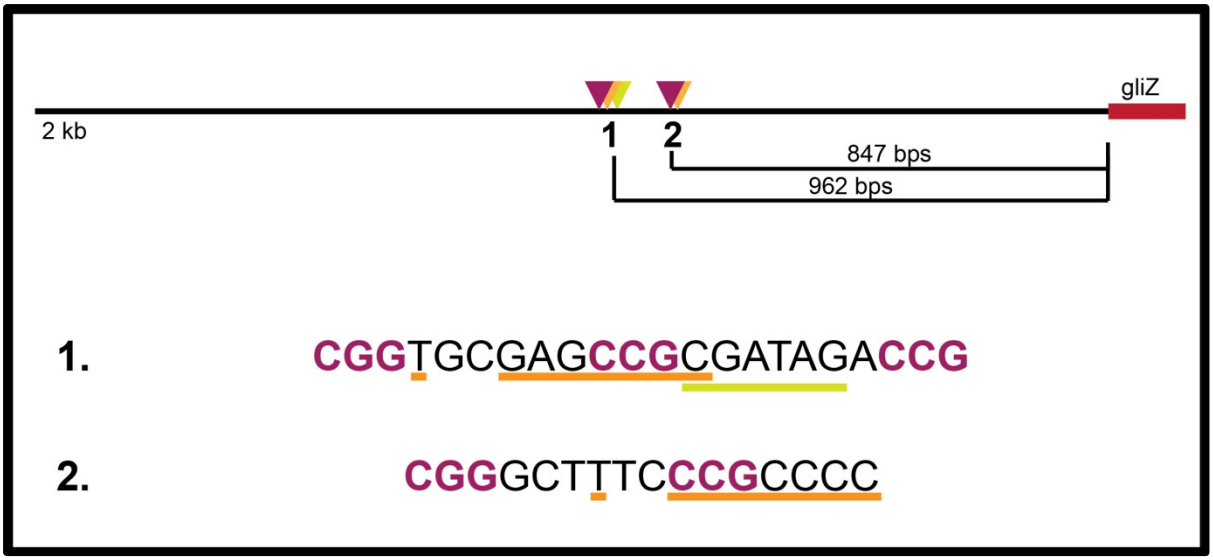


Figure 7.2. Layout of two potential GipA binding sites that are embedded in putative GliZ binding sites in the *gliZ* promoter. GliZ putative trinucleotide repeats are purple, the putative GipA binding sites are signified with orange, and binding cluster 1 additionally contains an AreA recognition element (yellow).

asperthecin synthesis is reduced when *aflR* is deleted in an RsmA over-expression background. AflR is a $Zn_2Cys_6$ binuclear finger transcription factor necessary for expression of aflatoxin and sterigmatocystin secondary metabolism clusters. Therefore, RsmA exerts its effects on the asperthecin biosynthetic cluster through AflR, which is located in a separate cluster [84].

Interestingly, RsmA has recently been characterized in *A. fumigatus*. Similar to what is seen in *A. nidulans*, over-expression of RsmA results in a significant increase in gliotoxin production, as well as an increase in mRNA transcript levels of multiple gliotoxin-specific genes [108]. High-copy expression of *gipA* also induced the gliotoxin cluster (Fig.4.2), although contrary to what was observed with *rsmA*, loss of *gipA* significantly reduced the level of gliotoxin in surrounding medium (Fig. 4.5). RsmA cannot induce the gliotoxin cluster in the absence of either *gliZ* or *laeA*, suggesting that both proteins are necessary for RsmA-mediated signaling [108]. I found a similar pattern for GipA-mediated signaling, as loss of *gliZ* negatively affected the ability of GipA to induce *gliP* and *gliA*, although there was a slight increase in *gliA* mRNA transcript levels, compared to basal levels (Fig. 6.8). Therefore GliZ is essential for complete GipA-mediated induction. I did not test the high-copy *gipA* strain in a *ΔlaeA* background, but this test would be worthwhile, as chromatin remodeling could contribute to GipA binding. Based on microarray data from a *ΔlaeA* strain, GipA is not regulated by LaeA, as *gipA* gene expression was not altered with loss of *laeA*, compared to a wild-type strain. Interestingly, GipB showed a moderate up-regulation in gene expression in the *laeA* deletion mutant, suggesting that LaeA negatively regulates GipB, which could be a result of developmental regulation (personal communication, Nancy P. Keller).

Although the experiments I performed give evidence for my model connecting GliZ and GipA, additional models further including GipB are more speculative. For instance, one

model could involve GipB signaling upstream of GliZ and GipA, suggesting that both transcription factors are required for GipB-mediated *gliA* expression (Fig. 7.3). This is supported by the fact that high-copy expression of *gipB* could not induce *gliA* in the absence of either *gliZ* or *gipA*. However, this pattern was also observed with respect to *gliP* expression, even though the interdependency of *gliZ* and *gipA* was not present. One explanation for this pattern is that GipB signals through GliZ and GipA to induce all genes in the gliotoxin cluster. An alternative explanation is that the experiment itself was not conclusive for GipB-mediated induction. As discussed earlier, high-copy expression of *gipB* induces the gliotoxin cluster at 24 hours growth, but not 48 hours growth, possibly due to temporal control of the activation of GipB. The *gliA* and *gliP* mRNA levels I measured in response to high-copy expression of *gipB* in various deletion backgrounds were collected after 48 hours growth. Therefore the results could falsely exhibit a dependency of GipB signaling on GliZ and GipA, when in fact GipB is simply not activated at this time point and can therefore not induce these gliotoxin genes. A second model would involved GliZ and GipA acting in an interdependent fashion, as I have proposed, but also involving GipB positively regulating the gliotoxin cluster independently of GipA, but most likely through GliZ (Fig. 7.3).

Although the *ΔgipA/ΔgipB* double mutant did not display an additive phenotype with respect to gliotoxin production, it did exhibit a 50% reduction in sporulation. This sporulation defect was not observed with the *ΔgipA* single mutant or the *ΔgipB* single mutant, indicating that it was in fact an additive effect, possibly as a result of GipA and GipB being involved in separate signaling pathways. While the *ΔgipA* single mutant had significantly reduced gliotoxin production (50%), the loss of *gipB* did not significantly affect gliotoxin production, so loss of both might not display an additive reduction in gliotoxin levels, even if they are both involved in separate pathways. Therefore, the sporulation

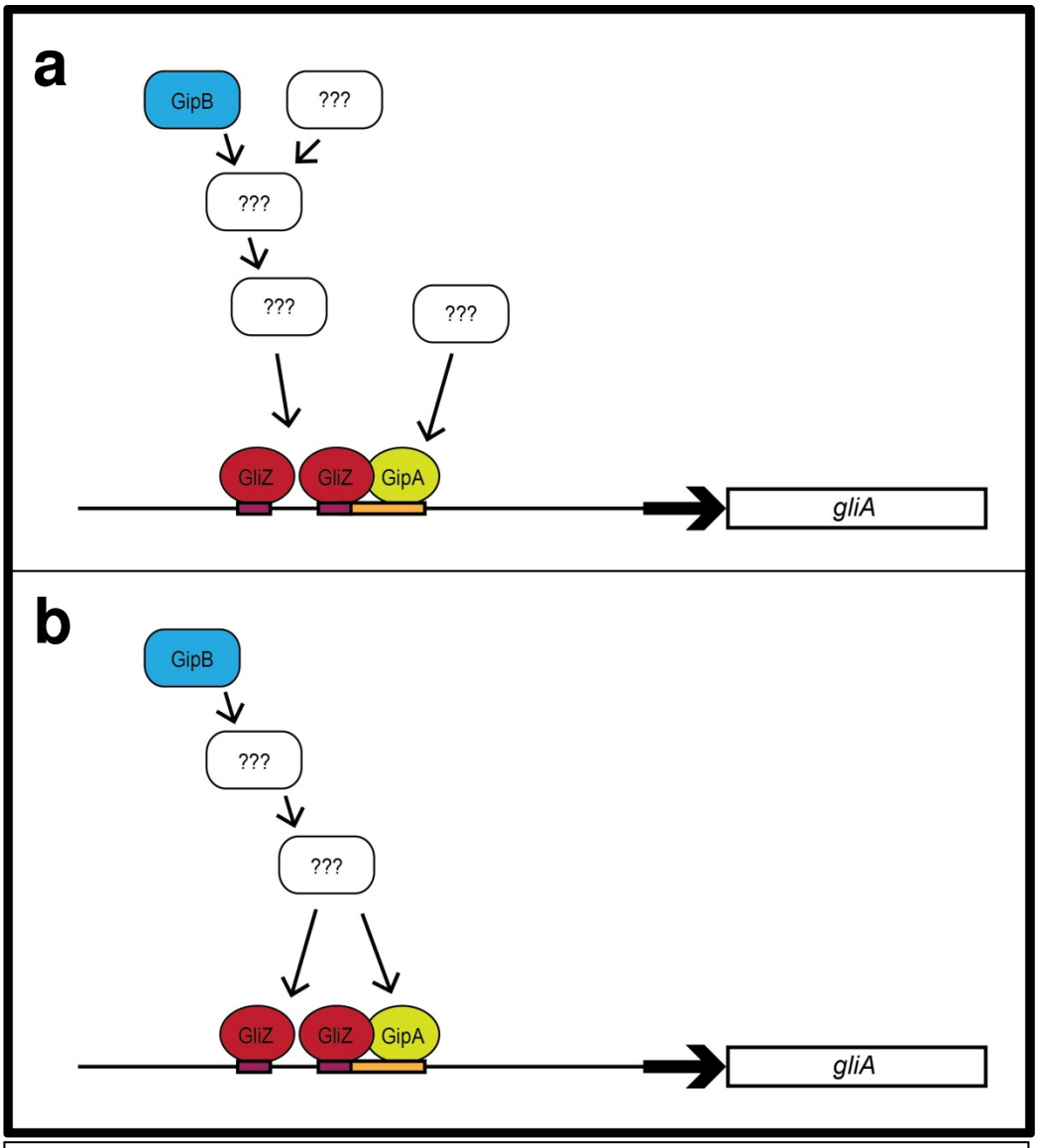


Figure 7.3. Possible models for *gliA* regulation involving GipB, GipA, and GliZ. (a) In this model, GipB is regulating *gliA* in a signaling pathway that is separate from GipA. Furthermore, there is possibly another hybrid sensor kinase that acts in a redundant fashion to GipB with respect to *gliA* expression. (b) In this model, GipB is regulating *gliA* upstream of both GipA and GliZ. All three proteins are involved in the same pathway.

phenotype of the *ΔgipA/ΔgipB* double mutant raises the possibility that GipB plays a role in regulating the gliotoxin cluster independently of GipA. The fact that the *ΔgipB* deletion strain did not significantly reduce gliotoxin production does not rule out the possibility that GipB is involved in gliotoxin gene cluster expression, as high-copy expression of *gipB* induces gliotoxin production. However, it is not clear if the positive effects exerted by GipB are direct (e.g. through a specific pathway) or indirect (e.g. altering other proteins that happen to effect gliotoxin production). If GipB is directly regulating the gliotoxin cluster, there could be other hybrid sensor kinases that play a redundant role in gliotoxin cluster expression, which would mask any effects from the loss of *gipB* alone. Further exploring these possibilities would serve to uncover a stronger model that explains the role of GipB in regulation of the gliotoxin cluster.

### 7.5 Future Perspectives

GipB and GipA are novel proteins in *A. fumigatus* that have not been characterized before my work. I originally discovered these proteins in a high-copy inducer screen searching for genes that induce a *gliA*$^{P}$*-lacZ* expression plasmid and presumably the entire gliotoxin cluster. Therefore, the work I completed for this project focused on gliotoxin production and *gliA* regulation specifically. Obviously there are many more experiments to be done to truly understand the mechanism by which GipB and GipA regulate *gliA* expression, as well as the gliotoxin cluster as a whole. For instance, as mentioned above, there are putative GipA binding sites in the intergenic regions upstream of every gliotoxin cluster gene, except *gliM*. There is a putative GipA binding site upstream of *gliM*, but it is upstream of the stop codon of the preceding gene. I showed from RNA dot blot analysis that GipA positively regulates multiple genes in the gliotoxin cluster. Although I obtained

evidence that GipA is directly binding to the *gliA* promoter, I do not know for certain whether GipA is regulating other genes in the cluster by directly binding to every promoter or through modulation of *gliZ* expression only. This could be tested through promoter mutagenesis of each promoter region, as was done for gliA, or through chromatin Immunoprecipitation.

Interestingly, there are two "binding clusters" in the upstream region of *gliZ* that contain a putative GipA binding site embedded within potential GliZ binding sites. I call these regions "potential GliZ binding sites" because of the presence of CGG trinucleotide repeats that are common recognition elements of $Zn_2Cys_6$ transcription factors, although the linker sequences are longer than those predicted for GliZ recognition. A potential GliZ binding site ($TCGGN_3CCGA$) has been proposed and is present upstream of every gliotoxin cluster gene, except *gliZ* and *gliA*, though this has not been experimentally studied [15]. In addition, these "binding clusters" that include putative binding sites for both GliZ and GipA are only present in the upstream regions of *gliZ* and *gliA*. Both "binding clusters" upstream of *gliZ* comprise 6 bp linker sequences, while the "binding cluster" upstream of *gliA* contains an 8 bp linker sequence. It would be advantageous to discover if either of the "binding clusters" in the *gliZ* upstream region are necessary for or contribute to *gliZ* expression, as was shown for the "binding cluster" in the *gliA* promoter, as would finding out if GipA directly binds to the promoter regions of the other gliotoxin cluster genes.

In verifying that GipA induces *gliA* through a particular GipA recognition site, I inadvertently discovered that GliZ also relies on this site for full *gliA* induction. Although I showed that mutation of part of the GipA binding site, which happened to contain a CCG trinucleotide, reduced GliZ-mediated induction of a $gliA^P$-*lacZ* expression plasmid, I did not experimentally verify direct binding of GliZ to this region. Although unlikely, GipA could be interacting with GliZ and directly binding to the DNA sequence, without GliZ directly binding

to the DNA. On the other hand, GliZ and GipA could be involved in a protein-protein interaction, in which, under certain conditions, GipA facilitates the direct binding of GliZ to a binding site that GliZ would not normally recognize, due to the longer linker sequence between the trinucleotide repeats. Further studies need to be performed to verify direct binding of GliZ to the *gliA* promoter, as well as the presence of a protein-protein interaction between GliZ and GipA. $C_2H_2$ transcription factors often contain zinc finger domains harboring the classical $C_2H_2$ motif, but some encode a natural variant, $C_2HC$, which displays an almost identical folding pattern to the $C_2H_2$ region [138]. This $C_2HC$ variation has been shown to be involved in protein-protein interactions in other organisms, although this is not considered to be ubiquitous to all $C_2HC$ variants [138]. As discussed above, GipA contains two zinc finger regions, one being the classical $C_2H_2$ motif and the other being the natural variation of $C_2HC$. Therefore, it is possible that GipA is directly interacting with GliZ through this $C_2HC$ domain. Uncovering such an interaction would greatly contribute to the understanding of the GliZ-GipA interdependent relationship with regards to *gliA* expression, and possibly *gliZ* expression as well.

GipB, being a hybrid sensor kinase, likely activates downstream proteins to induce the gliotoxin cluster. In fungal systems, these hybrid sensor kinases are generally thought to autophosphorylate in response to certain stimuli, followed by transfer of the phosphate to an HPt protein and subsequent transfer of the phosphate from the HPt protein to a response regulator. These response regulators can directly act on transcription factors or can activate signaling cascades, oftentimes composed of MAP kinase proteins. Therefore, it is likely that GipB is not directly activating the gliotoxin cluster, but is signaling through several proteins. Interestingly, research has provided evidence that only one HPt protein exists in all fungi that have been studied [127]. If GipB does activate downstream targets through this two-component relay system, it is highly likely that the single HPt protein in *A.*

*fumigatus*, which has not been characterized, is involved in this process. Research in other fungal species has suggested that cytosolic hybrid sensor kinases are likely involved in morphogenesis and development [127]. As the *gipB* DNA sequence does not show any obvious transmembrane domains, I predict that GipB is a cytosolic hybrid sensor kinase. Furthermore, RNA dot blot analysis indicated that GipB is activated during specific stages of conidiation, as high-copy expression of *gipB* induced gliotoxin production at 24 hours of growth, but not at 48 hours, which supports the possibility that GipB is involved in developmental processes. Studying a constitutively-active or constitutively-inactive form of GipB would be advantageous in elucidating a specific role for GipB activation.

The effects of nitrogen metabolite repression on gliotoxin production was studied by growing cultures in different nitrogen sources, however, other environmental regulatory networks were not researched for my project, including carbon catabolite repression and pH-mediated regulation. All growth conditions were under carbon catabolite repression, as repressing carbon sources were used throughout the experiments. Furthermore, pH-mediated induction was not observed, as medium was properly buffered preventing any pH changes to either acidic or alkaline conditions. In all conditions tested, *gipB* and *gipA* mRNA levels remained low, suggesting that nitrogen metabolite repression does not affect the expression of *gipA* or *gipB*. Upon examination of the promoter regions of both genes, I discovered a multitude of recognition elements belonging to global regulators, such as Area, CreA and PacC, and developmental regulators, such as AbaA, BrlA, and FlbC (Fig. 7.4). The presence of such recognition elements does not guarantee that they are actively recognized by the regulatory protein, but it does suggest that GipB and GipA may be under the control of both environmental global regulators and developmental regulatory networks. Further work focusing on uncovering specific regulators of *gipB* and *gipA* expression could contribute our understanding of these two novel proteins in *A. fumigatus*.

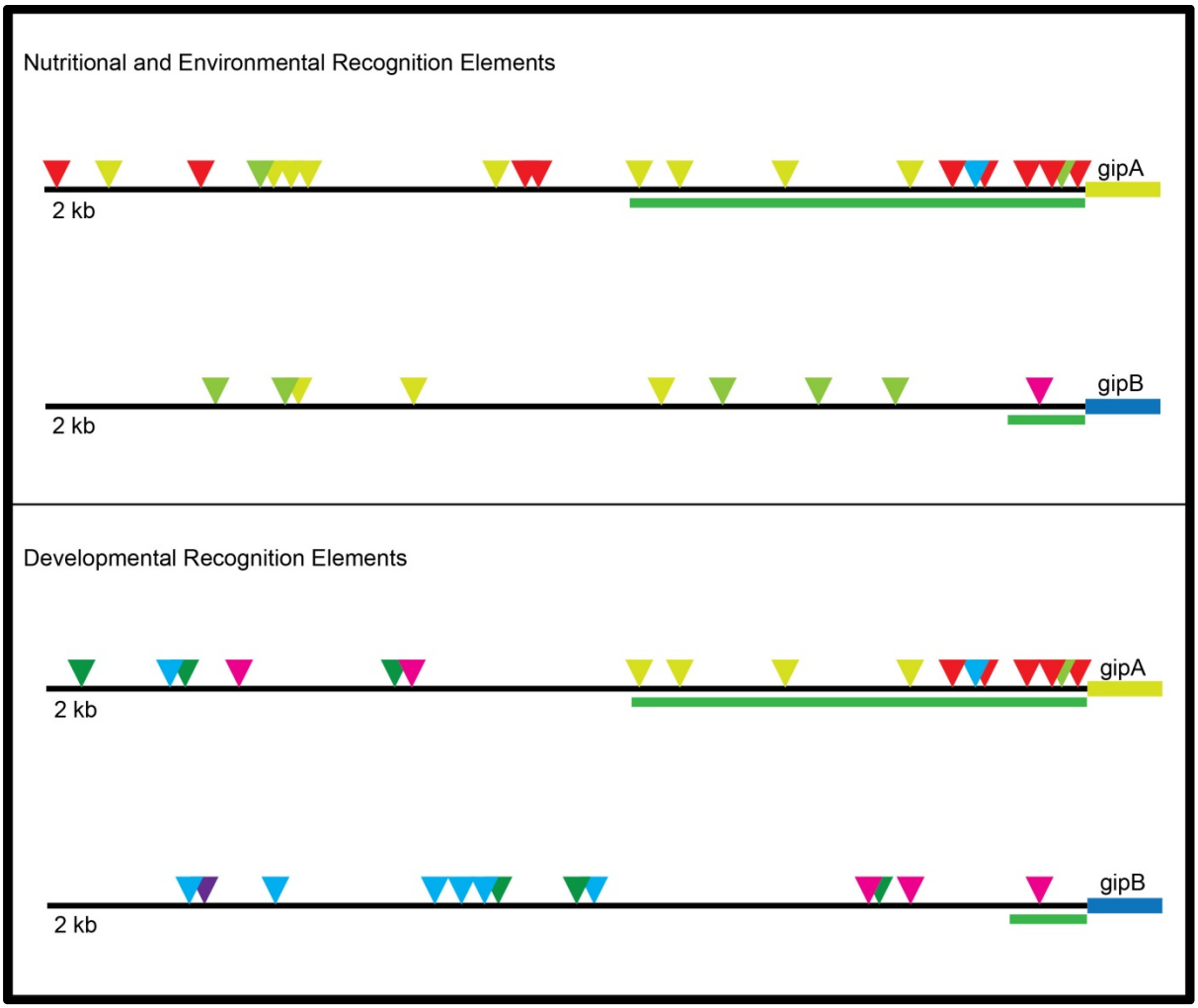


Figure 7.4. Layout of putative regulatory elements in the *gipA* and *gipB* promoter regions. The green bars represent the predicted 5' UTRs of each mRNA, based on data from the λ phage library screen. Binding sites displayed: CreA (red), AreA (yellow), PacC (light green), AbaA(green), FlbD (cyan), BrlA (magenta), and FlbC (purple).

# Chapter 8:

# References

## References


1. **Bayram, O. and G.H. Braus, *Coordination of secondary metabolism and development in fungi: the velvet family of regulatory proteins.* FEMS Microbiol Rev. 36(1): p. 1-24.**
2. **Keller, N.P., G. Turner, and J.W. Bennett, *Fungal secondary metabolism - from biochemistry to genomics.* Nat Rev Microbiol, 2005. 3(12): p. 937-47.**
3. **Brakhage, A.A., *Regulation of fungal secondary metabolism.* Nat Rev Microbiol. 11(1): p. 21-32.**
4. **Kamei, K. and A. Watanabe, *Aspergillus mycotoxins and their effect on the host.* Med Mycol, 2005. 43 Suppl 1: p. S95-9.**
5. **Calvo, A.M., R.A. Wilson, J.W. Bok, and N.P. Keller, *Relationship between secondary metabolism and fungal development.* Microbiol Mol Biol Rev, 2002. 66(3): p. 447-59, table of contents.**
6. **Latge, J.P., *Aspergillus fumigatus and aspergillosis.* Clin Microbiol Rev, 1999. 12(2): p. 310-50.**
7. **Gardiner, D.M., A.J. Cozijnsen, L.M. Wilson, M.S. Pedras, and B.J. Howlett, *The sirodesmin biosynthetic gene cluster of the plant pathogenic fungus Leptosphaeria maculans.* Mol Microbiol, 2004. 53(5): p. 1307-18.**
8. **Yu, J.H. and N. Keller, *Regulation of secondary metabolism in filamentous fungi.* Annu Rev Phytopathol, 2005. 43: p. 437-58.**
9. **Sigl, C., H. Haas, T. Specht, K. Pfaller, H. Kurnsteiner, and I. Zadra, *Among developmental regulators, StuA but not BrlA is essential for penicillin V production in Penicillium chrysogenum.* Appl Environ Microbiol. 77(3): p. 972-82.**

10. **Brakhage, A.A., P. Browne, and G. Turner, *Regulation of Aspergillus nidulans penicillin biosynthesis and penicillin biosynthesis genes acvA and ipnA by glucose.* J Bacteriol, 1992. 174(11): p. 3789-99.**

11. **Yu, J., D. Bhatnagar, and K.C. Ehrlich, *Aflatoxin biosynthesis.* Rev Iberoam Micol, 2002. 19(4): p. 191-200.**

12. **McDonagh, A., N.D. Fedorova, J. Crabtree, Y. Yu, S. Kim, D. Chen, O. Loss, T. Cairns, G. Goldman, D. Armstrong-James, K. Haynes, H. Haas, M. Schrettl, G. May, W.C. Nierman, and E. Bignell, *Sub-telomere directed gene expression during initiation of invasive aspergillosis.* PLoS Pathog, 2008. 4(9): p. e1000154.**

13. **Bok, J.W., D. Chung, S.A. Balajee, K.A. Marr, D. Andes, K.F. Nielsen, J.C. Frisvad, K.A. Kirby, and N.P. Keller, *GliZ, a transcriptional regulator of gliotoxin biosynthesis, contributes to Aspergillus fumigatus virulence.* Infect Immun, 2006. 74(12): p. 6761-8.**

14. **Gardiner, D.M. and B.J. Howlett, *Bioinformatic and expression analysis of the putative gliotoxin biosynthetic gene cluster of Aspergillus fumigatus.* FEMS Microbiol Lett, 2005. 248(2): p. 241-8.**

15. **Fox, E.M., D.M. Gardiner, N.P. Keller, and B.J. Howlett, *A Zn(II)2Cys6 DNA binding protein regulates the sirodesmin PL biosynthetic gene cluster in Leptosphaeria maculans.* Fungal Genet Biol, 2008. 45(5): p. 671-82.**

16. **Todd, R.B. and A. Andrianopoulos, *Evolution of a fungal regulatory gene family: the Zn(II)2Cys6 binuclear cluster DNA binding motif.* Fungal Genet Biol, 1997. 21(3): p. 388-405.**

17. **Ehrlich, K.C., B.G. Montalbano, and J.W. Cary, *Binding of the C6-zinc cluster protein, AFLR, to the promoters of aflatoxin pathway biosynthesis genes in Aspergillus parasiticus.* Gene, 1999. 230(2): p. 249-57.**

18. **Liang, S.D., R. Marmorstein, S.C. Harrison, and M. Ptashne, *DNA sequence preferences of GAL4 and PPR1: how a subset of Zn2 Cys6 binuclear cluster proteins recognizes DNA.* Mol Cell Biol, 1996. 16(7): p. 3773-80.**

19. **Vashee, S., H. Xu, S.A. Johnston, and T. Kodadek, *How do "Zn2 cys6" proteins distinguish between similar upstream activation sites? Comparison of the DNA-binding specificity of the GAL4 protein in vitro and in vivo.* J Biol Chem, 1993. 268(33): p. 24699-706.**

20. **Yin, W. and N.P. Keller, *Transcriptional regulatory elements in fungal secondary metabolism.* J Microbiol. 49(3): p. 329-39.**

21. **Kupfahl, C., T. Heinekamp, G. Geginat, T. Ruppert, A. Hartl, H. Hof, and A.A. Brakhage, *Deletion of the gliP gene of Aspergillus fumigatus results in loss of gliotoxin production but has no effect on virulence of the fungus in a low-dose mouse infection model.* Mol Microbiol, 2006. 62(1): p. 292-302.**

22. **Cramer, R.A., Jr., M.P. Gamcsik, R.M. Brooking, L.K. Najvar, W.R. Kirkpatrick, T.F. Patterson, C.J. Balibar, J.R. Graybill, J.R. Perfect, S.N. Abraham, and W.J. Steinbach, *Disruption of a nonribosomal peptide synthetase in Aspergillus fumigatus eliminates gliotoxin production.* Eukaryot Cell, 2006. 5(6): p. 972-80.**

23. **Spikes, S., R. Xu, C.K. Nguyen, G. Chamilos, D.P. Kontoyiannis, R.H. Jacobson, D.E. Ejzykowicz, L.Y. Chiang, S.G. Filler, and G.S. May, *Gliotoxin production in Aspergillus fumigatus contributes to host-specific differences in virulence.* J Infect Dis, 2008. 197(3): p. 479-86.**

24. **Kwon-Chung, K.J. and J.A. Sugui, *What do we know about the role of gliotoxin in the pathobiology of Aspergillus fumigatus?* Med Mycol, 2009. 47 Suppl 1: p. S97-103.**

25. **Gardiner, D.M., R.S. Jarvis, and B.J. Howlett, *The ABC transporter gene in the sirodesmin biosynthetic gene cluster of Leptosphaeria maculans is not***

***essential for sirodesmin production but facilitates self-protection.*** **Fungal Genet Biol, 2005. 42(3): p. 257-63.**

**26. Fox, E.M. and B.J. Howlett, *Biosynthetic gene clusters for epipolythiodioxopiperazines in filamentous fungi.* Mycol Res, 2008. 112(Pt 2): p. 162-9.**

**27. Schrettl, M., S. Carberry, K. Kavanagh, H. Haas, G.W. Jones, J. O'Brien, A. Nolan, J. Stephens, O. Fenelon, and S. Doyle, *Self-protection against gliotoxin--a component of the gliotoxin biosynthetic cluster, GliT, completely protects Aspergillus fumigatus against exogenous gliotoxin.* PLoS Pathog, 2010. 6(6): p. e1000952.**

**28. Krijgsheld, P., R. Bleichrodt, G.J. van Veluw, F. Wang, W.H. Muller, J. Dijksterhuis, and H.A. Wosten, *Development in Aspergillus.* Stud Mycol. 74(1): p. 1-29.**

**29. Bruns, S., M. Seidler, D. Albrecht, S. Salvenmoser, N. Remme, C. Hertweck, A.A. Brakhage, O. Kniemeyer, and F.M. Muller, *Functional genomic profiling of Aspergillus fumigatus biofilm reveals enhanced production of the mycotoxin gliotoxin.* Proteomics. 10(17): p. 3097-107.**

**30. Park, H.S. and J.H. Yu, *Genetic control of asexual sporulation in filamentous fungi.* Curr Opin Microbiol. 15(6): p. 669-77.**

**31. Sarikaya Bayram, O., O. Bayram, O. Valerius, H.S. Park, S. Irniger, J. Gerke, M. Ni, K.H. Han, J.H. Yu, and G.H. Braus, *LaeA control of velvet family regulatory proteins for light-dependent development and fungal cell-type specificity.* PLoS Genet. 6(12): p. e1001226.**

**32. Park, H.S., O. Bayram, G.H. Braus, S.C. Kim, and J.H. Yu, *Characterization of the velvet regulators in Aspergillus fumigatus.* Mol Microbiol.**

33. Osherov, N. and G. May, *Conidial germination in Aspergillus nidulans requires RAS signaling and protein synthesis.* Genetics, 2000. 155(2): p. 647-56.

34. Juvvadi, P.R., J.R. Fortwendel, N. Pinchai, B.Z. Perfect, J. Heitman, and W.J. Steinbach, *Calcineurin localizes to the hyphal septum in Aspergillus fumigatus: implications for septum formation and conidiophore development.* Eukaryot Cell, 2008. 7(9): p. 1606-10.

35. Adams, T.H., J.K. Wieser, and J.H. Yu, *Asexual sporulation in Aspergillus nidulans.* Microbiol Mol Biol Rev, 1998. 62(1): p. 35-54.

36. Sheppard, D.C., T. Doedt, L.Y. Chiang, H.S. Kim, D. Chen, W.C. Nierman, and S.G. Filler, *The Aspergillus fumigatus StuA protein governs the up-regulation of a discrete transcriptional program during the acquisition of developmental competence.* Mol Biol Cell, 2005. 16(12): p. 5866-79.

37. Tao, L. and J.H. Yu, *AbaA and WetA govern distinct stages of Aspergillus fumigatus development.* Microbiology. 157(Pt 2): p. 313-26.

38. O'Gorman, C.M., H. Fuller, and P.S. Dyer, *Discovery of a sexual cycle in the opportunistic fungal pathogen Aspergillus fumigatus.* Nature, 2009. 457(7228): p. 471-4.

39. Arratia-Quijada, J., O. Sanchez, C. Scazzocchio, and J. Aguirre, *FlbD, a Myb transcription factor of Aspergillus nidulans, is uniquely involved in both asexual and sexual differentiation.* Eukaryot Cell. 11(9): p. 1132-42.

40. Adams, T.H. and J.H. Yu, *Coordinate control of secondary metabolite production and asexual sporulation in Aspergillus nidulans.* Curr Opin Microbiol, 1998. 1(6): p. 674-7.

41. Lee, B.N. and T.H. Adams, *The Aspergillus nidulans fluG gene is required for production of an extracellular developmental signal and is related to prokaryotic glutamine synthetase I.* Genes Dev, 1994. 8(6): p. 641-51.

42. **Lee, B.N. and T.H. Adams, *FluG and flbA function interdependently to initiate conidiophore development in Aspergillus nidulans through brlA beta activation.* EMBO J, 1996. 15(2): p. 299-309.**

43. **Yu, J.H., *Heterotrimeric G protein signaling and RGSs in Aspergillus nidulans.* J Microbiol, 2006. 44(2): p. 145-54.**

44. **Seo, J.A., K.H. Han, and J.H. Yu, *Multiple roles of a heterotrimeric G-protein gamma-subunit in governing growth and development of Aspergillus nidulans.* Genetics, 2005. 171(1): p. 81-9.**

45. **Shimizu, K. and N.P. Keller, *Genetic involvement of a cAMP-dependent protein kinase in a G protein signaling pathway regulating morphological and chemical transitions in Aspergillus nidulans.* Genetics, 2001. 157(2): p. 591-600.**

46. **Yu, J.H., J.H. Mah, and J.A. Seo, *Growth and developmental control in the model and pathogenic aspergilli.* Eukaryot Cell, 2006. 5(10): p. 1577-84.**

47. **Tag, A., J. Hicks, G. Garifullina, C. Ake, Jr., T.D. Phillips, M. Beremand, and N. Keller, *G-protein signalling mediates differential production of toxic secondary metabolites.* Mol Microbiol, 2000. 38(3): p. 658-65.**

48. **Fillinger, S., M.K. Chaveroche, K. Shimizu, N. Keller, and C. d'Enfert, *cAMP and ras signalling independently control spore germination in the filamentous fungus Aspergillus nidulans.* Mol Microbiol, 2002. 44(4): p. 1001-16.**

49. **Park, H.S., M. Ni, K.C. Jeong, Y.H. Kim, and J.H. Yu, *The role, interaction and regulation of the velvet regulator VelB in Aspergillus nidulans.* PLoS One. 7(9): p. e45935.**

50. **Bok, J.W., S.A. Balajee, K.A. Marr, D. Andes, K.F. Nielsen, J.C. Frisvad, and N.P. Keller, *LaeA, a regulator of morphogenetic fungal virulence factors.* Eukaryot Cell, 2005. 4(9): p. 1574-82.**

51. **Bok, J.W. and N.P. Keller, *LaeA, a regulator of secondary metabolism in Aspergillus spp.* Eukaryot Cell, 2004. 3(2): p. 527-35.**

52. **Bayram, O., S. Krappmann, M. Ni, J.W. Bok, K. Helmstaedt, O. Valerius, S. Braus-Stromeyer, N.J. Kwon, N.P. Keller, J.H. Yu, and G.H. Braus, *VelB/VeA/LaeA complex coordinates light signal with fungal development and secondary metabolism.* Science, 2008. 320(5882): p. 1504-6.**

53. **Sanchez, J.F., A.D. Somoza, N.P. Keller, and C.C. Wang, *Advances in Aspergillus secondary metabolite research in the post-genomic era.* Nat Prod Rep, 2012. 29(3): p. 351-71.**

54. **Ruger-Herreros, C., J. Rodriguez-Romero, R. Fernandez-Barranco, M. Olmedo, R. Fischer, L.M. Corrochano, and D. Canovas, *Regulation of conidiation by light in Aspergillus nidulans.* Genetics. 188(4): p. 809-22.**

55. **Bahn, Y.S., C. Xue, A. Idnurm, J.C. Rutherford, J. Heitman, and M.E. Cardenas, *Sensing the environment: lessons from fungi.* Nat Rev Microbiol, 2007. 5(1): p. 57-69.**

56. **Atoui, A., C. Kastner, C.M. Larey, R. Thokala, O. Etxebeste, E.A. Espeso, R. Fischer, and A.M. Calvo, *Cross-talk between light and glucose regulation controls toxin production and morphogenesis in Aspergillus nidulans.* Fungal Genet Biol. 47(12): p. 962-72.**

57. **Gonzalez, R., V. Gavrias, D. Gomez, C. Scazzocchio, and B. Cubero, *The integration of nitrogen and carbon catabolite repression in Aspergillus nidulans requires the GATA factor AreA and an additional positive-acting element, ADA.* EMBO J, 1997. 16(10): p. 2937-44.**

58. **Berger, H., A. Basheer, S. Bock, Y. Reyes-Dominguez, T. Dalik, F. Altmann, and J. Strauss, *Dissecting individual steps of nitrogen transcription factor***

***cooperation in the Aspergillus nidulans nitrate cluster.*** **Mol Microbiol, 2008. 69(6): p. 1385-98.**

**59. Berger, H., R. Pachlinger, I. Morozov, S. Goller, F. Narendja, M. Caddick, and J. Strauss, *The GATA factor AreA regulates localization and in vivo binding site occupancy of the nitrate activator NirA.* Mol Microbiol, 2006. 59(2): p. 433-46.**

**60. Marzluf, G.A., *Genetic regulation of nitrogen metabolism in the fungi.* Microbiol Mol Biol Rev, 1997. 61(1): p. 17-32.**

**61. Andrianopoulos, A., S. Kourambas, J.A. Sharp, M.A. Davis, and M.J. Hynes, *Characterization of the Aspergillus nidulans nmrA gene involved in nitrogen metabolite repression.* J Bacteriol, 1998. 180(7): p. 1973-7.**

**62. Margelis, S., C. D'Souza, A.J. Small, M.J. Hynes, T.H. Adams, and M.A. Davis, *Role of glutamine synthetase in nitrogen metabolite repression in Aspergillus nidulans.* J Bacteriol, 2001. 183(20): p. 5826-33.**

**63. Macios, M., M.X. Caddick, P. Weglenski, C. Scazzocchio, and A. Dzikowska, *The GATA factors AREA and AREB together with the co-repressor NMRA, negatively regulate arginine catabolism in Aspergillus nidulans in response to nitrogen and carbon source.* Fungal Genet Biol. 49(3): p. 189-98.**

**64. Krappmann, S. and G.H. Braus, *Nitrogen metabolism of Aspergillus and its role in pathogenicity.* Med Mycol, 2005. 43 Suppl 1: p. S31-40.**

**65. Arst, H.N., Jr. and D.J. Cove, *Nitrogen metabolite repression in Aspergillus nidulans.* Mol Gen Genet, 1973. 126(2): p. 111-41.**

**66. Caddick, M.X., D. Peters, and A. Platt, *Nitrogen regulation in fungi.* Antonie Van Leeuwenhoek, 1994. 65(3): p. 169-77.**

**67. Feng, G.H. and T.J. Leonard, *Culture conditions control expression of the genes for aflatoxin and sterigmatocystin biosynthesis in Aspergillus parasiticus and A. nidulans.* Appl Environ Microbiol, 1998. 64(6): p. 2275-7.**

68. Ruijter, G.J. and J. Visser, *Carbon repression in Aspergilli.* FEMS Microbiol Lett, 1997. 151(2): p. 103-14.

69. Mogensen, J., H.B. Nielsen, G. Hofmann, and J. Nielsen, *Transcription analysis using high-density micro-arrays of Aspergillus nidulans wild-type and creA mutant during growth on glucose or ethanol.* Fungal Genet Biol, 2006. 43(8): p. 593-603.

70. Brakhage, A.A., P. Sprote, Q. Al-Abdallah, A. Gehrke, H. Plattner, and A. Tuncher, *Regulation of penicillin biosynthesis in filamentous fungi.* Adv Biochem Eng Biotechnol, 2004. 88: p. 45-90.

71. Wheeler, K.A., B.F. Hurdman, and J.I. Pitt, *Influence of pH on the growth of some toxigenic species of Aspergillus, Penicillium and Fusarium.* Int J Food Microbiol, 1991. 12(2-3): p. 141-9.

72. Tilburn, J., S. Sarkar, D.A. Widdick, E.A. Espeso, M. Orejas, J. Mungroo, M.A. Penalva, and H.N. Arst, Jr., *The Aspergillus PacC zinc finger transcription factor mediates regulation of both acid- and alkaline-expressed genes by ambient pH.* EMBO J, 1995. 14(4): p. 779-90.

73. Keller, N.P., C. Nesbitt, B. Sarr, T.D. Phillips, and G.B. Burow, *pH Regulation of Sterigmatocystin and Aflatoxin Biosynthesis in Aspergillus spp.* Phytopathology, 1997. 87(6): p. 643-8.

74. Diez, E., J. Alvaro, E.A. Espeso, L. Rainbow, T. Suarez, J. Tilburn, H.N. Arst, Jr., and M.A. Penalva, *Activation of the Aspergillus PacC zinc finger transcription factor requires two proteolytic steps.* EMBO J, 2002. 21(6): p. 1350-9.

75. Penas, M.M., A. Hervas-Aguilar, T. Munera-Huertas, E. Reoyo, M.A. Penalva, H.N. Arst, Jr., and J. Tilburn, *Further characterization of the signaling*

***proteolysis step in the Aspergillus nidulans pH signal transduction pathway.*** **Eukaryot Cell, 2007. 6(6): p. 960-70.**

**76. Bignell, E., S. Negrete-Urtasun, A.M. Calcagno, K. Haynes, H.N. Arst, Jr., and T. Rogers, *The Aspergillus pH-responsive transcription factor PacC regulates virulence.* Mol Microbiol, 2005. 55(4): p. 1072-84.**

**77. Flaherty, J.E., A.M. Pirttila, B.H. Bluhm, and C.P. Woloshuk, *PAC1, a pH-regulatory gene from Fusarium verticillioides.* Appl Environ Microbiol, 2003. 69(9): p. 5222-7.**

**78. Krappmann, S., E.M. Bignell, U. Reichard, T. Rogers, K. Haynes, and G.H. Braus, *The Aspergillus fumigatus transcriptional activator CpcA contributes significantly to the virulence of this fungal pathogen.* Mol Microbiol, 2004. 52(3): p. 785-99.**

**79. Hoffmann, B., O. Valerius, M. Andermann, and G.H. Braus, *Transcriptional autoregulation and inhibition of mRNA translation of amino acid regulator gene cpcA of filamentous fungus Aspergillus nidulans.* Mol Biol Cell, 2001. 12(9): p. 2846-57.**

**80. Hood, H.M., D.E. Neafsey, J. Galagan, and M.S. Sachs, *Evolutionary roles of upstream open reading frames in mediating gene regulation in fungi.* Annu Rev Microbiol, 2009. 63: p. 385-409.**

**81. Hinnebusch, A.G., *eIF3: a versatile scaffold for translation initiation complexes.* Trends Biochem Sci, 2006. 31(10): p. 553-62.**

**82. Elliott, C.E., E.M. Fox, R.S. Jarvis, and B.J. Howlett, *The cross-pathway control system regulates production of the secondary metabolite toxin, sirodesmin PL, in the ascomycete, Leptosphaeria maculans.* BMC Microbiol. 11: p. 169.**

83. **Busch, S., H.B. Bode, A.A. Brakhage, and G.H. Braus, *Impact of the cross-pathway control on the regulation of lysine and penicillin biosynthesis in Aspergillus nidulans.* Curr Genet, 2003. 42(4): p. 209-19.**

84. **Yin, W.B., S. Amaike, D.J. Wohlbach, A.P. Gasch, Y.M. Chiang, C.C. Wang, J.W. Bok, M. Rohlfs, and N.P. Keller, *An Aspergillus nidulans bZIP response pathway hardwired for defensive secondary metabolism operates through aflR.* Mol Microbiol. 83(5): p. 1024-34.**

85. **Abad, A., J.V. Fernandez-Molina, J. Bikandi, A. Ramirez, J. Margareto, J. Sendino, F.L. Hernando, J. Ponton, J. Garaizar, and A. Rementeria, *What makes Aspergillus fumigatus a successful pathogen? Genes and molecules involved in invasive aspergillosis.* Rev Iberoam Micol, 2010. 27(4): p. 155-82.**

86. **Brand, A., *Hyphal growth in human fungal pathogens and its role in virulence.* Int J Microbiol. 2012: p. 517529.**

87. **Comera, C., K. Andre, J. Laffitte, X. Collet, P. Galtier, and I. Maridonneau-Parini, *Gliotoxin from Aspergillus fumigatus affects phagocytosis and the organization of the actin cytoskeleton by distinct signalling pathways in human neutrophils.* Microbes Infect, 2007. 9(1): p. 47-54.**

88. **Pahl, H.L., B. Krauss, K. Schulze-Osthoff, T. Decker, E.B. Traenckner, M. Vogt, C. Myers, T. Parks, P. Warring, A. Muhlbacher, A.P. Czernilofsky, and P.A. Baeuerle, *The immunosuppressive fungal metabolite gliotoxin specifically inhibits transcription factor NF-kappaB.* J Exp Med, 1996. 183(4): p. 1829-40.**

89. **Dagenais, T.R. and N.P. Keller, *Pathogenesis of Aspergillus fumigatus in Invasive Aspergillosis.* Clin Microbiol Rev, 2009. 22(3): p. 447-65.**

90. **Hohl, T.M. and M. Feldmesser, *Aspergillus fumigatus: principles of pathogenesis and host defense.* Eukaryot Cell, 2007. 6(11): p. 1953-63.**

91. **Perrin, R.M., N.D. Fedorova, J.W. Bok, R.A. Cramer, J.R. Wortman, H.S. Kim, W.C. Nierman, and N.P. Keller, *Transcriptional regulation of chemical diversity in Aspergillus fumigatus by LaeA.* PLoS Pathog, 2007. 3(4): p. e50.**

92. **Scharf, D.H., T. Heinekamp, N. Remme, P. Hortschansky, A.A. Brakhage, and C. Hertweck, *Biosynthesis and function of gliotoxin in Aspergillus fumigatus.* Appl Microbiol Biotechnol, 2012. 93(2): p. 467-72.**

93. **Bernardo, P.H., N. Brasch, C.L. Chai, and P. Waring, *A novel redox mechanism for the glutathione-dependent reversible uptake of a fungal toxin in cells.* J Biol Chem, 2003. 278(47): p. 46549-55.**

94. **Waring, P., N. Newcombe, M. Edel, Q.H. Lin, H. Jiang, A. Sjaarda, T. Piva, and A. Mullbacher, *Cellular uptake and release of the immunomodulating fungal toxin gliotoxin.* Toxicon, 1994. 32(4): p. 491-504.**

95. **Yoshida, L.S., S. Abe, and S. Tsunawaki, *Fungal gliotoxin targets the onset of superoxide-generating NADPH oxidase of human neutrophils.* Biochem Biophys Res Commun, 2000. 268(3): p. 716-23.**

96. **Tsunawaki, S., L.S. Yoshida, S. Nishida, T. Kobayashi, and T. Shimoyama, *Fungal metabolite gliotoxin inhibits assembly of the human respiratory burst NADPH oxidase.* Infect Immun, 2004. 72(6): p. 3373-82.**

97. **Ben-Ami, R., R.E. Lewis, and D.P. Kontoyiannis, *Enemy of the (immunosuppressed) state: an update on the pathogenesis of Aspergillus fumigatus infection.* Br J Haematol, 2010. 150(4): p. 406-17.**

98. **Stanzani, M., E. Orciuolo, R. Lewis, D.P. Kontoyiannis, S.L. Martins, L.S. St John, and K.V. Komanduri, *Aspergillus fumigatus suppresses the human cellular immune response via gliotoxin-mediated apoptosis of monocytes.* Blood, 2005. 105(6): p. 2258-65.**

99. Pardo, J., C. Urban, E.M. Galvez, P.G. Ekert, U. Muller, J. Kwon-Chung, M. Lobigs, A. Mullbacher, R. Wallich, C. Borner, and M.M. Simon, *The mitochondrial protein Bak is pivotal for gliotoxin-induced apoptosis and a critical host factor of Aspergillus fumigatus virulence in mice.* J Cell Biol, 2006. 174(4): p. 509-19.

100. Gardiner, D.M., P. Waring, and B.J. Howlett, *The epipolythiodioxopiperazine (ETP) class of fungal toxins: distribution, mode of action, functions and biosynthesis.* Microbiology, 2005. 151(Pt 4): p. 1021-32.

101. Lewis, R.E., N.P. Wiederhold, M.S. Lionakis, R.A. Prince, and D.P. Kontoyiannis, *Frequency and species distribution of gliotoxin-producing Aspergillus isolates recovered from patients at a tertiary-care cancer center.* J Clin Microbiol, 2005. 43(12): p. 6120-2.

102. Kupfahl, C., A. Michalka, C. Lass-Florl, G. Fischer, G. Haase, T. Ruppert, G. Geginat, and H. Hof, *Gliotoxin production by clinical and environmental Aspergillus fumigatus strains.* Int J Med Microbiol, 2008. 298(3-4): p. 319-27.

103. Shin, K.S., H.S. Park, Y.H. Kim, and J.H. Yu, *Comparative proteomic analyses reveal that FlbA down-regulates gliT expression and SOD activity in Aspergillus fumigatus.* J Proteomics.

104. Mukherjee, P.K. and C.M. Kenerley, *Regulation of morphogenesis and biocontrol properties in Trichoderma virens by a VELVET protein, Vel1.* Appl Environ Microbiol. 76(7): p. 2345-52.

105. Shin, K.S., N.J. Kwon, and J.H. Yu, *Gbetagamma-mediated growth and developmental control in Aspergillus fumigatus.* Curr Genet, 2009. 55(6): p. 631-41.

106. Xiao, P., K.S. Shin, T. Wang, and J.H. Yu, *Aspergillus fumigatus flbB encodes two basic leucine zipper domain (bZIP) proteins required for proper asexual development and gliotoxin production.* Eukaryot Cell. 9(11): p. 1711-23.

107. Twumasi-Boateng, K., Y. Yu, D. Chen, F.N. Gravelat, W.C. Nierman, and D.C. Sheppard, *Transcriptional profiling identifies a role for BrlA in the response to nitrogen depletion and for StuA in the regulation of secondary metabolite clusters in Aspergillus fumigatus.* Eukaryot Cell, 2009. 8(1): p. 104-15.

108. Sekonyela, R., J.M. Palmer, J.W. Bok, S. Jain, E. Berthier, R. Forseth, F. Schroeder, and N.P. Keller, *RsmA Regulates Aspergillus fumigatus Gliotoxin Cluster Metabolites Including Cyclo(L-Phe-L-Ser), a Potential New Diagnostic Marker for Invasive Aspergillosis.* PLoS One. 8(5): p. e62591.

109. Jain, R., V. Valiante, N. Remme, T. Docimo, T. Heinekamp, C. Hertweck, J. Gershenzon, H. Haas, and A.A. Brakhage, *The MAP kinase MpkA controls cell wall integrity, oxidative stress response, gliotoxin production and iron adaptation in Aspergillus fumigatus.* Mol Microbiol, 2011. 82(1): p. 39-53.

110. Reyes, G., A. Romans, C.K. Nguyen, and G.S. May, *Novel mitogen-activated protein kinase MpkC of Aspergillus fumigatus is required for utilization of polyalcohol sugars.* Eukaryot Cell, 2006. 5(11): p. 1934-40.

111. Osherov, N., D.P. Kontoyiannis, A. Romans, and G.S. May, *Resistance to itraconazole in Aspergillus nidulans and Aspergillus fumigatus is conferred by extra copies of the A. nidulans P-450 14alpha-demethylase gene, pdmA.* J Antimicrob Chemother, 2001. 48(1): p. 75-81.

112. da Silva Ferreira, M.E., M.R. Kress, M. Savoldi, M.H. Goldman, A. Hartl, T. Heinekamp, A.A. Brakhage, and G.H. Goldman, *The akuB(KU80) mutant deficient for nonhomologous end joining is a powerful tool for analyzing pathogenicity in Aspergillus fumigatus.* Eukaryot Cell, 2006. 5(1): p. 207-11.

113. May, G.S., *The highly divergent beta-tubulins of Aspergillus nidulans are functionally interchangeable.* J Cell Biol, 1989. 109(5): p. 2267-74.

114. Maniatis, T., E.F. Fritsch, and J. Sambrook, *Molecular Cloning: A Laboratory Manual*. 1982: Cold Spring Harbor Laboratory. 521.

115. Xue, T., C.K. Nguyen, A. Romans, D.P. Kontoyiannis, and G.S. May, *Isogenic auxotrophic mutant strains in the Aspergillus fumigatus genome reference strain AF293.* Arch Microbiol, 2004. 182(5): p. 346-53.

116. Nierman, W.C., A. Pain, M.J. Anderson, J.R. Wortman, H.S. Kim, J. Arroyo, M. Berriman, K. Abe, D.B. Archer, C. Bermejo, J. Bennett, P. Bowyer, D. Chen, M. Collins, R. Coulsen, R. Davies, P.S. Dyer, M. Farman, N. Fedorova, T.V. Feldblyum, R. Fischer, N. Fosker, A. Fraser, J.L. Garcia, M.J. Garcia, A. Goble, G.H. Goldman, K. Gomi, S. Griffith-Jones, R. Gwilliam, B. Haas, H. Haas, D. Harris, H. Horiuchi, J. Huang, S. Humphray, J. Jimenez, N. Keller, H. Khouri, K. Kitamoto, T. Kobayashi, S. Konzack, R. Kulkarni, T. Kumagai, A. Lafon, J.P. Latge, W. Li, A. Lord, C. Lu, W.H. Majoros, G.S. May, B.L. Miller, Y. Mohamoud, M. Molina, M. Monod, I. Mouyna, S. Mulligan, L. Murphy, S. O'Neil, I. Paulsen, M.A. Penalva, M. Pertea, C. Price, B.L. Pritchard, M.A. Quail, E. Rabbinowitsch, N. Rawlins, M.A. Rajandream, U. Reichard, H. Renauld, G.D. Robson, S. Rodriguez de Cordoba, J.M. Rodriguez-Pena, C.M. Ronning, S. Rutter, S.L. Salzberg, M. Sanchez, J.C. Sanchez-Ferrero, D. Saunders, K. Seeger, R. Squares, S. Squares, M. Takeuchi, F. Tekaia, G. Turner, C.R. Vazquez de Aldana, J. Weidman, O. White, J. Woodward, J.H. Yu, C. Fraser, J.E. Galagan, K. Asai, M. Machida, N. Hall, B. Barrell, and D.W. Denning, *Genomic sequence of the pathogenic and allergenic filamentous fungus Aspergillus fumigatus.* Nature, 2005. 438(7071): p. 1151-6.

117. Magnani, E., L. Bartling, and S. Hake, *From Gateway to MultiSite Gateway in one recombination event.* BMC Mol Biol, 2006. 7: p. 46.

118. Lam, K.N., H. van Bakel, A.G. Cote, A. van der Ven, and T.R. Hughes, *Sequence specificity is obtained from the majority of modular C2H2 zinc-finger arrays.* Nucleic Acids Res, 2011. 39(11): p. 4680-90.

119. Aleksenko, A. and A.J. Clutterbuck, *Autonomous plasmid replication in Aspergillus nidulans: AMA1 and MATE elements.* Fungal Genet Biol, 1997. 21(3): p. 373-87.

120. Gems, D., I.L. Johnstone, and A.J. Clutterbuck, *An autonomously replicating plasmid transforms Aspergillus nidulans at high frequency.* Gene, 1991. 98(1): p. 61-7.

121. Kebaara, B.W. and A.L. Atkin, *Long 3'-UTRs target wild-type mRNAs for nonsense-mediated mRNA decay in Saccharomyces cerevisiae.* Nucleic Acids Res, 2009. 37(9): p. 2771-8.

122. Brayer, K.J. and D.J. Segal, *Keep your fingers off my DNA: protein-protein interactions mediated by C2H2 zinc finger domains.* Cell Biochem Biophys, 2008. 50(3): p. 111-31.

123. Brown, R.S., *Zinc finger proteins: getting a grip on RNA.* Curr Opin Struct Biol, 2005. 15(1): p. 94-8.

124. Lionakis, M.S., R.E. Lewis, G.S. May, N.P. Wiederhold, N.D. Albert, G. Halder, and D.P. Kontoyiannis, *Toll-deficient Drosophila flies as a fast, high-throughput model for the study of antifungal drug efficacy against invasive aspergillosis and Aspergillus virulence.* J Infect Dis, 2005. 191(7): p. 1188-95.

125. Khaldi, N., F.T. Seifuddin, G. Turner, D. Haft, W.C. Nierman, K.H. Wolfe, and N.D. Fedorova, *SMURF: Genomic mapping of fungal secondary metabolite clusters.* Fungal Genet Biol, 2010. 47(9): p. 736-41.

126. Santos, J.L. and K. Shiozaki, *Fungal histidine kinases.* Sci STKE, 2001. 2001(98): p. re1.

127. Bahn, Y.S., *Master and commander in fungal pathogens: the two-component system and the HOG signaling pathway.* Eukaryot Cell, 2008. 7(12): p. 2017-36.

128. Liebmann, B., M. Muller, A. Braun, and A.A. Brakhage, *The cyclic AMP-dependent protein kinase a network regulates development and virulence in Aspergillus fumigatus.* Infect Immun, 2004. 72(9): p. 5193-203.

129. Dhingra, S., D. Andes, and A.M. Calvo, *VeA regulates conidiation, gliotoxin production, and protease activity in the opportunistic human pathogen Aspergillus fumigatus.* Eukaryot Cell. 11(12): p. 1531-43.

130. Lin, Z. and W.H. Li, *Evolution of 5' untranslated region length and gene expression reprogramming in yeasts.* Mol Biol Evol. 29(1): p. 81-9.

131. Luukkonen, B.G., W. Tan, and S. Schwartz, *Efficiency of reinitiation of translation on human immunodeficiency virus type 1 mRNAs is determined by the length of the upstream open reading frame and by intercistronic distance.* J Virol, 1995. 69(7): p. 4086-94.

132. Muro-Pastor, M.I., R. Gonzalez, J. Strauss, F. Narendja, and C. Scazzocchio, *The GATA factor AreA is essential for chromatin remodelling in a eukaryotic bidirectional promoter.* EMBO J, 1999. 18(6): p. 1584-97.

133. Berg JM, T.J., Stryer L, *Examination of Three-Dimensional Structure Enhances Our Understanding of Evolutionary Relationships*, in *Biochemistry*. 2002, W H Freeman: New York.

134. Wanke, C., S. Eckert, G. Albrecht, W. van Hartingsveldt, P.J. Punt, C.A. van den Hondel, and G.H. Braus, *The Aspergillus niger GCN4 homologue, cpcA, is transcriptionally regulated and encodes an unusual leucine zipper.* Mol Microbiol, 1997. 23(1): p. 23-33.

135. Garzia, A., O. Etxebeste, E. Herrero-Garcia, U. Ugalde, and E.A. Espeso, *The concerted action of bZip and cMyb transcription factors FlbB and FlbD induces brlA expression and asexual development in Aspergillus nidulans.* Mol Microbiol. 75(5): p. 1314-24.

136. Garzia, A., O. Etxebeste, E. Herrero-Garcia, R. Fischer, E.A. Espeso, and U. Ugalde, *Aspergillus nidulans FlbE is an upstream developmental activator of conidiation functionally associated with the putative transcription factor FlbB.* Mol Microbiol, 2009. 71(1): p. 172-84.

137. Kwon, N.J., K.S. Shin, and J.H. Yu, *Characterization of the developmental regulator FlbE in Aspergillus fumigatus and Aspergillus nidulans.* Fungal Genet Biol. 47(12): p. 981-93.

138. Matthews, J.M., K. Kowalski, C.K. Liew, B.K. Sharpe, A.H. Fox, M. Crossley, and J.P. MacKay, *A class of zinc fingers involved in protein-protein interactions biophysical characterization of CCHC fingers from fog and U-shaped.* Eur J Biochem, 2000. 267(4): p. 1030-8.

139. Fox, A.H., C. Liew, M. Holmes, K. Kowalski, J. Mackay, and M. Crossley, *Transcriptional cofactors of the FOG family interact with GATA proteins by means of multiple zinc fingers.* EMBO J, 1999. 18(10): p. 2812-22.

140. Bergmann, S., A.N. Funk, K. Scherlach, V. Schroeckh, E. Shelest, U. Horn, C. Hertweck, and A.A. Brakhage, *Activation of a silent fungal polyketide biosynthesis pathway through regulatory cross talk with a cryptic nonribosomal peptide synthetase gene cluster.* Appl Environ Microbiol. 76(24): p. 8143-9.

Taylor Jane Schoberle was born in Dallas, Texas on May 26, 1981, the daughter of Catherine Saunders Schoberle and Carl Joseph Schoberle III. She completed an internship at The University of Texas Southwestern Medical Center in Dallas, Texas in the spring of 1999. After receiving a high school degree from Lake Highlands High School in 1999, she entered Southwestern University in Georgetown, Texas. She received a Bachelor of Arts with a major in Biology and a minor in French from Southwestern University in May 2003. In August of 2005, she entered The University of Texas Health Science Center at Houston Graduate School of Biomedical Sciences. She received a Master of Science degree in 2008 in Genes and Development and Molecular Biology and reentered The University of Texas Health Science Center at Houston Graduate School of Biomedical Sciences for a Doctor of Philosophy degree.

Permanent Address:
6 Rosewood Rd.
Stony Brook, NY 11790